KONINKLIJK BELGISCH INSTITUUT VOOR NATUURWETENSCHAPPEN
OD NATUUR – BEHEERSEENHEID VAN HET MATEMATISCH MODEL

MOnitoring en MOdellering van het cohesieve sedimenttransport en evaluatie van de effecten op het mariene ecosysteem ten gevolge van bagger- en stortoperatie (MOMO)

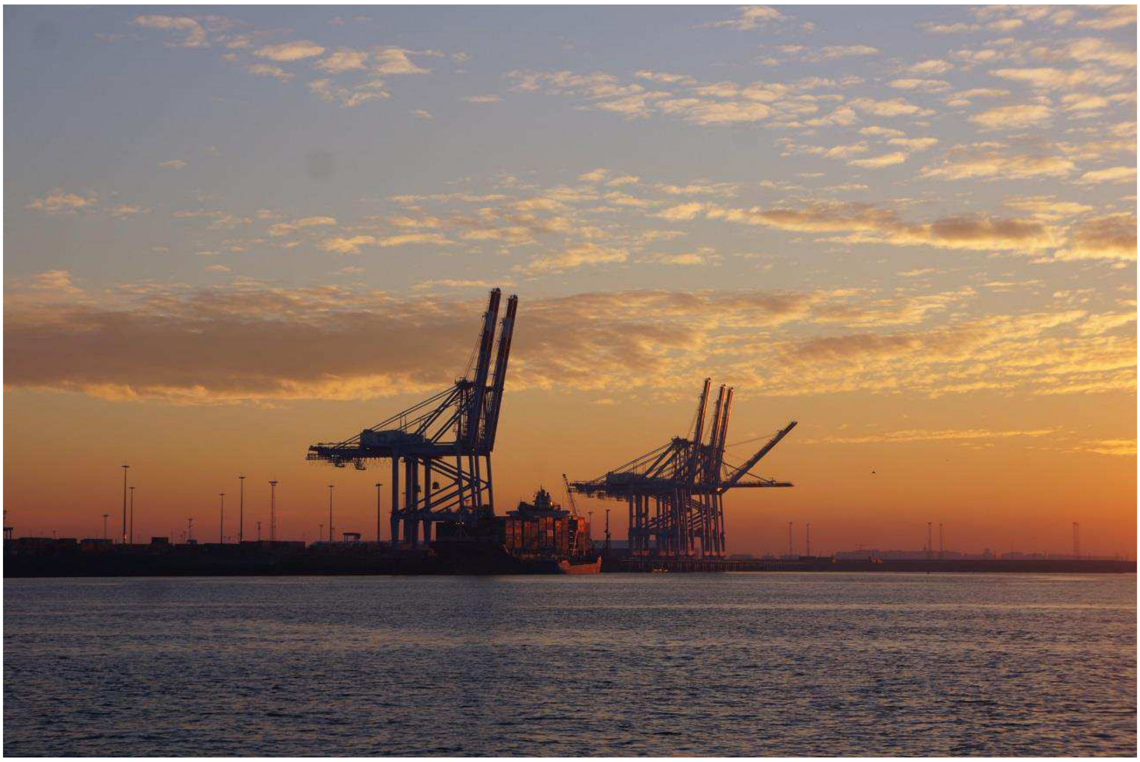

Activiteitsrapport (1 juli 2015 - 31 december 2015)

Michael Fettweis, Matthias Baeye, Frederic Francken, Dries Van den Eynde, Sylvie Thant[1]

MOMO/7/MF/201603/NL/AR/4

[1] huidig adres: Antea Group, Roderveldlaan 1, 2600 Antwerpen

museum
Operational Directorate Natural Environment
OD Nature I OD Natuur I DO Nature

KBIN-OD Natuur - BMM
Gulledelle 100
B–1200 Brussel
België

Inhoudstafel

1. Inleiding

1.1. Voorwerp van deze opdracht

Het MOMO-project (MOnitoring en MOdellering van het cohesieve sedimenttransport en de evaluatie van de effecten op het mariene ecosysteem ten gevolge van bagger- en stort-operatie) maakt deel uit van de algemene en permanente verplichtingen van monitoring en evaluatie van de effecten van alle menselijke activiteiten op het mariene ecosysteem waaraan België gebonden is overeenkomstig het Verdrag inzake de bescherming van het mariene milieu van de noordoostelijke Atlantische Oceaan (1992, OSPAR-Verdrag). De OSPAR Commissie heeft de objectieven van haar huidig "Joint Assessment and Monitoring Programme" (JAMP) gedefinieerd tot 2010 met de publicatie van een holistisch Quality Status Report Noordzee en waarvoor de federale overheid en de gewesten technische en wetenschappelijke bijdragen moeten afleveren ten laste van hun eigen middelen.

De menselijke activiteit die hier in het bijzonder wordt beoogd, is het storten in zee van baggerspecie waarvoor OSPAR een uitzondering heeft gemaakt op de algemene regel "alle stortingen in zee zijn verboden" (zie OSPAR-Verdrag, Bijlage II over de voorkoming en uitschakeling van verontreiniging door storting of verbranding). Het algemene doel van de opdracht is het bestuderen van de cohesieve sedimenten op het Belgisch Continentaal Plat (BCP) en dit met behulp van zowel numerieke modellen als het uitvoeren van metingen. De combinatie van monitoring en modellering zal gegevens kunnen aanleveren over de transportprocessen van deze fijne fractie en is daarom fundamenteel bij het beantwoorden van vragen over de samenstelling, de oorsprong en het verblijf ervan op het BCP, de veranderingen in de karakteristieken van dit sediment ten gevolge van de bagger- en stortoperaties, de effecten van de natuurlijke variabiliteit, de impact op het mariene ecosysteem in het bijzonder door de wijziging van habitats, de schatting van de netto input van gevaarlijke stoffen op het mariene milieu en de mogelijkheden om deze laatste twee te beperken.

Een samenvatting van de resultaten uit de voorbije vergunningsperioden kan gevonden worden in de Syntheserapportten over de effecten op het mariene milieu van baggerspeciestortingen (Lauwaert et al. 2004; 2006; 2008; 2009a, 2009b, 2011a, 2011b, 2014) die gepubliceerd werden conform art. 10 van het K.B. van 12 maart 2000 ter definiëring van de procedure voor machtiging van het storten in de Noordzee van bepaalde stoffen en materialen.

1.2. Algemene doelstellingen

Het onderzoek uitgevoerd in het MOMO project kadert in de algemene doelstellingen om de baggerwerken op het BCP en in de kusthavens te verminderen en om een gedetailleerd inzicht te verwerven van de fysische processen die plaatsvinden in het mariene kader waarbinnen deze baggerwerken worden uitgevoerd. Dit impliceert enerzijds beleidsondersteunend onderzoek naar de vermindering van de sedimentatie op de baggerplaatsen en het evalueren van alternatieve stortmethoden. Anderzijds is onderzoek naar knelpunten voor het plannen en schatten van de effecten van de baggerwerken vereist. Dit is specifiek gericht op het dynamische gedrag van silb in de waterkolom en op de bodem en zal uitgevoerd worden met behulp van modellen en in situ metingen. De specifieke acties die binnen dit onderzoek uitgevoerd worden om de algemene doelstellingen in te vullen zijn:

1. Streven naar een efficiënter stortbeleid door:

- optimalisatie van de stortlocaties. Gebaseerd op onderzoek uitgevoerd in de voorbije jaren (zie vorige syntheserapporten) zal een terreinproef worden uitgevoerd om de efficiëntie van een stortlocatie ten westen van Zeebrugge te bepalen;
- gebruik te maken van een operationeel stortmodel. Dit model zal geïntegreerd worden in de binnen BMM beschikbare operationele modellen. Het model zal gebruikt worden om in functie van de voorspelde fysische (wind, stroming, golven, sedimenttransport, recirculatie), economische (afstand, grootte baggerschip) en ecologische aspecten op korte termijn een keuze te kunnen maken tussen de beschikbare stortlocaties. Hiervoor zal binnen de huidige periode het slibtransportmodel gevalideerd worden op de geografische variabiliteit van de turbiditeitszones en de flocculatie van het slib.

2. Continue monitoring van het fysisch-sedimentologische milieu waarbinnen de baggerwerken worden uitgevoerd en aanpassing van de monitoring aan de nog op te stellen targets voor het bereiken van de goede milieutoestand (GES), zoals gedefinieerd zal worden binnen MSFD;

3. Uitbouw en optimalisatie van het numerieke modelinstrumentarium, ter ondersteuning en verfijning van acties 1 en 2.

1.3. Onderzoek Januari 2014 – December 2016

In het bijzonder is bij het opstellen van de hieronder vermelde taken rekening gehouden met de aanbevelingen voor de minister ter ondersteuning van de ontwikkeling van een versterkt milieubeleid zoals geformuleerd in het “Syntheserapport over de effecten op het mariene milieu van baggerspeciestortingen (2011)” dat uitgevoerd werd conform art. 10 van het K.B. van 12 maart 2000 ter definiëring van de procedure voor machtiging van het storten in de Noordzee van bepaalde stoffen en materialen

Taak 1: In situ metingen en data analyse

Monitoring moet gericht zijn op het begrijpen van processen, zodoende dat de waargenomen variabiliteit in een correcte kader geplaatst kan worden. In vele kustzones is er een gebrek aan langdurige en hoogfrequente data over sleutelparameters die de milieutoestand beschrijven, zoals turbiditeit en SPM concentratie. De tripodemetingen in het kader van het MOMO project te MOW1 vormen een uitzondering hierop gezien hun langdurig karakter. De eerste verankeringen werden in 2004 uitgevoerd, vanaf november 2009 worden er continue metingen gedaan. Deze data laten toe om om zowel de natuurlijke variabiliteit, de langdurige trends en de effecten van menselijke ingrepen op de turbiditeit te achterhalen. Een groot deel van de activiteiten is daarom gericht op zowel het uitvoeren van de metingen, het garanderen van kwalitatief hoogwaardige data en het archiveren, rapporteren en interpreteren ervan.

Taak 1.1 Langdurige metingen

Sinds eind 2009 worden er continue metingen uitgevoerd te MOW1 met behulp van een meetframe (tripode). Met dit frame worden stromingen, slibconcentratie, korrelgrootte-verdeling van het suspensiemateriaal, saliniteit, temperatuur, waterdiepte en zeebodem altimetrie gemeten. Om een continue tijdreeks te hebben, wordt gebruik gemaakt van 2 tripodes. Na ongeveer 1 maand wordt de verankerde tripode voor onderhoud aan wal gebracht en wordt de tweede op de meetlocatie verankerd.

In 2013 werd gestart met langdurige metingen met behulp van een OBS-5 sensor vastgemaakt aan de AW boei; deze metingen zullen verdergezet worden. De data geven informatie over de SPM concentratie aan het oppervlak en zijn aldus complementair aan de bodemnabije metingen met de tripode. De data zijn ook van belang voor het calibreren en valideren van de oppervlakte SPM concentraties uit satellietbeelden.

Taak 1.2 Calibratie van sensoren tijdens in situ metingen

Tijdens 4 meetcampagnes per jaar met de R/V Belgica zullen een voldoende aantal 13-uursmetingen uitgevoerd worden met als hoofdoel het calibreren van optische of akoestische sensoren en het verzamelen van verticale profielen. De metingen zullen plaatsvinden in het kustgebied van het BCP. De optische metingen (transmissometer, Optical Backscatter Sensor) zullen gecalibreerd worden met de opgemeten hoeveelheid materie in suspensie (gravimetrische bepalingen na filtratie) om te komen tot massa concentraties. Naast de totale hoeveelheid aan suspensiemateriaal (SPM) wordt ook de concentratie aan POC/PON, chlorophyl (Chl-a, Chl-b) en phaeofytine (a, b) bepaald. Stalen van suspensiemateriaal zullen genomen worden met de centrifuge om de samenstelling ervan te bepalen.

Taak 1.3: Data archivering en rapportage

De meetdata worden gearchiveerd en er wordt een kwaliteitsanalyse uitgevoerd, zodat de goede data onderscheiden kunnen worden van slechte of niet betrouwbare data. Slechte data kunnen bv optreden doordat het instrument slecht heeft gewerkt en verkeerd werd ingesteld. Niet betrouwbare data zijn typisch geassicieerd met bv biofouling. De data en metadata worden gearchiveerd.

Taak 1.4: Verwerking en interpretatie van metingen

De metingen vergaard tijdens de 13-uursmetingen aan boord van de Belgica en met de tripode worden verwerkt en geïnterpreteerd. Hiervoor werden in het verleden reeds heel wat procedures (software) toegepast of ontwikkeld, zoals de berekening van de bodem-schuifspanning uit turbulentiemetingen, entropieanalyse op partikelgrootteverdelingen, de opsplitising van multimodale partikelgrootteverdeling in een som van lognormale verdelingen, het groeperen van de data volgens getij, meteorologie, klimatologie en seizoenen. Deze methodes (zullen opgenomen worden) zijn opgenomen in de standaardverwerking van de data. De aldus verwerkte data dienen als basis voor het verder gebruik binnenin wetenschappelijke vragen (zie taak 2.2, 2.3 en 4.2, 4.4).

Taak 2: Onderzoek en monitoring alternatieve stortstrategie onderhoudsbaggerwerk voorhaven Zeebrugge

De BMM is auteur van de voorbereidende studies voor de terreinproef en zal de terreinproef mee opvolgen. BMM-OD Natuur zal verantwoordelijk zijn voor het uitvoeren van de langdurige frame metingen (lopen tot eind april 2014) en de statistische verwerking van de resultaten (Taak 2.1). De resultaten van de metingen zullen gebruikt worden bij de analyse van de efficiëntie van de baggerproef (Taak 2.3). Door de BMM-OD Natuur zullen ook met behulp van het Automatic Underway Monitoring System (AUMS) op het onderzoeksschip Belgica opnames gemaakt worden van de sedimentconcentratie binnen de haven (Taak 2.2). Deze gegevens zullen ter beschikking gesteld worden voor verdere verwerking. BMM-OD Natuur zal deel uitmaken van de stuurgroep.

Taak 2.1: Uitvoeren van lange termijn metingen in de omgeving van de haven van Zeebrugge voor het opvolgen van de terreinproef, en het bestuderen van de interne sedimentdynamiek in de haven

Voor dit deel van de opdracht is de BMM-OD Natuur verantwoordelijk voor het uitvoeren van de metingen en het aanleveren van de gevalideerde data voor verdere verwerking in de factual data rapportering en omzetting naar het standaardformaat. Het betreft twee meetframes, een ter hoogte van de meetpaal MOW 1 (als achtergrondwaarde, zie Taak

1.1) en een ander ter hoogte van de ingang van de haven van Zeebrugge (WZ-boei). Deze meetframes dienen afdoend de saliniteit, stromingen, sedimentconcentratie en korrelgrootteverdeling te meten.

Taak 2.2: Beschrijving van de omgevingscondities

Gedurende de meetperiode van de langdurige metingen dienen ook de verschillende externe factoren die een invloed kunnen hebben op de interne slibdynamiek in de haven nauwkeurig bijgehouden worden en dit gedurende dezelfde periode als de metingen in taak 2.1. De BMM-OD Natuur is verantwoordelijk voor het opleveren van informatie over de sedimentconcentraties uit het AUMS aan boord van de Belgica.

Taak 2.3: Analyse efficiëntie baggerproef

Na afloop van de baggerproef dient de efficiëntie van de uitgevoerde proef geschat te worden. Hiervoor dient als eerste een T0 toestand gedefinieerd te worden, waarbij op basis van de binnen Taak 2.1 en Taak 2.2 verzamelde data een inschatting kan gemaakt worden van de mogelijke events die tijdens de proef hebben plaatsgevonden, en hun invloed op de resultaten van de baggerproef. De BMM-OD Natuur zal een statistische benadering van de efficiëntie van de baggerproef uitvoeren, waarbij nagegaan wordt in hoeverre de tijdens de baggerproef gemeten waardes op de twee frames afwijken van de waardes die gemeten werden buiten de stortproef. Deze analyse werd reeds toegepast bij de evalueren van de baggerproef in het Albert II dok.

Taak 3: Uitbouw en optimalisatie van het modelinstrumentarium

Taak 3.1: Validatie van het slibtransportmodel

Het tijdens de voorbije jaren verbeterde en aangepaste slibtransportmodel zal worden gevalideerd met behulp van de langdurige meetreeksen en de satellietbeelden. Hierbij zal dezelfde methode als in Baeye et al. (2011) en zoals in taak 1.4 worden gebruikt om de modelresultaten te groeperen en te klasseren volgens windrichting, weertype en getij. Het voordeel van deze werkwijze is dat niet zozeer gekeken wordt of de correlatie tussen meting en modelresultaat in één of meerder punt goed is, maar dat globaal nagegaan wordt of het model de SPM dynamica op het BCP goed kan reproduceren. Deze taak zal in nauwe samenwerking met het WLH gebeuren die eenzelfde benadering zullen toe passen op hun model (contacten zijn gelegd met B De Maerschalk).

Taak 3.2: Operationeel stortmodel

Dit model zal geïntegreerd worden in de binnen BMM-OD Natuur beschikbare operationele modellen. Het model zal gebruikt worden om in functie van de voorspelde fysische (wind, stroming, golven, sedimenttransport, recirculatie), economische (afstand, grootte baggerschip) en ecologische aspecten op korte termijn een keuze te kunnen maken tussen de beschikbare stortlocaties. Hiervoor zal binnen de huidige periode het slibtransportmodel gevalideerd worden op de geografische variabiliteit van de turbiditeitszones en de flocculatie van het slib.

Taak 4: Oplossingen voor knelpunten

Taak 4.1: Kwaliteitscontrole van de data en de integratie ervan in de monitoing voor de KRMS

Taak 4.1.1: KRMS monitoring

De data verzameld in Taak 1, zullen worden opgenomen in de nog op te zetten monitoringsverplichtingen van de Belgische Staat (07/2014) in het kader van de Kaderrichtlijn Mariene Strategie (MFSD). De KRMS monitoring zal in 2015 starten en zal dienen om de toestand van het mariene milieu te evalueren aan de goede milieutoestand

(GES), zoals opgetseld door de Belgische Staat in 2012 (Belgische Staat 2012a, 2012b).

Er zal verder geëvalueerd worden of het MOMO meetprogramma aan de monitorings-verplichtingen die voor de KRMS (MFSD) moeten worden opgesteld zal voldoen en/of er aanpassingen nodig zijn. De wetenschappelijke vragen die hier bekeken worden hebben vooral betrekking op de geografische spreiding van de data. Is het voldoende om – zoals nu gebeurt – te berusten op satellietbeelden voor de geografische en in situ meetreeksen voor de temporele spreiding of dienen we te opteren voor één vast meetpunt (MOW1) en bijkomend een aantal andere punten (Nieuwpoort, Kwintebank, Gootebank) waar random in de tijd gemeten wordt met een tripode gedurende telkens een periode van ongeveer 1 maand. Hiervoor zou bv de tripode die nu ingezet wordt voor de terreinproef gebruikt kunnen worden.

Taak 4.1.2:Kwaliteitscontrole

Een belangrijk aandachtspunt bij deze langdurige datareeksen is het garanderen van een gelijke kwaliteit in de tijd van de verzamelde data. De vraag die zich bij onze SPM concentratiemetingen stelt is niet zozeer het opmeten van hogere of lagere waarden, mogelijks veroozaakt door het toepassen van een andere stortstrategie, maar het garanderen dat deze waarden inderdaad veroorzaakt worden door menselijke activiteiten (bv storten) en niet het effect zijn van natuurlijke fluctuaties. De natuurlijke variabiliteit van SPM concentratie is groot en wordt veroorzaakt door de getijwerking, doodtij-springtijcyclus en meteorologische en klimatologische phenomenen. De tijdschalen gaan van seconden tot seizoenen, met mogelijks langere fluctuaties voor (nodale cylus, klimaatsverandering, zeespiegelstijging,...). Langdurige variaties kunnen bv geïdentifceerd worden als een trend of een cosinusfunctie met lage frequentie. Om kwaliteitsvolle data te kunnen leveren over een lange periode, die gebruikt kunnen worden om langdurige trends te identificeren, is het nodig om een rigoureuze kwaliteitscontrole uit te voeren. OBS alsook akoestische sensoren zijn gevoelig aan de samenstelling en korrelgrootte van het gesuspendeerde materiaal. Dit kan varieren in functie van de boven vermelde frequenties, maar hieromtrent is er nog geen afdoende duidelijkheid wat de metingen te MOW1 betreft.

- Hoe veranderen de calibratieconstanten i.f.v. externe parameters (doodtij-springtij, zomer-winter)? Hoe dikwijls moeten de sensoren in situ gecalibreerd worden om de rekening te kunnen houden met de mogelijke fluctuaties in samenstelling van het suspensiemateriaal?
- Wat is de fout op de metingen? Het uitvoeren van directe (waterstaal) en indirecte metingen (OBS, akoestische backscatter) van SPM concentratie gaat inherent gepaard met onzekerheden (meetfouten). In situ metingen zijn steeeds onderhevig aan onzekerheden tengevolge van random meetfouten (gebrek aan precisie), systematische fouten (onnauwkeurigheid), menselijke fouten, en de statistische variabiliteit van de parameter. De fouten hebben hun oorsprong in de onnauwkeurigheid en het gebrek aan precisie van het meetinstrument of de procedures (bv. waterstaalname en filtratie). Doel is om de fout op de verschillende onderdelen van de metingen (filtratie, calibratie, langdurige trends...) te schatten.

Taak 4.1.3: Aanvulling van ontbrekende data met behulp van statistische methodes

Het gebeurt regelmatig in de metingen te MOW1 dat de OBS sensoren verzadigen (vooral deze op 0.2 m) of uitvallen en er aldus gedurende een korte of langere perioden geen (betrouwbare) data beschikbaar zijn. In de statistiek bestaan technieken de ontbrekende data te reconstrueren. Er zal nagegaan worden wat de meets geschikte methode is om de tijdseries te vervolledigen.

Taak 4.2: Biologische effecten en de seizoenale variaties in SPM concentratie

De correlatie tussen biomassa (zoals o.a. POC en chlorophyl) en vlokgrootte en vorm wordt dikwijls aangehaald in de literatuur, maar dit bleek sterk plaatsgebonden te zijn en dikwijls gebaseerd op korte meetperioden. De lange tijdsreeks te MOW1 werd geanalyseerd in combinatie met satelliet data, de omgekeerde correlatie tussen de chlorophyll en de SPM concentratie is opvallend. Er werd de hypothese opgesteld, dat door de algenbloei in de lente de concentratie aan kleverige organische moleculen (TEPs) wordt verhoogd, waardoor meer macrovlokken gevormd worden, het SPM sneller bezinkt en moeilijker kan eroderen en aldus de SPM concentratie gaat afnemen. erder onderzoek richt zich naar:

1) Analyse van TEP concentraties. Tot nu toe worden geen TEP analyses uitgevoerd, nochthans is dit noodzakelijk om deze hypothese te toetsen. Er zal nagegaan worden hoe de TEPs geanalyseerd kunnen worden in waterstalen, wat en hoe dit meet-programma uitgevoerd kan worden. Er wordt geopteerd om tegen 2015 met de eerste metingen te kunnen beginnen.
2) De invloed van lichthoeveelheid op de start van de algenbloei in de lente en de afname van de SPM concentratie;
3) Wat gebeurt er met het SPM dat uit de waterkolom verdwijnt door snellere sedimentatie in de zomer? Heeft dit een effect op de frequentie van hooggeconcentreerde slibsuspensies en mogelijks aanslibbing van vaargeulen en havens?
4) Verdere ontwikkeling van het flocculatiemodel zodat seizoenale effecten in rekening gebracht kunnen worden. Simulatie in 2D/3D met dit flocculatiemodel teneinde het model te valideren.

Taak 4.3: Alternatieve Stortstrategies Nieuwpoort

Er zal ondersteuning gegeven worden aan MDK in verband met het opzetten van een wetenschappelijke terreinproef om de impact van het verpompen van baggerspecie uit de haven van Nieuwpoort op een stortzone te evalueren. Details hiervan zullen op een vergadering van de technische werkgroep besproken worden.

Taak 4.4: Golfsystemen en hun impact op de zeebodem en de SPM concentratie

Er bestaan verschillende sorten golven en golfsystemen (korte golven, deining) die een impact hebben op de zeebodem. Tot nu toe werd dit aspect nog niet in rekening gebracht in de analyse van de data. Wat is de impact van deinig of korte golven op de resuspensie van sedimenten? Wat zijn de belangrijkste parameters en wat is hun belang voor waterbouwkundige werken (baggeren)?

1.4. Gerapporteerde en/of uitgevoerde taken

Periode Januari 2014 – Juni 2014

Taak 1.1: De meetreeks te MOW1 werd verdergezet.
Taak 1.2: Calibratie van sensoren werd uitgevoerd tijdens RV Begica campagnes 2014/01 en 2014/11
Taak 1.4: Verwerking en interpretatie van OBS meetdata (gerapporteerd in activiteitsrapport MOMO/7/MF/201408/NL/AR/1)
Taak 2.1: De metingen aan de WZ boei werden beëindigd eind maart 2014.

Periode Juli 2014 – December 2014

Taak 1.1: De meetreeks te MOW1 werd verdergezet.
Taak 1.2: Calibratie van sensoren werd uitgevoerd tijdens RV Begica campagnes 2014/22, 2014/28 en 2014/31
Taak 1.4: Verwerking en interpretatie van LISST meetdata (gerapporteerd in activiteitsrapport MOMO/7/MF/201501/NL/AR/2).
Taak 2.2: ADCP data gemeten aan boord van de Belgica en de satellietbeelden tijdens

de stortproef werden verwerkt en de data opgeleverd.

Taak 4.2: Wat gebeurt er met het SPM dat uit de waterkolom verdwijnt door snellere sedimentatie in de zomer? (gerapporteerd in activiteitsrapport MOMO/7/MF/201501/NL/AR/2, voorgesteld op PiE 2014, PECS 2014, VLIZ Young Scientist day 2015 en gepubliceerd in JGR in augustus 2015).

Periode Jaunari 2015 – Juni 2015

Taak 1.1: De meetreeks te MOW1 werd verdergezet.

Taak 1.2: Calibratie van sensoren werd uitgevoerd tijdens RV Begica campagnes 2015/01 en 2015/10.

Taak 2 Terreinproef, analyse efficiëntie baggerproef (zie activiteitsrapport MOMO/7/MF/201508/NL/AR/3).

Periode Juli 2015 – December 2015

Taak 1.1: De meetreeks te MOW1 werd verdergezet.

Taak 1.2: Calibratie van sensoren werd uitgevoerd tijdens RV Begica campagnes 2015/32.

Taak 2 Terreinproef (voorgesteld op INTERCOH 2015).

Taak 4.1.2 Kwaliteitscontrole (voorgesteld op INTERCOH 2015).

Taak 4.4 Golfsystemen en hun impact op de zeebodem en de SPM concentratie (gerapporteerd in activiteitsrapport MOMO/7/MF/201603/NL/AR/4, voorgesteld INTERCOH 2015).

1.5. Publicaties (januari 2014 – december 2015)

Hieronder wordt een overzicht gegeven van publicatie (rapporten, papers, thesissen en presentatie op workshops en conferenties) waar resultaten en data uit het MOMO project in werden gebruikt.

Activiteits-, Meet- en Syntheserapporten

Fettweis M, Baeye M, Francken F, Van den Eynde D, Thant S. 2016. MOMO activiteitsrapport (1 juli – 31 december 2015). BMM-rapport MOMO/7/MF/201603/NL/AR/4, 25pp + app.

Fettweis M, Baeye M, Francken F, Vn den Eynde D. 2015. MOMO activiteitsrapport (1 januari – 30 juni 2015). BMM-rapport MOMO/7/MF/201508/NL/AR/3, 76pp + app.

Van den Eynde D, Fettweis M. 2015. Modellering van een alternatieve stortstrategie voor de onderhoudsbaggerwerken in de voorhaven van Zeebrugge. Technisch rapport MOMO/7/DVDE/201506/NL/TR01, 17pp.

Fettweis M, Baeye M, Francken F. 2015. MOMO activiteitsrapport (1 juli – 31 december 2014). BMM-rapport MOMO/7/MF/201501/NL/AR/2, 41pp + app.

Backers J, Francken F, Hindryckx K, Vanaverbeke W. 2014. Rapport van de RV Belgica Meetcampagnes en Verankering van Meetsystemen MOMO – 2013. BMM-rapport BMM-MDO/2014-10/MOMO/2013, 213pp.

Fettweis M, Baeye M, Francken F, Van den Eynde D. 2014. MOMO activiteitsrapport (1 januari - 30 juni 2014). BMM-rapport MOMO/7/MF/201408/NL/AR/1, 43pp + app.

Lauwaert B, Fettweis M, De Witte B, Devriese L, Van Hoei G, Timmermans S, Martens C. 2014. Vooruitgangsrapport (juni 2014) over de effecten op het mariene milieu van baggerspeciestortingen (vergunningsperiode 01/01/2012 – 31/12/2016). Rapport uitgevoerd door KBIN-BMM, ILVO, CD, aMT. BL/2014/01, 20pp + app.

Conferenties/Workshops

Dujardin A, Vanlede J, Van Hoestenberghe T, Van Poucke L, Fettweis M, Cardoso C, Velez C, Martens M. 2015. Factors influencing top sediment layer and SPM concentration in the Zeebrugge harbor. INTERCOH, 7-11 September, Leuven (Belgium).

Fettweis M, Baeye M, Verney R. 2015. Uncertainty of in situ SPM concentration measurements. INTERCOH, 7-11 September, Leuven (Belgium).

Fettweis M, Baeye M, Francken F, Van den Eynde D, Van Hoestenberghe T, Van Poucke L, Dujardin A, Martens C. 2015. In situ measurements of SPM concentration to evaluate the impact of the disposal of fine grained sediments from maintenance dredging. INTERCOH, 7-11 September, Leuven (Belgium).

Lee BJ, Bi Q, Toorman EA, Fettweis M, Weilbeer H. 2015. Two-Class Flocculation kinetic model: Development and application to large-scale, multi-dimensional cohesive sediment transport. INTERCOH, 7-11 September, Leuven (Belgium).

Thant S, Fettweis M, Baeye M, Monbaliu J. 2015. Wave systems and their impact on the seabed and water column turbidity in the Belgian coastal zone. INTERCOH, 7-11 September, Leuven (Belgium).

Van den Eynde D, Baeye M, Fettweis M, Francken F, Van Lancker V. 2015. Validation of modelled bottom shear stress under the influence of currents and waves using long-term measurements. INTERCOH, 7-11 September, Leuven (Belgium).

Fettweis M, Baeye M. 2015. Seasonality in concentration, size and settling velocity of muddy marine snow in the southern North Sea and their effects on the the sea bed. VLIZ Young Marine Scientists' Day, 20 February, Brugge (Belgium).

Fettweis M, Baeye M. 2015. SPM dynamics at the marine limit of influence of the Westerschelde estuary. Ems-Scheldt workshop, 12-13 February, Delmenhorst (Germany).

Fettweis M, Baeye M, Francken F. 2014. Seasonality of the near bed SPM dynamics in the southern North Sea. PECS, 20-24 October, Porto de Galinhas (Brazil).

Fettweis M, Baeye M. 2014. Variability in concentration, size and settling velocity of muddy marine flocs from the southern North Sea. Particles in Europe, 7-9 October, Esbjerg (Denmark).

Fettweis M, Lee B, Toorman E. 2014. Multimodal particle size distribution of fine-grained cohesive sediments: Observation and simulation. Reactive Transport Workshop, 20 May, Louvain-la-Neuve (Belgium).

Baeye M, Francken F, Fettweis M, Van den Eynde D. 2014. The first buoy for continuous measuring of surface Suspended Particulate Matter concentration on the Belgian inner shelf. VLIZ Young Marine Scientists' Day, 7 March, Brugge (Belgium) (poster).

Fettweis M, Baeye M, Van der Zande, Van den Eynde D, Lee BJ. 2014. Seasonality of nearshore marine snow in the southern North Sea. VLIZ Young Marine Scientists' Day, 7 March, Brugge (Belgium).

Thant S, Baeye M, Fettweis M, Monbaliu J, Van Rooij D. 2014. Extreme values of Suspended Particulate Matter concentration and their relation to wave systems along the Belgian inner shelf. VLIZ Young Marine Scientists' Day, 7 March, Brugge (Belgium).

<u>Publicaties (tijdschriften, hoofdstuk in boeken, proceedings)</u>

Toorman E, Mertens T, Fettweis M, Vanlede J (Eds). 2015. INTERCOH2015. 13th International Conference on Cohesive Sediment Transport Processes. Leuven, Belgium, 7-11 September 2015. Hydraulics Division, Department of Civil Engineering, KU Leuven. VLIZ Special Publication 74 – Flanders Marine Institute (VLIZ). Oostende, Belgium. xii+224pp.

Fettweis M, Baeye M. 2015. Seasonal variation in concentration, size and settling velocity of muddy marine flocs in the benthic boundary layer. Journal of Geophysical Research Oceans, doi: 10.1002/2014JC010644

Van Lancker V, Deronde B, De Vos K, Fettweis M, Houthuys R, Martens C, Mathys M. 2015. Kust en Zee. In: Borremans M. (Ed.) Geologie van Vlaanderen. Academia Press/Genootschap van Gentse Geologen.

Van den Eynde D, Fettweis M**.** 2014. Towards the application of an operational sediment transport model for the optimisation of dredging works in the Belgian coastal zone (southern North Sea). In: Dahlin H., Flemming N.C., Petersson S.E. (Eds.). Sustainable Operational Oceanography, 250-260.

Fettweis M, Baeye M, Van der Zande D, Van den Eynde D, Lee BJ. 2014. Seasonality of floc strength in the southern North Sea. Journal of Geophysical Research Oceans, 119, 1911-1926. doi:10.1002/2013JC09750

Lee BJ, Toorman E, Fettweis M. 2014. Multimodal particle size distribution of fine-grained sediments: Mathematical modeling and field investigations. Ocean Dynamics 64, 429-441. doi: 10.1007/s10236-014-0692-y

<u>Thesis</u>

Nelson M. 2015. Soft sediment dynamics in a high-turbidity environment, Belgian coastal zone. Master thesis in Marine and Lacustrine Science and Management. UA, UGent

and VUB. 38pp+app.
Thant S. 2014. Study on wave systems and their impact on the seabed and water column turbidity in the Belgian coastal zone. Master thesis in Marine and Lacustrine Science and Management. UA, UGent and VUB. 43pp+app.

2. Golfsystemen en hun impact op de zeebodem en de SPM concentratie

In dit hoofdstuk wordt de impact van extreme weersomstandigheden op de resuspensie van fijnkorrelige sedimenten en op het voorkomen van estreem hoge SPM concentraties bestudeerd. Tijdseries van SPM concentratie verzameld te MOW1 gedurende de periode 2005-2013 werden hiervoor gebruikt. Voor de detectie van extreme gebeurtenissen werd gebruik gemaakt van de SPM concentratie afgeleid uit de ADP, terwijl de SPM concentratie afgeleid uit de OBS gebruikt werd voor verdere analyse. Meteorologische en golfdata werden gecombineerd om de impact van golfsystemen bij het voorkomen van extreme SPM concentraties te verklaren.

Extreme SPM concentraties komen voor tijdens twee soorten gebeurtenissen, met name noordwesten- (NW) en zuidwestenstormen (SW). De eerste gebeurtenissen zijn gekenmerkt door golfperioden met een gemiddelde periode van 6 s, die zorgen voor hoge resuspensie en erosie van de zeebodem door de hoge bodemschuifspanningen. SW stormen zijn gekenmerkt door golfperioden van 4 s en genereren een extreme SPM concentratie bijna uitsluitend tijdens doodtij, wanneer de fluffy lag geresuspendeerd wordt. Beide stormtypes hebben enkel een kleine invloed op de langdurige SPM dynamica in de Belgische kustzone en hebben geen significant effect op de langdurig gemiddelde SPM concentratie.

2.1. Introduction

Knowledge on suspended particulate matter (SPM), resuspension, deposition, sediment transport and the origin of high turbidity zones is important for the construction of coastal structures, dredging of navigation channels, sand extraction and dredging and disposal operations (Fettweis and Van den Eynde 2003; Dobrynin et al. 2010). The duration, intensity and frequency of sediment mixing in the water column, for example, may influence the primary production in the marine realm (Chang et al. 2001). Long term suspension of sediments causes attenuation of the available light and inhibits phytoplankton growth (Lawrence et al. 2004; Thompson et al. 2011). Resuspension of bed material may contribute to the redistribution of pollutants in the higher water column (Hakanson 2006). A good understanding of the natural and anthropogenic variation in concentration and behavior of SPM is therefore necessary to develop sustainable exploitation strategies and to assess the human footprint on the marine ecosystem (Fettweis et al. 2010).

Although in general storm events have a significant influence on sediment processes in coastal high turbidity zones, they are not well documented. Pepper and Stone (2004) state that their general models for sediment resuspension and transport during fair-weather and storms will deviate significantly depending on the meteorological conditions, the local geology and bathymetry and the physical character of the currents of the study area. So will a setting in the Mediterranean differ to one along the coastline of the United States (Ferré et al. 2005). According to Green et al. (1995) measurements of suspended sediment concentration and sediment transport during storms are more difficult to acquire since the driving processes causing sediment movement cannot be extrapolated from fair-weather conditions and storm data is rare. The existing studies from the Belgian nearshore area that deal with the wind and storm influence (Baeye et al. 2011; Fettweis et al. 2010) on SPM concentrations remain focused on specific events. Up to now a general study on the role of storm systems and the occurrence of extreme SPM concentrations events is missing. This paper discusses therefore the impact of extreme weather conditions on sediment resuspension and on extreme SPM concentrations in the Belgian Coastal Zone (BCZ) by combining time series of in situ SPM concentration for the period 2005 - 2013, and of meteorological and wave data for the same period in order to distinguish different extreme weather/wave conditions and their effect on extreme SPM concentration. The scope of this paper is to investigate both the cause and consequences of events in extreme SPM concentration. Study area characteristics, such as sediment type, local bathymetry and sediment supply are accounted for. Characteristics of storm types, coinciding with external features such as tides, spring-neap cycles and currents are used to quantify variations and patterns in resuspension and erosion of the bed. Consequently, the full overlying water column is considered when looking at an event with increased SPM concentration. Furthermore, a quantitative estimation of the impact of extreme weather conditions on the sediment processes in the navigation channels is presented.

2.2. Study area

The study area covers the Belgian coastal zone situated in the southern Bight of the North Sea. The relatively well protected Southern Bight is mainly tidal dominated as compared with other shallow areas in the North Sea where wave influences are more pronounced (Fettweis et al. 2012). Southwesterly winds dominate the overall wind climate, followed by winds from the NE sector (Héquette et al. 2008; Fettweis et al. 2010; Pietrzak et al. 2011). Although the maximum wind speeds coincide with the southwesterly winds, the largest waves are generated under the influence of northwesterly winds (Baeye et al. 2011). Wind sea, is the dominant wave system in the coastal zone (62.9%) while combined systems of wind sea and fresh or matured swell account for 13% and 11.2% respectively. Sole swell and multiple wave systems are less represented (Boukhanovsky et al. 2007). The Belgian coastal zone has a semi-diurnal tidal regime, often characterized by tidal asymmetry. These tidal currents and the residual water transport are directed northeast. The average tidal range at Zeebrugge for spring - neap tide amounts 4.3 and 2.3m respectively. The salinity is generally between 28 and 34; changes in salinity are caused by the advection of marine and Scheldt water masses (Arndt et al. 2011). The residual alongshore currents at MOW1 are in 80% of the time directed towards the SW (i.e. in ebb direction) and salinity is then around 30 psu. During the prevailing SW wind salinity may increase up to 34 and marine water with generally lower SPM concentration enters the area; the residual alongshore current is then directed towards the NE. SW-NE direction corresponds with the alignment of the coastline.

Depths in the nearshore zone range between 0 - 20 m with an exception for the mouth of the Westerschelde where depths can surpass this 20 m. The depth at measuring station MOW1 is about 9 m MLLWS. The MOW1 measuring site is situated in a coastal turbidity maximum area with SPM concentrations between 0.02 and more than 0.1 g/l at the surface and between 0.1 and more than 3 g/l near the bed; lower values (<0.01 g/l) occur offshore (Baeye et al. 2011; Fettweis et al. 2012). The SPM concentration, floc size, and settling velocity have a distinct seasonal signal (Fettweis and Baeye 2015). An acoustic detection method using ADV and ADP altimetry revealed bed boundary level changes up to 0.2 m in the nearshore area during tidal and spring-neap cycles suggesting the occurrence of lutoclines, and possibly of fluid mud layers (Baeye et al. 2012). The occurrences of brownish colored fluffy layers have frequently been observed in Van Veen grab and box core samples taken at the measuring site.

The seabed is dominated by fine to medium Quaternary sandy deposits whereby nearshore deposits contain a variable concentration of mud (Lanckneus et al. 2001; Fettweis and Van den Eynde 2003; Mathys 2009). In the eastern part of the Belgian continental shelf (nearshore area) cohesive sediments, such as mud and clay, with different consolidation state occur, ranging from Eocene clay to Holocene and freshly deposited mud. The latter one occurs as thin fluffy layers or as thicker, more consolidated soft mud layers. Their presence is mainly restricted to the area around dumping sites, navigation channels and harbors, which are efficient sediment sinks. The Holocene, medium consolidated muds, are characterized by intercalations of thin sandy horizons (Fettweis et al. 2010). The SPM samples have the same mineralogical signature as these Holocene muds (Adriaens 2015).

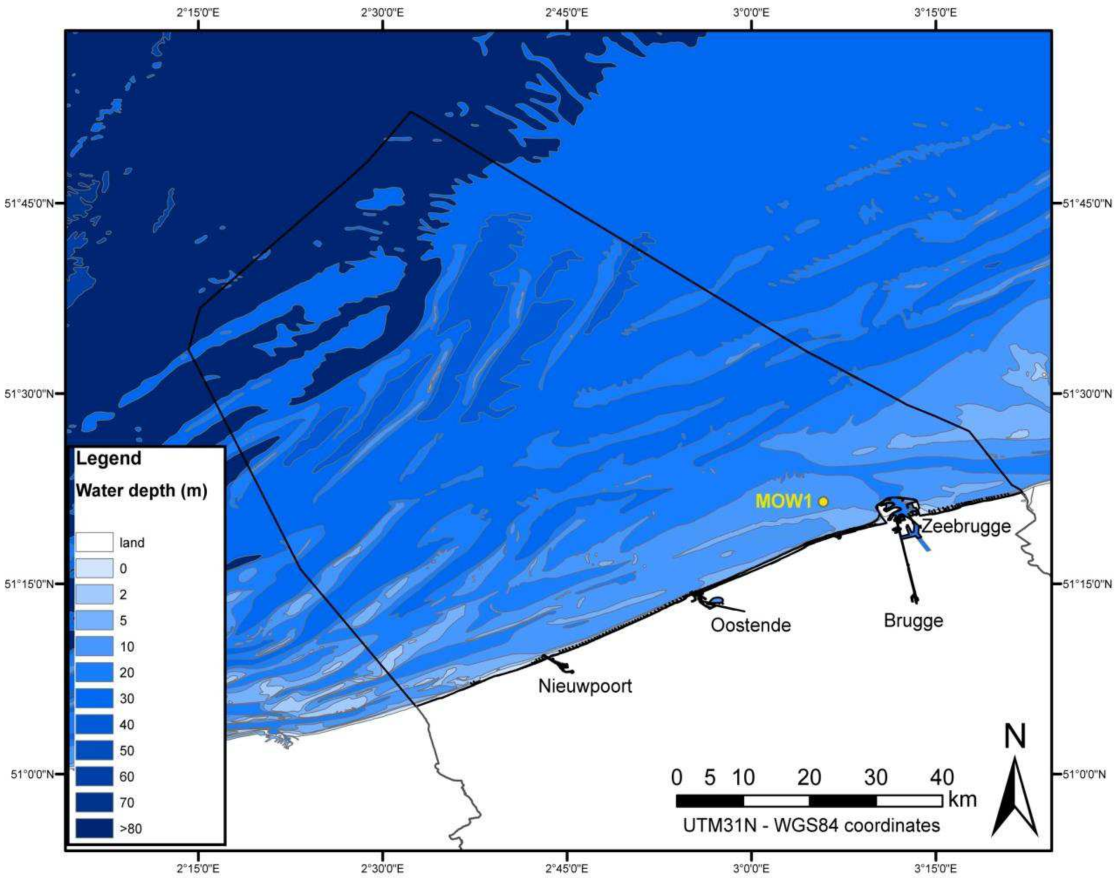

Figure 2.1: Belgian coastal zone with indication of the measuring station MOW1.

2.3. Methodology

2.3.1. SPM Concentration from optic and acoustic sensors

Time series of SPM concentration and other oceanographic parameters have been collected at the measuring site MOW1 (51.358°N and 3.098°E), west of Zeebrugge (Figure 2.1). Current velocity, salinity, SPM concentration and altimetry were collected with tripods. The instrumentation suite consisted amongst others of a downward looking ADP profiler (3 MHz SonTek Acoustic Doppler Profiler), two D&A optical backscatter point sensors (OBS3+) and a Sea-bird SBE37 CT. The data were collected in bursts every 10 or 15 min for the OBS while the ADP was set to record a profile every 1 min. The OBS's were mounted at 0.2 and 2.3 m above bed (mab), see Figure 2. The tripods were moored between 3 and 6 weeks and then replaced with similar tripod systems to ensure continuous time series. The SPM concentration was derived from optical (OBS) and acoustical instruments (ADP). The ADP profilers were attached at 2.3 mab and down-looking, measuring current and acoustic intensity profiles with a bin resolution of 0.25 m starting at 1.8 mab (Figure 2.2). The backscattered acoustic signal strength, from ADP, was used to estimate SPM concentrations. After conversion to decibels, the signal strength was corrected for geometric spreading, and water and sediment attenuation (Thorne and Hanes 2002). The upper OBS-derived SPM concentration estimates were used to calibrate the ADP's first bin. The different sensitivity of acoustic and optic sensors to changes in the SPM particle size and characteristic is reflected in the correlation coefficient between the ADP backscatter (in dB) and the OBS-derived SPM concentration of R^2=0.53. The R^2 is better for the lower SPM concentrations and the regression model thus accounts for less variance for the higher SPM concentrations.

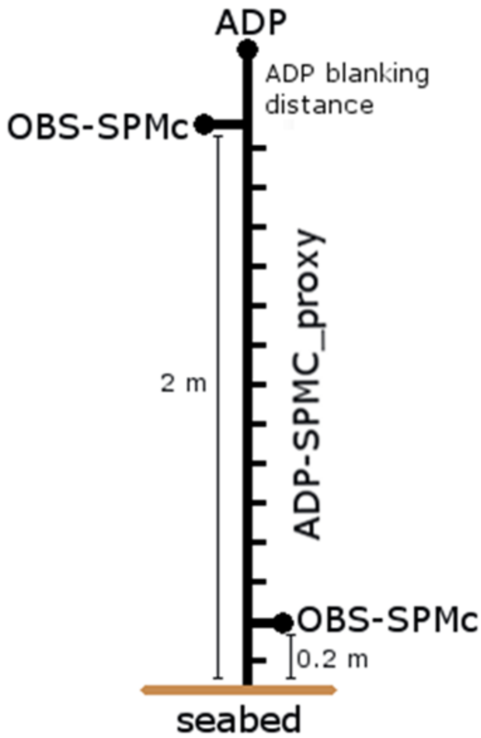

Figure 2.2: Schematic overview of the positioning of the ADP and OBS sensors above the seabed.

The result is a proxy for the evolution of SPM concentration near the seabed (Figure 2.3). In order to highlight strong anomalous SPM concentrations over the whole near-bed profile, the ADP derived SPM concentration proxy distribution was low-passed filtered and by using peak detection these extreme events were focused on (Figure 2.2). Typically, the signal over a period of 14 days (1 spring tide and 1 neap tide) was low-passed filtered, with a moving window to detect anomalous peaks in the signal. The detected peaks are not necessarily corresponding with the maxima in the low-pass filtered signal, but with a short term increase that pops up from the neap-spring signal (Figure 2.3).

The OBS voltage readings were converted into NTU using Amco clear turbidity standards and then into SPM mass concentration (g/l) by calibration against filtered water samples collected during four tidal cycles a year. A linear regression was used to fit a straight line between the OBS signal (in NTU) and the filtered SPM concentration (in g/l). The regression coefficient (R^2) is generally higher than 0.90; the uncertainty on the OBS derived SPM concentrations was estimated as 10% (Fettweis, 2008). The stability of the OBS was further controlled by calibrating them against Amco clear solution about once a year. Uncertainties of the OBS's arose also due to the measuring range that what set to 1.5 or 3 g/l depending on the sensor. During high energy conditions, near bed SPM concentrations at MOW1 were regularly higher than 1.5 or 3 g/l. Under these circumstances the OBS saturated and underestimated the actual SPM concentration. The ADP derived SPM concentration time series was used to identify periods with anomalous SPM concentrations, as the time series from this instruments are more continuous and without saturated peaks. Because of the higher accuracy of the OBS derived SPM concentration the analysis was based on the latter by selecting the period that correspond to the peak of the event ± 1 day (Figure 2.3). By doing so each event corresponds to about 4 to 5 tidal cycles that were then ensemble averaged.

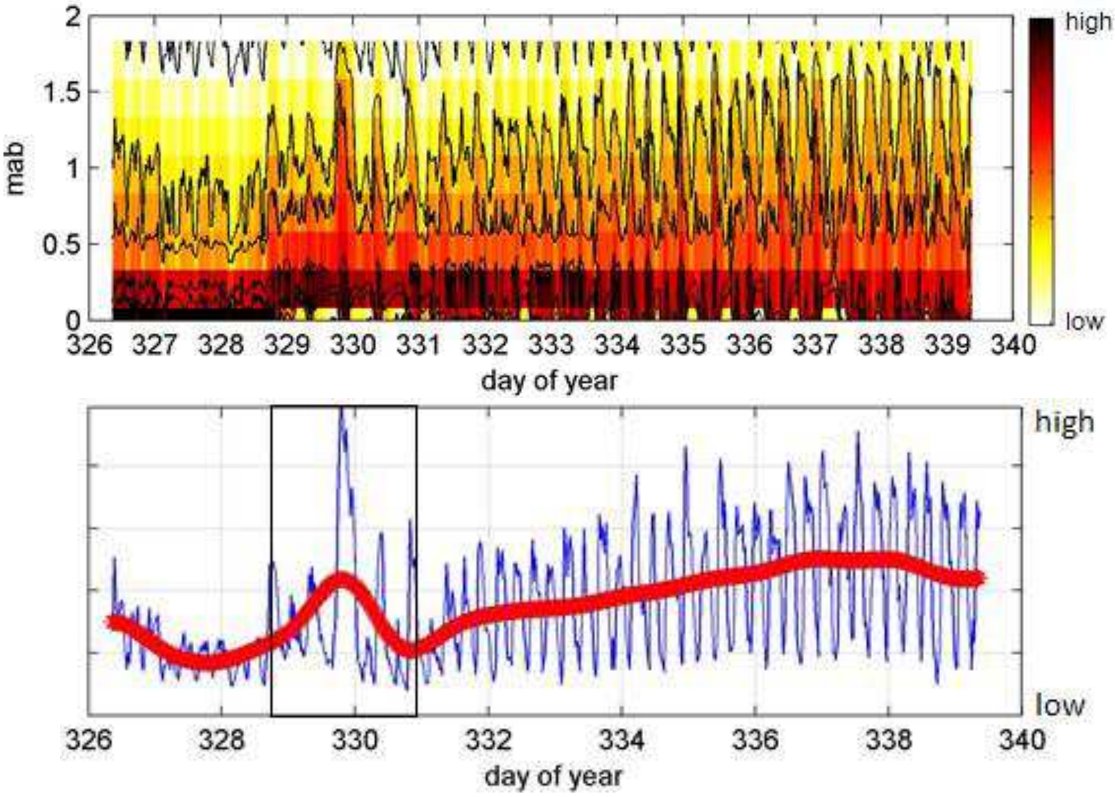

Figure 3.3: (above) ADP backscatter data as a proxy for SPM concentration near the sea-bed (down) Peak detection of events of extreme SPM concentration.

2.3.2. Wave data

Wave rider buoys measure the wave spectra from which the wave height, period and E10 were derived. E10 is used as a proxy for longer-than-average waves. E10 is derived from the wave energy spectra, taking into account all energy within all waves with a period larger than 10 s. The wave orbital velocity and wave induced shear stress were calculated using the following:

$$Ub = \pi H / T \sinh(kh)$$

where H is the wave height, T the wave period, h the total water depth and k the wave-number defined as k = 2π/L, L representing the wave length (Soulsby 1997). The shear stress induced by waves was calculated by (Soulsby 1997):

$$\tau w = ½ * \rho w * fw * Ub^2$$

2.4. Results

2.4.1. Meteorological conditions during the event

The extreme SPM concentration events captured in the ADP derived SPM concentrations have been classified into two groups (Table 2.1). The first group consist of 10 events that are characterised by Southwestern storms (SW storms), a common weather system characterised by low pressure (LP) above the British Isles. The second group are Nortwestern storms (NW storms) that are less common and only occurring in winter (October to March), when a strong LP is situated above central Europe, during which streamlines are south directed on the western side of the LP-cyclone. This case concerns 11 events.

Table 2.1: Occurrence and duration of detected events of extreme SPM concentrations, classified by causing storm type (NW storms and SW storms).

Type	Beginning of storm event		End of storm event	
SW storm	20/05/2006	10:00	21/05/2006	5:00
SW storm	11/01/2007	5:00	12/01/2007	8:00
SW storm	23/11/2009	10:45	24/11/2009	9:00
SW storm	25/12/2009	5:00	26/12/2009	2:00
SW storm	26/05/2011	5:00	27/05/2011	12:00
SW storm	18/10/2011	2:00	19/10/2011	16:00
SW storm	16/07/2012	14:00	17/07/2012	8:00
SW storm	17/04/2013	22:00	19/04/2013	2:00
SW storm	13/10/2013	0:30	13/10/2013	22:00
SW storm	28/10/2013	0:45	29/10/2013	1:00
NW storm	24/11/2005	20:00	26/11/2005	2:00
NW storm	8/11/2007	23:00	10/11/2007	4:00
NW storm	21/11/2008	8:00	23/11/2008	0:00
NW storm	12/10/2009	2:00	12/10/2009	12:00
NW storm	16/10/2009	12:00	17/10/2009	14:00
NW storm	30/11/2009	20:00	1/12/2009	6:00
NW storm	23/12/2010	16:00	24/12/2010	8:00
NW storm	5/01/2012	12:00	6/01/2012	16:00
NW storm	10/09/2013	19:00	11/09/2013	6:00
NW storm	10/10/2013	13:00	11/10/2013	6:00
NW storm	5/12/2013	12:00	7/12/2013	8:00

Southwestern storms are typically characterised by 1.5 m waves with mean wave periods of 4.3 s. The E10 energy amounts on average 30 cm² s. NW storms can easily be recognised by their correspondence to mean wave periods of 6s, whereas on average wave periods vary around 3.7 s (Table 2.2). Low frequency wave energy is significantly higher during these storm events, resulting in median and mean E10 values of respectively 880 cm² s and 1050 cm² s. The average duration of a NW storm is about 24 hours with higher variations ranging between less than 12 hours and up to almost 48 hours. In contrast, SW storms have a duration that is in general about 24 hours. Extreme SPM concentration events in the time series associated with NW storm occurred during neap (4 times) and spring tide (7 times), while those associated with SW events only occurred during lower tidal ranges (around neap tide conditions).

In order to compare these two groups of extreme SPM concentration events with other situations, further groups have been defined. Because most of the extreme events occur during winter the selection has been limited to the winter period (October to March), the following groups have been defined:

- NW Storm (SPM): all periods with extreme SPM concentration during NW storms;
- NW Storm (meteo): all periods with Hs>1.25m and wave period > 5s, including those that are not necessarily having an extreme SPM concentration event;
- SW Storm (SPM): all periods with extreme SPM concentration during SW storms;
- SW Storm (meteo): all periods with Hs>1.25m and wave period < 5s, including those that are not necessarily having an extreme SPM concentration event;
- Winter (no NW and SW storm): winter SPM concentration during periods with Hs < 1.25m;
- Winter: all data from October until March.

Table 2.2: Mean and median values for significant wave height (Hs), period (T) and wave energy from waves with period larger than 10s (E10) for whole the period of 2005 – 2013, and the NW events and SW events with extreme SPM concentrations.

	Hs (m)		T (s)		E10 (cm² s)	
	mean	median	mean	median	mean	median
2005-2013	0.8	0.68	3.74	3.66	19.5	3.5
NW events	2.65	2.67	5.96	6	1054.0	878.3
SW events	1.52	1.46	4.32	4.35	32.4	14.2

2.4.2. Wave induced shear stress

Figure 2.4 indicates the higher induced shear stresses during NW storm events (up to 26 Pa) compared to SW storm events (up to 4 Pa). These higher shear stresses are caused by the high wave orbital velocities, which are due to significantly enhanced wave heights and longer wave periods. For both storm types, shear stress declines with water depth, however, it can be observed that at water depths of 18 m (e.g. as occurring in the navigation channel towards the harbour of Zeebrugge, Pas van het Zand) shear stresses during SW storms are reduced to zero whereas NW storm events still retain shear stresses of 4-5 Pascal, more than the maximum shear stress reached during SW storm events.

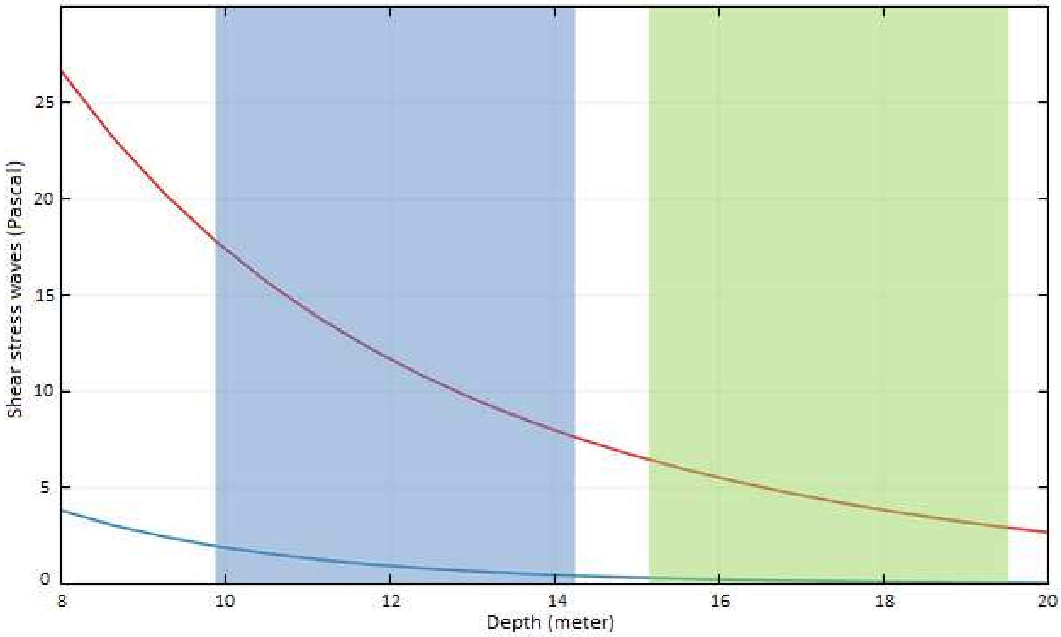

Figure 2.4: Shear stresses calculated during Northwestern storms (red) and Southwestern storms (blue) as a function of water depths. Water depths highlighted in blue and green indicate respectively the water depths representative for MOW1 and Pas van het Zand.

2.4.3. OBS derived SPM concentration

The OBS derived SPM concentrations show a different behaviour during SW and NW storm events. At 0.2 mab SPM concentrations are in both cases significantly increased (although higher during NW storm than SW storm conditions) in comparison with normal conditions (Figure 5). At 2 mab, during NW storms, SPM concentrations are still higher than during normal conditions. However, during SW storms the observed increase in SPM concentration at 0.2 mab is not visible at 2 mab (Figure 2.5).

Figure 2.5 indicates that the highest SPM concentrations occur around 1.5 hour before low water (LW) and a smaller peak at 1 hour before and after high water (HW). On average a maximum of 0.62 g/l and 0.37 g/l are observed at respectively 0.2 and 2.0 mab. During NW storms peaks of on average 0.7 g/l (0.2 mab) and 0.4 (2 mab) are monitored. During extreme NW-SPM storm events SPM concentrations close to the bottom can increase up to > 1 g/l. SW storm SPM concentrations vary around 0.55 g/l and 0.25 g/l at 0.2 mab and 2.0 mab respectively. It can be clearly observed that at both heights above the bed SPM concentrations are always higher under NW storm events compared to SW storm events.

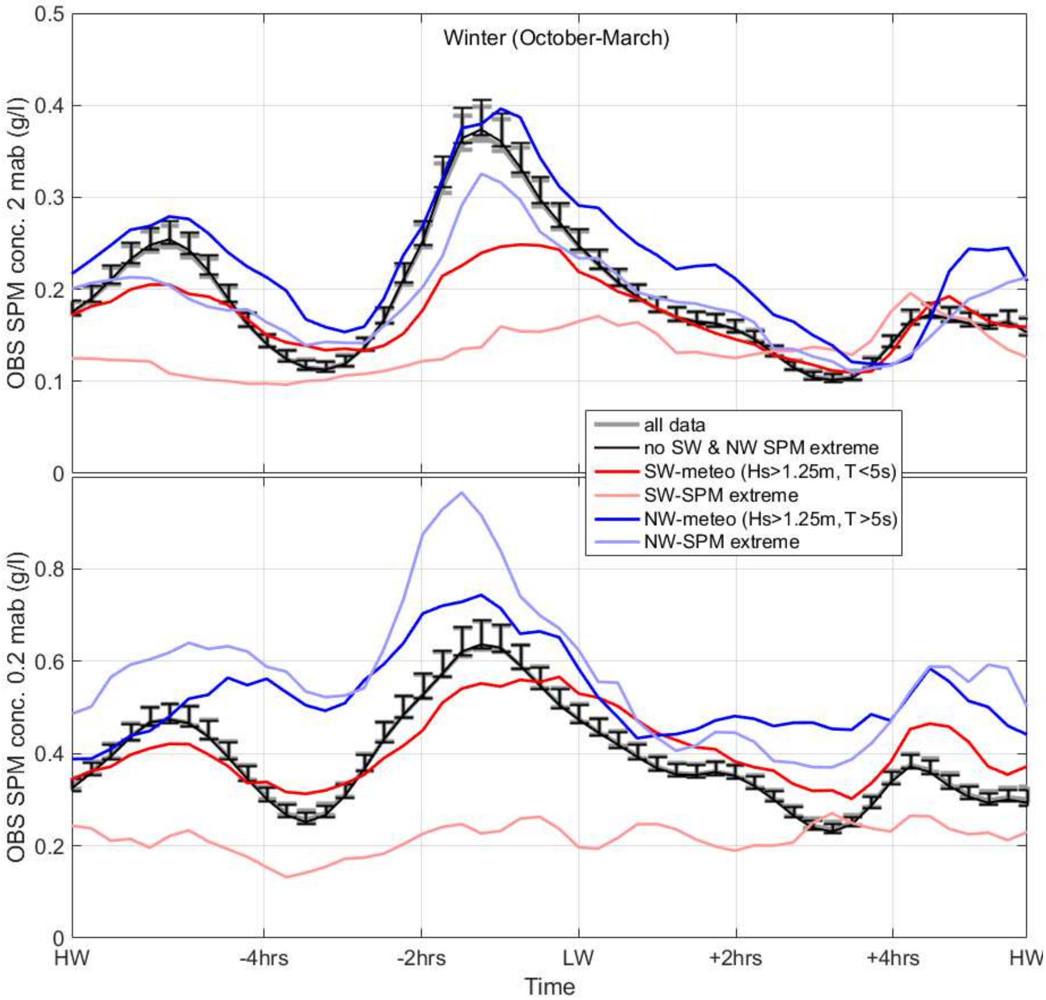

Figure 2.5: Ensemble averaged OBS-SPM concentration (g/l) at 0.2 and 2.0 mab during different conditions. Indication of SPM concentrations during SW events (red), NW events (blue), winter (all data) (grey) and winter excluding the detected storm events (black) for the winter period (October – March).

2.5. Discussion

2.5.1. Frequency of long period Northwestern waves

E10 values >250 cm² s are always associated with NW storm events, and are occurring only 1% of the time. They were not recorded during summer months. The 11 observed events occur all between September and January. The models of Dobrynin et al. (2010) already indicated 2 patterns in SPM dynamics in the North Sea. The first pattern is observed during calm conditions in the summer months (15 April – 15 October) when SPM dynamics are predominantly defined by currents, the second in the period 15 October – 15 April when SPM dynamics and vertical mixing are determined by wave action and high energetic values during storms. The 11 NW-SPM events detected fit this second pattern type of SPM dynamics.

2.5.2. Relevance of the NW waves regarding the SW-stormy turbidity

events

As mentioned earlier, all SW storm events of increased SPM concentrations that were detected as extreme events occurred during or near to neap tide. This makes the effect of a storm to be more pronounced as hydrodynamic conditions are then reduced. During neap tide, SPM has a higher probability to be deposited on the bed leading to the formation of a fluffy layer. The SPM concentration during these periods is lower than during tides with larger tidal range. SW storms occurring during/directly after neap tide will stir up the fluffy layer, leading to a sudden and significant increase in SPM concentration. The change and peak in SPM concentration will be more significant and higher compared to other SW storm events, taking place for example around spring tide. The latter missing the presence of a thick fluffy layer, having instead a high SPM concentration background caused by the stronger hydrodynamics, leading the event to be less pronounced (Fettweis et al. 2010). Because of this, SW storm events will often barely be noticed in the SPM concentration signal.

As SW storm events are almost only detected if coinciding with neap tide, NW storm events are not limited to a specific tidal range condition. Wave orbital velocities and induced shear stresses are in these cases high enough to cause large sediment resuspension at all times. The effect of the storm on the SPM concentration is significantly pronounced compared to background values. Spring-tide can however enhance the strength and the impact of the storm significantly (even though the absence of a fluffy layer) for both SW and NW storms. As Bartholomä et al. (2009) discussed, the duration and the impact intensity of a storm event are highly dependent on the way wind/wave direction and tidal phase interact. However, it can be concluded from Figure 2.5 that both storm events only play a minor role on the overall SPM dynamics at the Belgian Coastal Zone. The extreme events are hardly visible in the averaged signal (all data vs no SW and NW SPM extreme) and it is the tidal range and seasonal variation determining the general SPM dynamics. The effects of extreme energy events (storms) can, during the storm, overprint these periodic variations in SPM and the sediment budget can be changed temporarily or even permanently (Bartholomä et al. 2009). The impact of severe storms at the Belgian Coastal Zone is however not sufficient to cause permanent changes in the sediment budget.

Bartholomä et al. (2009), Ulses et al. (2008) and Dufois et al. (2014) indicate the important impact of storm events in the German Wadden Sea and the Rhone River prodelta. Bartholomä et al. (2099) highlighted the importance of storm “Britta” (November 2006), causing seriously increased SPM concentrations and a large export of sediment towards the North Sea. In the study of Dufois et al. (2014) 2 extreme storm events were discussed, each causing an export of 2.1Mt of sediment out of the prodelta area. The 2 winter storms analyzed by Ulses et al. (2008) caused a serious resuspension of shelf sediment and the export of sediment was estimated on 9.1Mt (Gulf of Lions). They found, 41% and 26% of the total sediment export was caused by the winter storms of respectively December 2003 and February 2004. These reported impacts are far stronger than the effects on SPM concentration observed during our 11 NW and 10 SW storm events (again illustrated by figure 5). This is further confirmed by Ferré et al. (2005) who observed a tenfold increase in SPM concentration during storms compared to “calm” conditions, which is far more enhanced then the increases detected in our SW and NW events.

2.5.3. Erosive behaviour of different mud layers

The SPM concentrations encountered during a storm event are strongly depending on meteorological conditions such as wind direction and the availability of erodible sediments in the area (coastal zone). This causes the impact of every storm to be different, depending on its meteorological and sedimentological history. According to Fettweis et al. (2010), the critical erosion threshold (τ_{ce}) of the top layer (fluffy layer) of sediments in the study area varies between 0.5 and 2.5 Pa. For the Holocene mud layers τ_{ce} increases up to 13 Pa. The generated shear stresses of up to 26 Pa during a NW storm event will thus cause full resuspension of the fluffy layer and a serious erosion of the Holocene mud. These high shear stresses originate from the high wave heights and long periods that could build up because of the large fetch of the Northwestern winds (North Sea). Waves during a SW storm are lower and have a smaller period (limited fetch, winds coming from the English Channel), leading to the mentioned shear stresses of 4 Pa. The SW storm event will be able to bring the material of the fluffy layer into suspension, but will not erode the bed itself, even in combination with induced shear stresses of tidal currents (which on itself can also not erode the bed). NW storms will thus have a stronger impact on SPM concentration (Figure 5).

This difference in resuspension/erosion capacity between the 2 storms is supported by the study of Sheremet et al. (2005), the latter mentioning a deficit of short motion waves to cause resuspension and declaring long waves to be responsible for higher turbulences and thus resuspension. In our case short waves (SW storm events) still cause resuspension of the fluffy layer, this can be due to e.g. different bathymetric settings. The overall pattern of short waves (SW) to be less energetic than long waves (NW), causing by consequence less resuspension, however remains. As mentioned before, storms characterized by similar physical properties such as wave height, period and induced shear stresses can have different impact intensity due to changes in the sediment composition, earlier meteorological/seabed conditions or different biological community compositions (Palinkas et al. 2010). Ferré et al. (2005) also mention 2 phases of SPM concentration during a storm : in the beginning of the storm (e.g. first 2 hours) there is a resuspension of finer particles of the local sediment (this would be the case during both SW and NW events), in the second phase there is also bed armouring, enhancing SPM concentrations even more (in this case this would only occur under NW storm conditions).

2.5.4. Spatial impact of longer-period-than-average waves

The sediments in the navigation channels (Scheur, Pas van het Zand) consist of thick layers (45 cm) of freshly deposited mud above slightly consolidated mud (Fettweis et al. 2010). The critical erosion shear stress of the upper layer for these sediments is 1 - 4 Pa and for the lower part more than 4 Pa. The shear stresses of NW storms varying around 6 Pa at 15 m depth are still high enough to cause resuspension of the freshly deposited mud and erosion of the slightly consolidated mud layer. Contrary, SW storms have no effect on sediment resuspension in the navigation channels (shear stress equals zero). Aside during NW storm events the slightly consolidated mud layer will only be entrained during e.g. dredging maintenance works.

Fettweis et al. (2010) concluded that navigation channels are a major source of fine-grained sediments during storms. This indicates that the very high SPM concentrations during storms originate from the fine-grained material that is deposing in the deepened areas or that accumulates on some disposal sites. The measuring site is situated at the marine limit of the Western Scheldt estuary. Deepening of the navigation channels leads to increases in up-estuary sediment transport and increased SPM concentrations. The deepening of the Ems river has led to higher sediment loads, e.g. higher SPM concentrations, in the river because of the higher up-river sediment transport that is induced by a gravitational and enhanced salinity circulation and a decreased river flushing. This research was aside the Ems also conducted for e.g. the Elbe and Loire. Enhanced siltation rates additionally increase the SPM concentrations (Winterwerp 2011; Winterwerp et al. 2013; van Maren et al. 2015). Also new sources of SPM material can be created when re-moving normally non-erodible layers during maintenance works, then acting as a new source of sediment materials that can be suspended during storm activity (de Jonge et al. 2014). Also Stanev et al. (2009) highlight the importance of fine grained sediment availability, as they observed that at the Dogger Bank high shear stresses coincided with low SPM concentrations, leading to the conclusion of a deficit in fine grained material in this area. For the Belgian coast it are the increased SPM concentrations due to channel deepening, the sediment input through the Strait of Dover, the local erosion of Holocene mud deposits and the shallowness of the area that cause high siltation rates and the turbidity maximum in front of Zeebrugge (Fettweis and Van den Eynde 2003). All this available fine grained sediment will then be entrained into suspension during the SW and NW storm events.

2.6. Conclusions

Extreme events in SPM concentration near the seabed and in the water column were investigated for the Belgian coastal zone. Events were detected by ADP-SPM concentration data, while OBS-SPM concentrations were used for further analysis. SPM concentration data was obtained at the measuring station MOW1, together with the corresponding meteorological data and wave data. Events of extreme SPM concentrations were classified in 2 groups: Northwestern storm events and Southwestern storm events.

Northwestern storms are recognised by their correspondence to mean wave periods of 6s. They generate shear stresses of up to 26 Pa in shallow areas, causing a full resuspension of the fluffy layer and a serious erosion of the Holocene mud layer. At 15m depth shear stresses are still high enough (6 Pa) to cause resuspension of the freshly deposited mud and erosion of the slightly consolidated mud layer in the navigation channels. These NW storm events are rare, occurring only 1% of the time, only recorded during winter months.

Southwestern storm events will be able to bring material of the fluffy layer into suspension (generated shear stresses up to 4 Pa), but will not erode the bed itself. Furthermore they have no effect on sediment resuspension in the navigation channels (shear stress equals zero). SW storm events are almost only detected if coinciding with neap tide, most of the time they are obscured by the effects of tidal range. NW storm events are not limited to a specific tidal range condition and are always clearly visible against the background values.

In general NW storms have a stronger impact on SPM concentration than SW storms. Especially close to the bottom the impact is very pronounced. However, both storm type events only play a minor role in long-term SPM dynamics at the Belgian Coastal Zone and have no significant effect on long-term SPM concentrations. The extreme SPM events are hardly visible in the averaged SPM signal and it is the tidal range and seasonal variation determining the general SPM dynamics. Effects of extreme energy events (storms) can, during the storm, overprint these periodic variations in SPM but will not cause permanent changes in the sediment budget.

3. Referenties

Adriaens R. 2015. Neogene and Quaternary clay minerals in the southern North sea. PhD thesis. KULeuven, pp 272.

Arndt S, Lacroix G, Gypens N, Regnier P, Lancelot C. 2011. Nutrient dynamics and phyto-plankton development along an estuary coastal zone continuum: A model study. Journal of Marine Systems, 84, 49-66.

Baeye M, Fettweis M, Voulgaris G, Van Lancker V. 2011. Sediment mobility in response to tidal and wind-driven flows along the Belgian inner shelf, southern North Sea. Ocean Dynamics, 61, 611-622.

Baeye M, Fettweis M, Legrand S, Dupont Y, Van Lancker V. 2012. Mine burial in the seabed of high-turbidity area: Findings of a first experiment. Continental Shelf Research, 43, 107-119.

Bartholomä A, Kubicki A, Badewien TH, Flemming BW. 2009. Suspended sediment transport in the German Wadden Sea: seasonal variations and extreme events. Ocean Dynamics, 59, 213-225.

Boukhanovsky AV, Lopatoukhin LJ, Soares CG. 20070 Spectral wave climate of the North Sea. Applied Ocean Research, 29 146-154.

Chang GC, Dickey TD, Williams AJ. 2001. Sediment resuspension over a continental shelf during Hurricanes Edouard and Hortense. Journal of Geophysical Research, 106, 9517-9531.

Chen MS, Wartel S, Van Eck BTM, van Maldegem D. 2005. Suspended matter in the Scheldt estuary. Hydrobiologia, 540, 79-104.

de Jonge VN, Schuttelaars HM, van Beusekom JEE, Talke SA, de Swart HE. 2014. The influence of channel deepening on estuarine turbidity levels and dynamics, as exemplified by the Ems estuary. Estuarine, Coastal and Shelf Science, 139, 46-59.

Dobrynin M, Gayer G, Pleskachevsky A, Günther H. 2010. Effect of waves and currents on the dynamics and seasonal variations of suspended particulate matter in the North Sea. Journal of Marine Systems, 82, 1-20.

Dufois F, Verney R, Le Hir P, Dumas F, Charmasson S. 2014. Impact of winter storms on sediment erosion in the Rhone River prodelta and fate of sediment in the Gulf of Lions (North Western Mediterranean Sea). Continental Shelf Research, 72, 57-72.

Fettweis M, Van den Eynde D. 2003. The mud deposits and the high turbidity in the Belgian–Dutch coastal zone, southern bight of the North Sea. Continental Shelf Research, 23, 669-691.

Fettweis M. 2008. Uncertainty of excess density and settling velocity of mud flocs derived from in situ measurements. Estuarine, Coastal and Shelf Science, 78, 426-436.

Fettweis M, Francken F, Van den Eynde D, Verwaest T, Janssens J, Van Lancker V. 2010. Storm influence on SPM concentrations in a coastal turbidity maximum area with high anthropogenic impact (southern North Sea). Continental Shelf Research, 30, 1417-1427.

Fettweis M, Monbaliu J, Baeye M, Nechad B, Van den Eynde D. 2012. Weather and climate induced spatial variability of surface suspended particulate matter concentration in the North Sea and the English Channel. Methods in Oceanography, 3-4, 25-39.

Fettweis M, Baeye M. 2015. Seasonal variation in concentration, size and settling velocity of muddy marine flocs in the benthic boundary layer. Journal of Geophysical Research, 120, 5648-5667.

Ferré B, Guizien K, de Madron X.D, Palanques A, Guillén J, Grémare A. 2005. Fine-grained sediment dynamics during a strong storm event in the inner-shelf of the Gulf of Lion (NW Mediterranean). Continental Shelf Research, 25, 2410-2427.

Green MO, Vincent CE, McCave IN, Dickson RR, Rees JM, Pearson ND. 1995. Storm sediment transport - observations from the british north-sea shelf. Continental Shelf Research, 15, 889-912.

Hakanson L. 2006. Suspended Particulate Matter in Lakes, Rivers and Marine Systems. The Blackburn Press, New Jersey.

Héquette A, Hemdane Y, Anthony EJ. 2008. Sediment transport under wave and current combined flows on a tide-dominated shoreface, northern coast of France. Marine Ge-

ology, 249, 226-242.
Lanckneus J, Van Lancker V, Moerkerke G, Van den Eynde D, Fettweis M, De Batist M, Jacobs P (2001) Investigation of the natural sand transport on the Belgian Continental shelf: BUDGET. Final Report. Federal Office for Scientific, Technical and Cultural Affairs (OSTC), pp 104
Lauwaert B, Fettweis M, Cooreman K, Hillewaert H, Moulaert I, Raemaekers M, Mergaert K, De Brauwer D. 2004. Syntheserapport over de effecten op het mariene milieu van baggerspeciestortingen. BMM, DVZ & aMT rapport, BL/2004/01, 52pp.
Lauwaert B, De Brauwer D, Fettweis M, Hillewaert H, Hostens K, Mergaert K, Moulaert I, Parmentier K, Verstraeten J. 2006. Syntheserapport over de effecten op het mariene milieu van baggerspeciestortingen (vergunningsperiode 2004-2006). BMM, ILVO & aMT rapport, BL/2006/01, 87pp.
Lauwaert B, Bekaert K, Berteloot M, De Brauwer D, Fettweis M, Hillewaert H, Hoffman S, Hostens K, Mergaert K, Moulaert I, Parmentier K, Vanhoey G, Verstraeten J. 2008. Syntheserapport over de effecten op het mariene milieu van baggerspeciestortingen (vergunningsperiode 2006-2008). BMM, ILVO, aK & aMT rapport, BL/2008/01, 128pp.
Lauwaert B, Bekaert K, Berteloot M, De Backer A, Derweduwen J, Dujardin A, Fettweis M, Hillewaert H, Hoffman S, Hostens K, Ides S, Janssens J, Martens C, Michielsen T, Parmentier K, Van Hoey G, Verwaest T. 2009a. Synthesis report on the effects of dredged material disposal on the marine environment (licensing period 2008-2009) Report by MUMM, ILVO, CD, aMT & WL, BL/2009/01. 73pp.
Lauwaert B, Bekaert K, Berteloot M, De Backer A, Derweduwen J, Dujardin A, Fettweis M, Hillewaert H, Hoffman S, Hostens K, Ides S, Janssens J, Martens C, Michielsen T, Parmentier K, Van Hoey G, Verwaest T. 2009b. Syntheserapport over de effecten op het mariene milieu van baggerspeciestortingen (vergunningsperiode 2008-2009). Rapport uitgevoerd door BMM, ILVO, CD, aMT & WL, BL/2009/01. 18pp.
Lauwaert B, Delgado R, Derweduwen J, Devriese L, Fettweis M, Hostens K, Janssens J, Robbens J, Timmermans S, Van Hoey G, Verwaest T. 2011a. Synthesis report on the effects of dredged material disposal on the marine environment (licensing period 2010-2011). Report by MUMM, ILVO, CD, aMT & WL, BL/2011/12, 85pp.
Lauwaert B, Delgado R, Derweduwen J, Devriese L, Fettweis M, Hostens K, Janssens J, Robbens J, Timmermans S, Van Hoey G, Verwaest T. 2011b. Synthese rapport over de effecten op het mariene milieu van baggerspeciestortingen (vergunningsperiode 2010-2011). Rapport uitgevoerd BMM, ILVO, CD, aMT & WL, BL/2011/12, 16pp.
Lauwaert B, Fettweis M, De Witte B, Van Hoey G, Timmermans S, Martens C. 2014. Vooruitgangsrapport (januari 2012 – juni 2014) over de effecten op het mariene milieu van baggerspeciestortingen. Rapport door KBIN-BMM, ILVO, CD & aMT, BL/2014/01, 21pp.
Lawrence D, Dagg MJ, Liu H, Cummings SR, Ortner PB, Kelble C. 2004. Wind events and benthic–pelagic coupling in a shallow subtropical bay in Florida. Marine Ecology Progress Series, 266, 1–13.
Mathys M. 2009. The Quaternary geological evolution of the Belgian Continental Shelf, southern North Sea. PhD thesis. Gent University, 382pp.
Palinkas CM, Ogston AS, Nittrouer CA. 2010. Observations of event-scale sedimentary dynamics with an instrumented bottom boundary-layer tripod. Marine Geology, 274, 151-164.
Pepper DA, Stone GW. 2004. Hydrodynamic and sedimentary responses to two contrasting winter storms on the inner shelf of the northern Gulf of Mexico. Marine Geology, 210, 43-62.
Pietrzak JD, de Boer GJ, Eleveld MA. 2011. Mechanisms controlling the intra-annual mesoscale variability of SST and SPM in the southern North Sea. Continental Shelf Research, 31, 594-610.
Sheremet A, Mehta AJ, Liu B, Stone GW. 2005. Wave–sediment interaction on a muddy inner shelf during Hurricane Claudette. Estuarine, Coastal and Shelf Science, 63, 225-233.
Soulsby R. 1997. Dynamics of Marine Sands : A Manual for Practical Applications. Thomas Telford Publications, London.

Stanev EV, Dobrynin M, Pleskachevsky A, Grayek S, Günther H. 2009. Bed shear stress in the southern North Sea as an important driver for suspended sediment dynamics. Ocean Dynamics, 59, 183-194.

Thompson CEL, Couceiro F, Fones GR, Helsby R, Amos CL, Black K, Parker ER, Greenwood N, Statham PJ, Kelly-Gerreyn BA. 2011. In situ flume measurements of resuspension in the North Sea. Estuarine, Coastal and Shelf Science, 94, 77-88.

Thorne PD, Hanes DM. 2002. A review of acoustic measurement of small-scale sediment processes. Continental Shelf Research, 22, 603-632.

Ulsesa C, Estournela C, Durrieu de Madronc X, Palanques A. 2008. Suspended sediment transport in the Gulf of Lions (NW Mediterranean): Impact of extreme storms and floods. Continental Shelf Research, 28, 2048-2070.

van Maren DS, van Kessel T, Cronin K, Sittoni L. 2015. The impact of channel deepening and dredging on estuarine sediment concentration. Continental Shelf Research, 95, 1-14.

Winterwerp JC. 2011. Fine sediment transport by tidal asymmetry in the high-concentrated Ems River: Indications for a regime shift in response to channel deepening. Ocean Dynamics, 61, 203-215.

Winterwerp JC, Wang ZB, van Braeckel A, van Holland G, Kösters F. 2013. Man-induced regime shifts in small estuaries—II: a comparison of rivers. Ocean Dynamics, 63, 1293-1306.

COLOPHON

Dit rapport werd voorbereid door de BMM in maart 2016
Zijn referentiecode is .MOMO/7/MF/201603/NL/AR/4

De scheepstijd met de RV Belgica werd voorzien door BELSPO en KBIN-OD Natuur

Indien u vragen hebt of bijkomende copies van dit document wenst te verkrijgen, gelieve een e-mail te zenden naar m.fettweis@mumm.ac.be, met vermelding van de referentie, of te schrijven naar:

Koninklijk Belgisch Instituut voor Natuurwetenschappen
OD Natuur – BMM
t.a.v. Michael Fettweis
Gulledelle 100
B–1200 Brussel
België

Tel: +32 2 773 2132
https://www.naturalsciences.be/en/science/do/98
http://www.mumm.ac.be/

BEHEERSEENHEID VAN HET MATHEMATISCH
MODEL VAN DE NOORDZEE

APPENDIX 1

Fettweis M, Baeye M. 2015. Seasonal variation in concentration, size and settling velocity of muddy marine flocs in the benthic boundary layer. Journal of Geophysical Research Oceans, 5648-5667. doi: 10.1002/2014JC010644.

AGU PUBLICATIONS

Journal of Geophysical Research: Oceans

RESEARCH ARTICLE
10.1002/2014JC010644

Seasonal variation in concentration, size, and settling velocity of muddy marine flocs in the benthic boundary layer

Michael Fettweis[1] **and Matthias Baeye**[1]

[1]Royal Belgian Institute of Natural Sciences—Operational Directorate Natural Environment, Brussels, Belgium

Key Points:
- SPM is better mixed throughout the water column in winter
- SPM is more concentrated in the benthic layer in summer
- Seasonality in SPM concentration is due to seasonality of the floc settling velocity

Correspondence to:
M. Fettweis,
michael.fettweis@naturalsciences.be

Citation:
Fettweis, M., and M. Baeye (2015), Seasonal variation in concentration, size, and settling velocity of muddy marine flocs in the benthic boundary layer, *J. Geophys. Res. Oceans*, *120*, 5648–5667, doi:10.1002/2014JC010644.

Received 11 DEC 2014
Accepted 22 JUL 2015
Accepted article online 24 JUL 2015
Published online 14 AUG 2015

Abstract Suspended Particulate Matter (SPM) concentration profiles of the lowest 2 m of the water column and particle size distribution at 2 m above the bed were measured in a coastal turbidity maximum area (southern North Sea) during more than 700 days between 2006 and 2013. The long-term data series of SPM concentration, floc size, and settling velocity have been ensemble averaged according to tidal range, alongshore residual flow direction, and season, in order to investigate the seasonal SPM dynamics and its relation with physical and biological processes. The data show that the SPM is more concentrated in the near-bed layer in summer, whereas in winter, the SPM is better mixed throughout the water column. The decrease of the SPM concentration in the water column during summer is compensated by a higher near-bed concentration indicating that a significant part of the SPM remains in the area during summer rather than being advected out of it. The opposite seasonality between near-bed layer and water column has to our knowledge not yet been presented in literature. Physical effects such as wave heights, wind climate, or storms have a weak correlation with the observed seasonality. The argument to favor microbial activity as main driver of the seasonality lies in the observed variations in floc size and settling velocity. On average, the flocs are larger and thus settling velocities higher in summer than winter.

1. Introduction

The behavior of cohesive sediments in a turbulent flow field differs from noncohesive ones due to their ability to change size, density, and thus settling velocity through flocculation [*Eisma*, 1986]. Flocculation occur in a turbulent flow field and combines aggregation, where the suspended particles form larger-sized clusters or flocs, and breakage, where the larger flocs are broken up into their constituting particles. The conceptual relationship between floc diameter, SPM concentration, and shear stress proposed by *Dyer* [1989] shows that turbulent flow is needed to enhance particle aggregation and to increase the size and settling velocity of the flocs. At very low turbulences, aggregation hardly occurs, and at too high turbulences, floc breakage is enhanced, resulting in a decrease in size and settling velocity of the flocs. The large flocs that occur during slack water will quickly settle, increase the near-bed SPM concentration, and form lutoclines that separates the water column with generally lower SPM concentration from the fluffy layers [*Mehta*, 1986; *Winterwerp*, 2002; *Lee et al.*, 2012; *Becker et al.*, 2013]. The particle-turbulence interactions and the stratification-induced turbulence damping contribute to the formation and stability of the lutocline and thus of these High Concentration Mud Suspensions (HCMS) or fluid mud layers [*Le Hir et al.*, 2000; *Toorman*, 2002; *Winterwerp*, 2006]. Fluid mud and HCMS are generally considered as high concentrations of fine-grained sediment in which settling is substantially hindered [*Mehta*, 1986; *Berlamont et al.*, 1993; *Winterwerp*, 2002; *McAnally et al.*, 2007a]. Often 10 g/L is suggested as a lower limit for SPM concentration in these layers; fluid mud layers have concentrations that are above the gelling point [*Winterwerp*, 2002]. The difference between fluid mud and HCMS is based on their flow behavior, which is near Newtonian for HCMS and non-Newtonian for fluid mud layers [*Mehta*, 1991]. In order to distinguish between both, measurements of viscosity, density, and/or pore pressure are thus needed [*McAnally et al.*, 2007b].

Coastal seas are often characterized by a high variability in concentration of Suspended Particulate Matter (SPM) as well as in content of cohesive sediments in the seabed [*van Ledden et al.*, 2004; *Fettweis et al.*, 2014]. On short time scales, the predominant forcings that cause these variations are related to tides, waves, and meteorological conditions. On longer time scales, neap-spring cycles, climate, and seasonal variations are significant. These forcings have an influence on the horizontal and vertical distribution of the SPM in the water column [*Mehta*, 1991; *Wan et al*., 2014]. Seasonal variations in SPM concentrations are typical for mid-latitude shelf seas such as the North Sea and are related to the seasonal patterns in wind forcing [e.g., *Howarth et al*., 1993] and/or the spring and summer phytoplankton blooms [e.g., *Jago et al*., 2007]. *Fettweis et al*. [2014] showed that the seasonality in SPM concentration in the Belgian nearshore area (southern North Sea) is mainly caused by the higher biological activity in spring and summer that triggers the formation of larger and stronger flocs and thus of higher settling rates rather than the relative small seasonality in wind strength and thus wave climate. They focused their analysis on a data set from 2011 measured at about 2 m above the bed in order to find a relation between SPM concentration, its particle size distribution, turbulence, and chlorophyll (Chl) concentration. Here a much longer time series from the same field site (2006–2013) is presented and the analysis of the data is extended to the lowest 2 m of the water column in order to investigate the seasonality of the near-bed SPM fluxes. A question that remained unanswered in the previous study [*Fettweis et al*., 2014] is related to the fate of the SPM throughout a year. How are the near-bed fluxes of SPM influenced by seasons and how does this relate to near-bed biogeophysical indicators? Is the reduction of the SPM concentration in the water column during spring and summer compensated by a higher near-bed concentration and possibly more frequent formation of HCMS, or does the residual transport have a seasonal component with a higher export of the fine-grained material out of the measuring area during summer?

The fine-grained sediment dynamics control not only the transport of cohesive sediments, but also of biogeochemical processes and of the substances that tend to be adsorbed to the fine particles, such as pollutants and nutrients [*Friedrichs et al*., 2008]. As such, they influence coastal eutrophication, algae blooms, fate of pollutants, ephemeral sealing of the seafloor by fluffy layers, benthic and pelagic ecosystems, and siltation of navigation channels and harbors [*Lancelot et al*., 1987; *Lee and Wiberg*, 2002; *Kirby*, 2011]. A better understanding of cohesive sediment dynamics allows a better prediction of changes caused by natural forcings as well as anthropogenic influences. As the seasonal variations are smaller and superimposed on the significant quarter-diurnal variations, long-term measurements that resolve all relevant time scales are needed to answer the question. We have used the long time series (several years) of SPM dynamics that are available from the Belgian nearshore area (southern North Sea) to investigate the links between settling velocity of the SPM, its concentration in the water column and in the near-bed layer, the residual alongshore current velocity, and the wave conditions using data classification and ensemble averaging techniques. The data have been collected with a benthic lander (tripod) equipped with a suite of state-of-the-art instrumentation, focusing on the lower 2 m of the water column.

2. Region of Interest

The Belgian nearshore area is situated in the southern North Sea and is characterized by semidiurnal tides, strong tidal currents (up to 1.5 m/s), and a coastal turbidity maximum area with SPM concentrations between 0.02 and more than 0.1 g/L at the surface and between 0.1 and more than 3 g/L near the bed; lower values (<0.01 g/L) occur offshore [*Baeye et al*., 2011; *Fettweis et al*., 2012b], see Figure 1. In situ measurements are available at MOW1 (51°21.63 N, 3°7.41 E) located about 5 km offshore in the coastal turbidity maximum zone and at a water depth of about 10 m MLLWS. The measuring location is situated at the marine limit of influence of the Westerscheldt estuary and the Rhine-Meuse delta [*Lacroix et al*., 2004; *Arndt et al*., 2011], where salinity is generally between 28 and 34. The strong tidal currents and the low freshwater discharges from rivers result in a well-mixed water column. Southwesterly winds dominate the overall wind climate, followed by winds from the NE sector. Maximum wind speeds coincide with southwesterly winds; nevertheless, the highest waves are generated under northwesterly winds.

The tidal current ellipses are elongated at the measuring location and vary on average between 0.2–0.8 m/s during spring tide and 0.2–0.5 m/s during neap tide at 2 m above the bed. Slack water occurs around 3 h before and 3 h after HW. Ebb (about 3 h after HW until about 3 h before HW) is directed toward the SW and flood toward the NE. Maximum currents occur during flood around 1 h before HW; the peak currents during ebb are slightly lower and occur around LW. An acoustic detection method using ADV and ADP altimetry revealed bed boundary level changes up to 0.2 m during tidal and spring-neap cycles suggesting the occurrence of lutoclines, which act as acoustic reflectors, and thus of HCMS or fluid mud layers in the nearshore area [*Baeye et al*., 2012]. The occurrence of brownish colored fluffy layers on top of consolidated black and

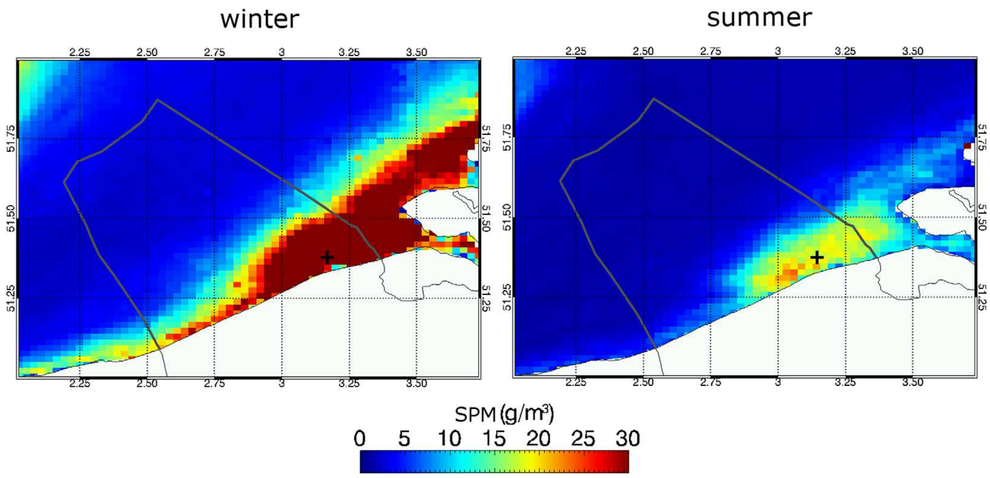

Figure 1. The mean surface SPM concentration during winter and summer in the Belgian coastal area (southern North Sea). Data are from MERIS satellite and cover the period 2003–2011 [see *Fettweis et al.*, 2014]. The cross indicates the in situ measuring station MOW1.

anoxic mud deposits of Holocene age, intercalated with thin sandy layers, have frequently been observed in Van Veen grab and box core samples taken at this location [*Fettweis et al.*, 2009]. *Gerritsen et al.* [2001] claim that the transport from the English Channel toward the North Sea is the main source of fine-grained sediments in the southern North Sea. Clay mineralogical analysis of the fine-grained sediments along the French, Belgian, and Dutch coast, however, points to erosion of the Holocene mud layers off the Belgian coast as main origin of the SPM in the coastal turbidity maximum zone [*Adriaens*, 2015].

3. Methods

3.1. Instrumentation and Data Processing

Current velocity, salinity, temperature, SPM concentration, and Particle Size Distribution (PSD) were collected with a tripod. The instrumentation suite consisted of a 5 MHz ADVOcean velocimeter, a 3 MHz SonTek Acoustic Doppler Profiler (ADP), two D&A optical backscatter point sensors (OBS), a Sea-bird SBE37 CT, and a Sequoia Scientific Laser In Situ Scattering and Transmissometer 100-X (type-C). All data (except LISST) were stored in two SonTek Hydra data logging systems. The data were collected in bursts every 10 or 15 min for the OBS, LISST, and ADV, while the ADP was set to record a profile every 1 min; later on, averaging was performed to a 15 min interval to match the sampling interval of the other sensors.

The tripod was moored at the MOW1 location between 3 and 6 weeks and was then recovered and from December 2009 on replaced with a similar tripod system to ensure continuous time series. More than 45 deployments were carried out between February 2006 and December 2013; 34 between November 2009 and December 2013. From these, a total of 1258 days of ADP data, 1153 days of OBS, and 721 days of LISST data remained after quality check. The OBSs were mounted at 0.2 and 2.3 m above the bed (hereafter referred to as mab) and the LISST at 2.3 mab. The ADP was downward looking and profiling the lowest 1.8 m of the water column. Rejection of ADP was mainly caused by instrument failure, and for the OBS due to biofouling or saturation. The number of good data increased significantly after installation of wipers on the OBS. Good quality data for the LISST have been selected if the optical transmission was between 15% and 98%, if no gradual or sudden increase or decrease in transmission or volume concentration occurred during the measurements and if the PSDs were smooth. A gradual decrease is often the result of biofouling and occurs mainly in spring and summer. A sudden decrease in transmission is generally caused by a physical obstruction (e.g., cord entangled in optical path). A misaligned laser beam may cause high peaks in a few size classes making the PSD not smooth; these peaks remain during the whole measurements. The LISST 100 is a delicate instrument, misalignment of the laser beam may occur during deployment or other physical disturbances (collision with fishing gear). The ADP and OBS data are more or less equally distributed over the seasons, whereas LISST data are for 80% from winter season due to low biofouling. The long deployments ensured sampling of conditions that include complete periods of neap and spring tides, seasons, as well as the occurrence of a variety of meteorological events.

3.2. SPM Concentration From Acoustic and Optic Instruments

The OBS signal was used to estimate SPM concentration. OBS voltage readings were converted into SPM concentration by calibration against filtered water samples collected during four tidal cycles every year, i.e., one in spring, summer, autumn, and winter. A linear regression was used to fit a straight line between the OBS signal (in FTU) and the filtered SPM concentration (in mg/L). The regression coefficient (R^2) is for more than 80% of the calibrations higher than 0.90; the uncertainty on the OBS-derived SPM concentrations was estimated as 10% [*Fettweis*, 2008]. The slope (a) and the intercept (b) of the fitted regression lines have larger variability with a mean slope of $a = 1.52 \pm 0.26$ and a mean intercept of $b = 11.3 \pm 13.1$. Further uncertainties of the OBSs arise because they were formatted to measure concentration of up to 1.5 or 3 g/L depending on the sensor. During high energy conditions, SPM concentrations at 0.2 mab were regularly higher than 1.5 or 3 g/L. Under these circumstances the OBS saturated and underestimated the actual SPM concentration. The OBS at 0.2 mab was in this state during about 3.2% of the time in summer and 1.4% of the time in winter. Although this represents relative short period of times, it significantly affects the mean SPM concentration, e.g., an underestimation of the peak SPM concentration during saturation by 2 g/L results in an underestimation of the mean SPM concentration in summer by 64 mg/L and in winter by 28 mg/L.

The ADP profiler was attached at 2.3 mab and down-looking, measuring current and acoustic intensity profiles with a bin resolution of 0.25 m starting at 1.8 mab. The lowest bin size that is not disturbed by the seabed is located at 0.5 mab. The backscattered acoustic signal strength, from ADP, was used to estimate SPM concentrations. After conversion to decibels, the signal strength was corrected for geometric spreading and water attenuation. Furthermore, an iterative approach [*Thorne and Hanes*, 2002] was used to also correct for sediment attenuation. The upper OBS-derived SPM concentration estimates were used to calibrate the ADP's first bin. Backscattering is affected by sediment type, color, size, composition and turbulence; optical and acoustical backscattering showing different sensitivities for these parameters [*Thorne et al.*, 1991; *Fugate and Friedrichs*, 2002; *Voulgaris and Meyers*, 2004; *Downing*, 2006; *Nauw et al.*, 2014]. The echo intensity of the backscattered acoustic signal gives an indication of SPM concentration variation if the particle size distribution and characteristics remain the same. This is often not the case in tidal environments where fine-grained sediments are subject to flocculation and where cohesive and non-cohesive sediments can both be in suspension during high flow velocities [*Baeye et al.*, 2011; *Fettweis et al.*, 2012a]. Flocs have a smaller influence on the backscatter than a sand grain of the same size due to their lower density [*Ha et al.*, 2011]. The strength of backscattered signal from flocs is mainly (but not solely) influenced by the building blocks of the flocs, i.e., the flocculi [*Fugate and Friedrichs*, 2002; *MacDonald et al.*, 2013; *Rouhnia et al.*, 2014]. The different sensitivity of acoustic and optic sensors to changes in the SPM particle size and characteristic is reflected in the correlation coefficient between the ADP backscatter (in dB) and the OBS-derived SPM concentration of $R^2 = 0.53$. The R^2 is better for the lower SPM concentrations and the regression model thus accounts for less variance for the higher SPM concentrations.

3.3. PSD Measurements and Curve Fitting

The LISST 100C uses laser diffraction technology to measure particle size and volume concentration in 32 logarithmically spaced size groups over the range of 2.5–500 μm [*Agrawal and Pottsmith*, 2000]. The volume concentration of each size group is estimated with an empirical volume calibration constant, which is obtained under a presumed sphericity of particles. Despite the uncertainties and limitations of the LISST-100C detectors, which are related to the characteristics of the particles occurring in nature [*Mikkelsen et al.*, 2006; *Andrews et al.*, 2010; *Davies et al.*, 2012; *Graham et al.*, 2012], and to the measuring principle itself [*Goossens*, 2008], it is well suited to collect long-time series of PSD autonomously. Limitations related to the particles in suspension are caused by their shape and size. For example, particles smaller than the size range affect the entire PSD, with an increase in the volume concentration of the smallest two size classes, a decrease in the next size classes and, an increase in the largest size classes [*Andrews et al.*, 2010; *Graham et al.*, 2012]. A rising tail in the lowest size classes of the LISST is frequently observed in our data and is interpreted as an indication of the presence of very fine particles rather than providing a correct number. This bias may further enhance the separation between the two peaks of primary particles and flocculi and develop a small peak of macroflocs during the peak flows. In case of low turbulent condition, it may also indicate the presence of very large particles [*Andrews et al*., 2010]. Particles exceeding the LISST size range of 500 μm also contaminate the PSD. *Davies et al*. [2012] reported that large out of range particles increase the volume concentration of particles in multiple size classes in the range between 250 and 400 μm and in the smaller size classes and recommended to interpret the PSD with care in case particles outside the size range may potentially occur. The importance of these spurious results depends on the number of large particles in the distribution [*Davies et al*., 2012]. No particle size data obtained with other methods (video system, holography) are available at the MOW1 site. Macrofloc sizes recorded by a video system at an estuarine site with similar tidal dynamics were generally smaller than 580 μm [*Winterwerp et al*., 2006], which indicates that most of the larger flocs are most probably not exceeding the size limit of the LISST.

The diameter of a particle is an exact proxy of its size if the particle is a sphere. Natural particles, such as flocs, have irregular shapes. Measurements by laser diffraction (or other methods) result thus intrinsically in a particle size distribution that is generally lognormally distributed. In case of SPM, the PSD is further characterized by a multimodal size distribution, which can be reduced to a four-level structure consisting of primary particles, flocculi, microflocs, and macroflocs [*Lee et al*., 2012]. Primary particles consist of various organic and mineral particles, flocculi are breakage-resistant aggregates of mainly clay minerals; microflocs are the medium size aggregates, and macroflocs are the large aggregates that can reach a few hundred micrometers. The decomposition of the multimodal PSD into these subordinate aggregate groups is based on the method of *Whitby* [1978] as described in *Fettweis et al*. [2012a] and *Lee et al*. [2012], which consist in writing the multimodal lognormal distribution as a sum of lognormal distribution functions representing the four aggregate groups:

$$\frac{dV}{dD}=\sum_{i=1}^{4}\frac{V_i}{\sqrt{2\pi}ln(\sigma_i)}\quad e^{-0.5\left(ln(D/D_i)/ln(\sigma_i)\right)^2} \tag{1}$$

where D is the particle diameter, V the volume concentration, D_i the geometric mean diameter, σ_i the multiplicative standard deviation, and V_i the volumetric fraction of an ith unimodal PSD. dV/dD is the normalized volumetric fraction by the width of the size interval and used for curve fitting to a lognormal distribution. For two modal peaks, fixed sizes of 3 μm (lowest size class of the LISST) and 15 μm were chosen; the modal peaks of the bigger fractions were variable and chosen in order to represent the larger size classes of the LISST instrument (15–200 and 150–500 μm). The standard deviations varied between 1 and 2.5.

3.4. Settling Velocity

The settling velocity is a function of the particle size and the effective density, and can be described by Stokes' Law under the assumption that the particle Reynolds number is smaller than one. However, the effective density cannot be measured directly by the LISST and has to be estimated from volume and mass concentration measurements [*Mikkelsen and Pejrup*, 2001]. As floc size increases, the effective density decreases, the larger flocs are thus loosely bound and lighter compared to smaller, tightly packed units. The settling velocity can then be derived if the relationship between effective density and floc size is established. This has been done, e.g., by assuming a self-similarity between primary particles and flocs based on fractal theory [*Kranenburg*, 1994; *Winterwerp*, 1998] or by using density functions that describe the mass distribution over the PSD [*Markussen and Andersen*, 2013]. The settling velocity was calculated for each of the four aggregate groups of primary particles, flocculi, microflocs, and macroflocs separately, using the modified Stokes' equation [*Lee et al*., 2012]:

$$w_{s,i}=\frac{\rho_p-\rho_w}{18\ \mu}g\ D_p^{3-nf_i}\ \frac{D_i^{nf_i-1}}{1+0.15Re_i^{0.687}} \tag{2}$$

where $w_{s,i}$ is the settling velocity of the ith aggregate group. The densities of primary particle and seawater (ρ_p and ρ_w) were fixed at 2475 and 1030 kg/m^3; and the size of primary particles (D_p) was set as 2 μm [*Fettweis*, 2008]. The gravitational acceleration and the fluid viscosity (g and μ) were 9.81 m/s^2 and 0.001 kg/m/s. Re_i represents the Reynolds number of an aggregate. Four stepwise fractal dimensions (nf_i) of 3, 2.5, 2.2, and 2.1 were used for the four discrete aggregate groups of primary particles, flocculi, microflocs, and macroflocs, respectively. These values are in the range of fractal dimensions for marine and estuarine flocs proposed in literature [e.g., *Winterwerp*, 1998]. The settling velocity value of the PSD is then the sum of the by volume concentration weighted settling velocities of the four aggregate groups. The volume concentrations of the four groups are obtained from the curve fitting analysis. The advantage of this approach is that the multimodality of a PSD is taken into account and that the settling velocity is estimated more accurately than with the median or mean particle size that is not accurately representing the PSD [*Lee et al*., 2012].

3.5. Turbulence Data

Turbulence in coastal areas controls the flocculation of fine-grained material and impacts the vertical and horizontal flux of SPM. The length scale of the smallest dissipating eddies (Kolmogorov microscale of turbulence, λ_k) generally limits the size of the flocs [*van Leussen*, 1999; *Cross et al*., 2013]. Assuming that turbulent kinetic energy production is equal to dissipation, this scale can be calculated as $\lambda_k = (\nu^3/\varepsilon)^{1/4}$, where ν is the kinematic viscosity (10^{-6} m^2 s^{-1}) and ε is the turbulent energy dissipation (m^2 s^{-3}). The turbulent dissipation can be derived from $\tau = \rho(\varepsilon\, \kappa\, z)^{2/3}$, where τ is the shear stress, *z* the elevation above the bed, κ the von Karman constant, and ρ the water density. The turbulent kinetic energy and the shear stress can be calculated using the variance of velocity fluctuation from the high-frequent ADV measurements [*Stapleton and Huntley*, 1995; *Thompson et al*., 2003]. MOW1 is situated in shallow waters where wave effects are important; therefore, the shear stress was corrected for the advection by waves following the approach of *Trowbridge and Elgar* [2001] and *Sherwood et al*. [2006]. With the turbulence dissipation known, the Kolmogorov length scale can be calculated. The length scale was low-pass filtered using the PL64 filter described in *Flagg et al*. [1976] with a 33 h half-amplitude cut off to remove tidal and higher-frequency signals. The low-pass Kolmogorov length scale can be used as a proxy of the nontidal (waves and wind) turbulence intensity in shallow waters [*Fettweis et al*., 2014].

3.6. Data Classification and Ensemble Averaging

The available data comprise of 1392 (LISST) up to 2428 (ADP) tidal cycles collected during different seasonal, tidal, and meteorological conditions. To every tidal cycle classification, parameters were assigned that take into account seasons, tidal range, alongshore current, and wave height. Each tidal cycle starts at high water (HW) and finishes at the following HW and was resampled to obtain 50 data points per cycle (i.e., every 15 min). The tidal cycles of each class were then ensemble averaged, and the standard error was calculated. The standard error estimates how far the sample mean is likely to be from the population mean and will decrease with increasing sample size.

Classification into seasons was limited to two periods, one with a lower SPM and a high Chl concentration in the water column (April–September: summer) and one with a higher SPM and low Chl concentration (October–March: winter), similar as in *Fettweis et al*. [2014]. The tidal range was calculated from the harmonic tidal signal and then grouped according to the P66 (3.95 m) and P33 (3.31 m) percentiles into a spring tide (SP, >P66), mean tide (MT, P66-P33), and neap tide (NT, <P33). This division in spring, mean, and neap tides is not necessarily corresponding to the astronomical definition of the spring-neap cycle, as some astronomical spring tides or neap tides can have sufficient small or large tidal ranges to be classified as mean tides. Remark also that the tidal range has a semiannual cycle at the measuring location. The highest and lowest tidal ranges occur during equinox, i.e., around March and September. The influence of weather systems on SPM concentration was investigated by grouping the tidal cycles according to the alongshore flow and the wave-induced turbulence. For each tidal cycle, the alongshore flow was estimated using the ADP current velocity data by calculating the residual flow using a low-passed filter (PL64) of 33 h half-amplitude cut off to remove tidal and higher-frequency signals [*Flagg et al*., 1976]. Subsequently, the tidal cycle was classified in terms of this residual alongshore current into two groups. One corresponds with the P10 (−0.12 m/s) and is SW-ward directed the other one with the P90 (0.02 m/s) and is NE-ward directed; SW-NE direction corresponds with the alignment of the coastline. The residual alongshore flow at the measuring location MOW1 is in 85% of the time directed toward the SW, i.e., in ebb direction. In order to investigate the wave influence, the data have been grouped according to the low-pass filtered Kolmogorov length scale into two classes. The first one corresponds with the P66 of highest ($\lambda_k < 0.36$ mm) and the second one with the P33 of lowest ($\lambda_k < 0.49$ mm) wave effects.

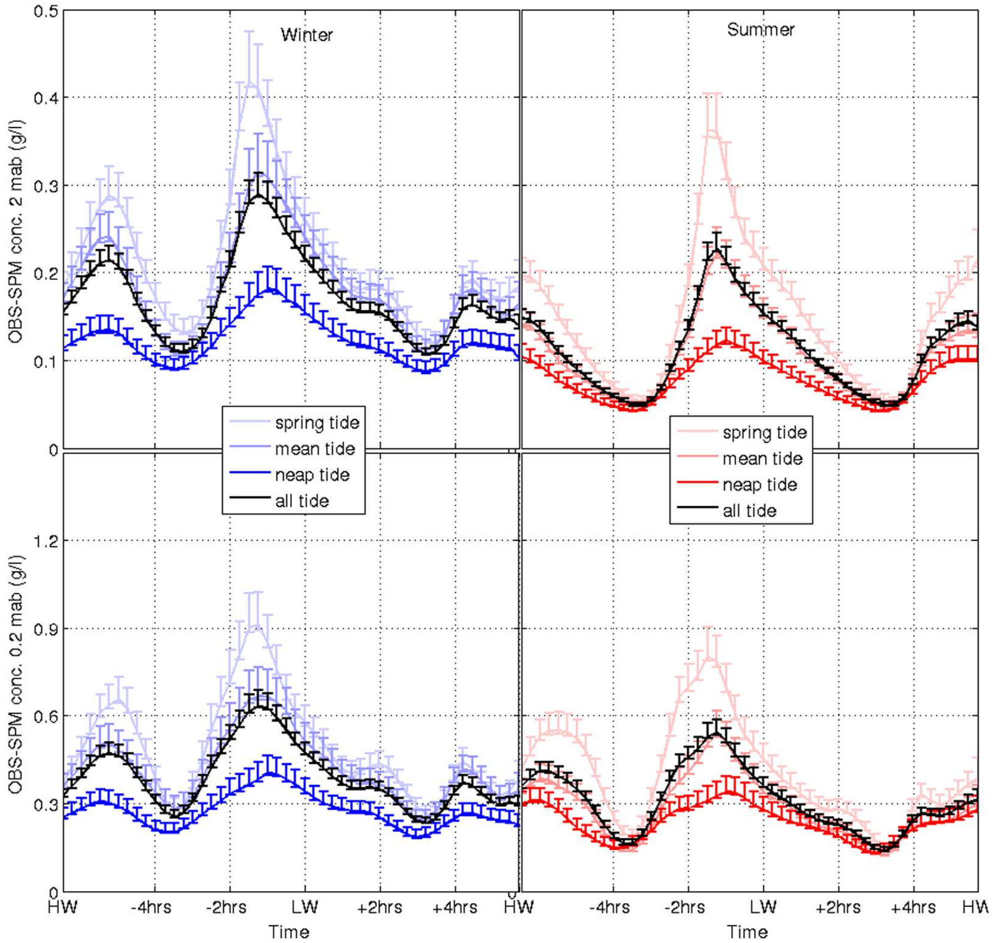

Figure 2. Ensemble averaged OBS-derived SPM concentration at 2 and 0.2 mab during a tidal cycle in (left) winter and (right) summer and for different tidal ranges. The black line is the seasonal averaged SPM concentration. The error bars are the standard errors.

4. Results

4.1. Seasonality of SPM Mass Concentration as a Function of Tidal Range

The SPM mass concentrations derived from OBS and ADP backscatter during winter and summer season and for different tidal ranges are shown in Figures 2 and 3. The SPM concentration varies typically with ebb-flood and with tidal range. The ADP-derived SPM concentration is better correlated with the current velocities than the OBS-derived concentration. Both sensors have lower SPM concentration during slack water in summer than in winter. Differences between OBS and ADP SPM concentrations are more pronounced during flood. The maximum ADP-derived SPM concentration corresponds with the maximum current velocity (1 h before HW), the maximum in the OBS signal is registered about 2 h later (1 h after HW), when current velocity has already decreased. The seasonal signal in the SPM concentration is slightly different in both sensors. The ADP has higher SPM concentration during ebb and flood at 0.5 mab and lower ones at 1.8 mab in summer, and the OBS has always registered lower SPM concentration in summer. Both sensors show lower SPM concentration during slack water in summer. The seasonal difference in the ADP decreases with increasing distance from the bed. At 1.8 mab, the SPM concentrations are always higher in winter and this during the entire tidal cycle. The ADP-derived SPM concentrations have further been averaged over the tidal cycle, ebb, flood, and slack waters and are plotted in Figure 4 as vertical profiles of the lowest 2 m of the water column. These profiles show the nonlinear increase in SPM concentration toward the bed, but they also show that the SPM concentration at 1.8 mab is lower during summer whereas the seasonal

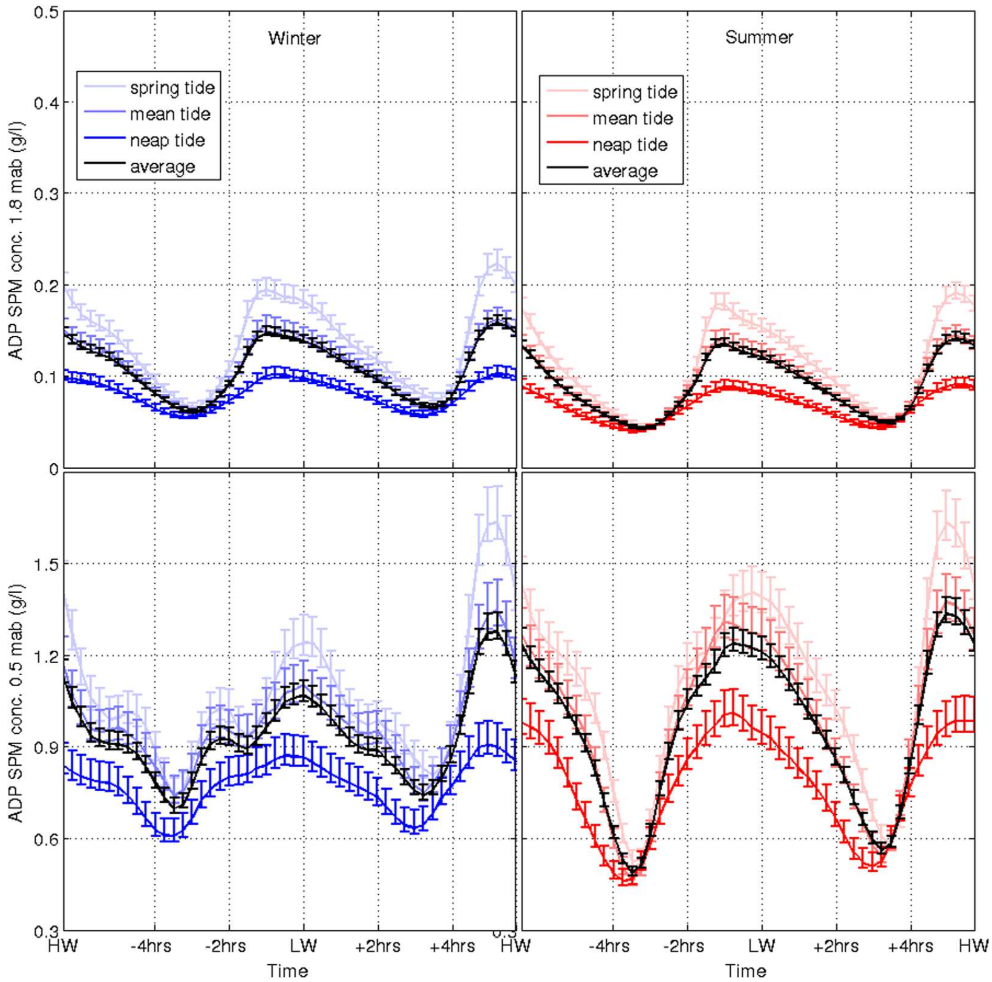

Figure 3. Ensemble averaged ADP backscatter-derived SPM concentration at 1.8 and 0.5 mab during a tidal cycle in (left) winter and (right) summer and for different tidal ranges. The black line is the seasonal averaged SPM concentration. The error bars are the standard errors.

differences are smaller at 0.5 mab or even reversed (summer is higher during ebb and flood). The mean SPM concentrations during winter and summer derived from the OBSs and the ADP is shown in Table 1. At 2 mab, the OBS records higher SPM concentration, whereas near the bed the ADP has larger values. These data reflect the uncertainties of the instruments that comprise different sensitivities of the backscattered signal with changing SPM characteristics and sensor limitation (OBS saturation), see section 3.2.

4.2. Seasonality of SPM Mass Concentration as a Function of Alongshore Flow and Turbulence

The effects of residual alongshore flow on the SPM mass concentration derived from the OBS are shown in Figure 5. The alongshore flow changes the SPM concentration during ebb and flood. The SPM concentration is generally higher in case that currents are directed in the same direction as the alongshore flow. Thus for ebb, the highest SPM concentration is recorded during SW-ward directed and for flood during NE-ward directed residual alongshore flow. SPM concentration differences between summer and winter show similar pattern as presented above (section 4.1). The effect of low and high turbulence, as indicated by the low-pass filtered Kolmogorov length scale, on the OBS-derived SPM concentration is shown in Figure 6. The low-pass filtered Kolmogorov length scale is a proxy of the wave and wind-induced turbulence intensity and takes into account the turbulence induced by spring-neap cycle variations. The SPM concentration near the bed is strongly influenced by turbulence (waves), higher up in the water column wave influences decreases. Although the effect of waves and wind forcing on turbulence is independent of the season, one can see that

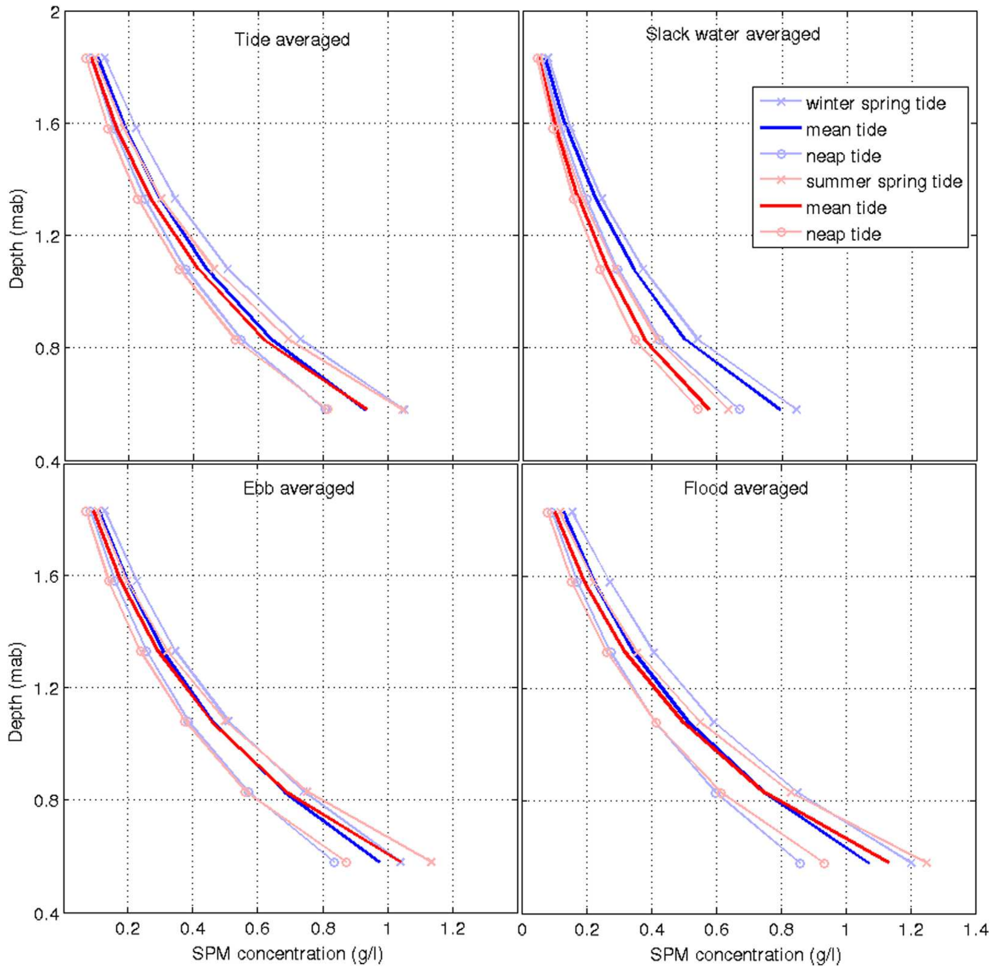

Figure 4. Ensemble averaged ADP backscatter-derived SPM concentration profiles averaged over a tidal cycle, slack water, ebb, and flood in winter and summer and for different tidal ranges.

the SPM concentration reacts differently in summer and winter. An increase of turbulence has a more pronounced effect on SPM concentration in the near-bed layer in summer than winter and vice versa at 2 mab. During periods with higher wave-induced turbulence, the increase of SPM concentration near the bed is stronger in summer, whereas in winter the wave effects are better visible higher up in the water column.

4.3. Seasonality of SPM Volume Concentration, Floc Size, and Settling Velocity

The geometric mean floc size, the SPM volume concentration, and the settling velocity at 2.2 mab during winter and summer season and for different tidal ranges are shown in Figure 7 and for different wave conditions in Figure 8. The figures show that seasonal differences are more pronounced for floc size and settling velocity than SPM volume concentrations. The SPM volume concentration is generally higher in winter than in summer. This corresponds with the SPM mass concentration recorded at 1.8 mab by the ADP and at 2 mab by the OBS. The geometric mean floc size is on average higher in summer than winter. The largest floc sizes occur during slack water and the smallest during peak ebb and flood currents. The course of floc size during a tidal cycle in summer differs somewhat from its course. For example,

Table 1. Geometric Mean SPM Concentration (mg/L) and Multiplicative Standard Deviation (Multiplied-Divided = */) During Winter and Summer as Derived From ADP and OBS Backscatter

	Winter	Summer
ADP 1.8 mab	103*/1.35	84*/1.46
OBS 2.0 mab	165*/1.55	102*/1.55
ADP 0.5 mab	926*/1.33	931*/1.33
OBS 0.2 mab	380*/1.27	331*/1.41

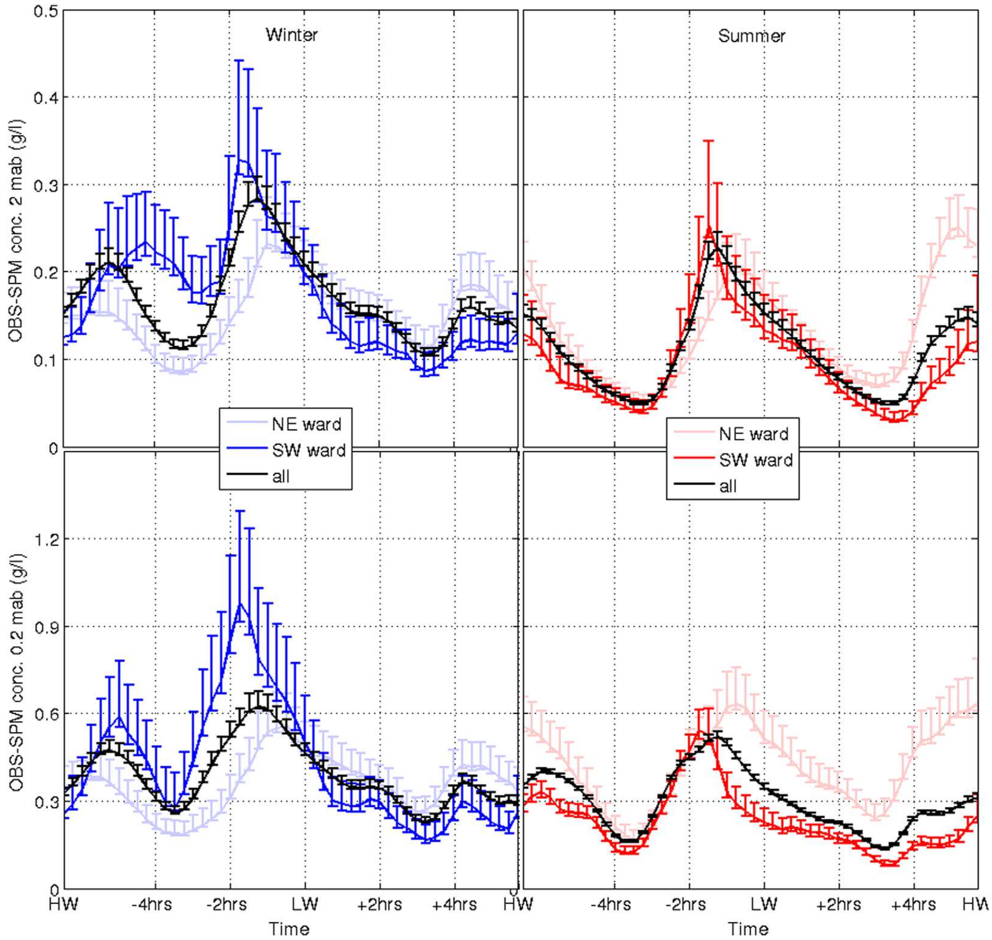

Figure 5. Ensemble averaged OBS-derived SPM concentration at 2 and 0.2 mab during a tidal cycle (g/L) in (left) winter and (right) summer for two different alongshore flows (NE = northeastward, SW = southwestward). The plotted data are the P90 (NE, 0.02 m/s) and P10 (−0.12 m/s, SW) percentiles. The error bars are the standard errors.

the floc sizes during flood in summer are higher than during ebb, which is not the case in winter. Similarly, the floc sizes in winter during ebb-flood slack water (3 h before HW) are smaller than the floc sizes during flood-ebb slack water (3 h after HW); during summer the differences are less pronounced except for the smallest and largest tidal ranges. The settling velocities are between 0.18 and 0.35 mm/s in winter and 0.18 and 0.45 mm/s in summer (Figure 7). Note that the settling velocities in summer are larger during whole the tidal cycle. The difference in settling velocity between winter and summer is significant when no seasonal variation in fractal dimensions is assumed; summer settling velocities are then on average 35% higher than winter ones. In order to take into account effects of organic matter enrichment on the density of macroflocs in summer, the fractal dimension of the macroflocs was changed from 2.1 to 2.0. Although this corresponds to about 50% reduction in effective density of the macroflocs and 0.03 mm/s reduction of the summer mean settling velocity (0.28–0.25 mm/s), the mean settling velocities are still about 20% higher in summer.

The larger floc sizes in summer are caused by higher frequency of macroflocs and larger sizes of micro and macroflocs in summer than in winter, see Table 2 and Figures 9 and 10 where the temporal frequency distribution of the four constituents of the PSDs (primary particles, flocculi, microflocs, and macroflocs) are shown for a neap-spring-neap cycle in winter and summer. Both periods are characterized by low wave condition so that turbulence is mainly a function of tidal current strength. The figures show that the geometric

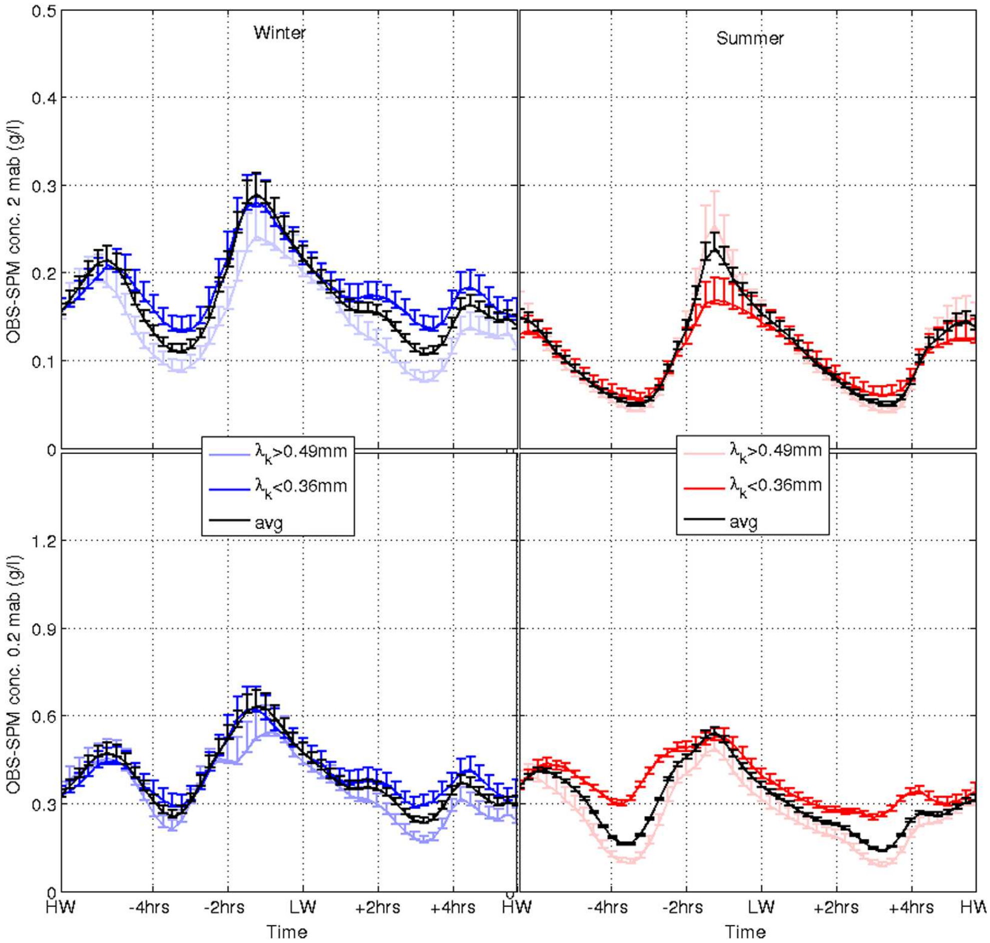

Figure 6. Ensemble averaged OBS-derived SPM concentration at 2 and 0.2 mab during a tidal cycle in (left) winter and (right) summer and for high ($\lambda_k < 0.36$ mm, D33) and low ($\lambda_k > 0.49$ mm, D66) low-pass filtered Komogorov microscale conditions. These conditions correspond roughly with periods where the significant wave heights are lower than 0.4 m and greater than approximately 0.9 m. The black line is the seasonal averaged SPM concentration. The error bars are the standard errors.

mean floc size depends on turbulent shear (as given by the Kolmogorov microscale). High turbulent shear (or low Kolmogorov scale) decreases the geometric mean floc diameter down to about 30 μm, whereas low turbulent shear concurred with an increase of the floc diameters up to about 180 μm. Figure 9 shows a period in winter 2011 (January), where primary particles and flocculi have variations opposite to those of micro and macroflocs. High frequencies of macroflocs and microflocs together with low frequencies of primary particles and flocculi occur during slack water when turbulence is low, and high frequencies of primary particles and flocculi together with low frequencies of micro and macroflocs occur during ebb and flood when turbulence is high. This is in contrast to a period end of April 2011 (Figure 10). During low turbulence, the variation in frequency of micro and macroflocs is not in concordance anymore, but reversed. The increase in frequency of macroflocs is compensated by a decrease in microflocs frequency. During breakup periods, the frequency of microflocs, flocculi, and primary particles increases. The shift from microflocs to macroflocs during low turbulence periods in summer is partially the result of the chosen parameter of the curve fitting (see section 3.3), but it reflects physical changes in flocculation type, from turbulence mediated flocculation in winter toward an additional biological mediated flocculation in summer. The data indicate that larger flocs are formed during slack water in summer through aggregation of microflocs and that during periods with high turbulent shear, the flocs break up in microflocs, flocculi, and primary particles. In winter, we observe that the floc population consists mainly of microflocs that have been formed through

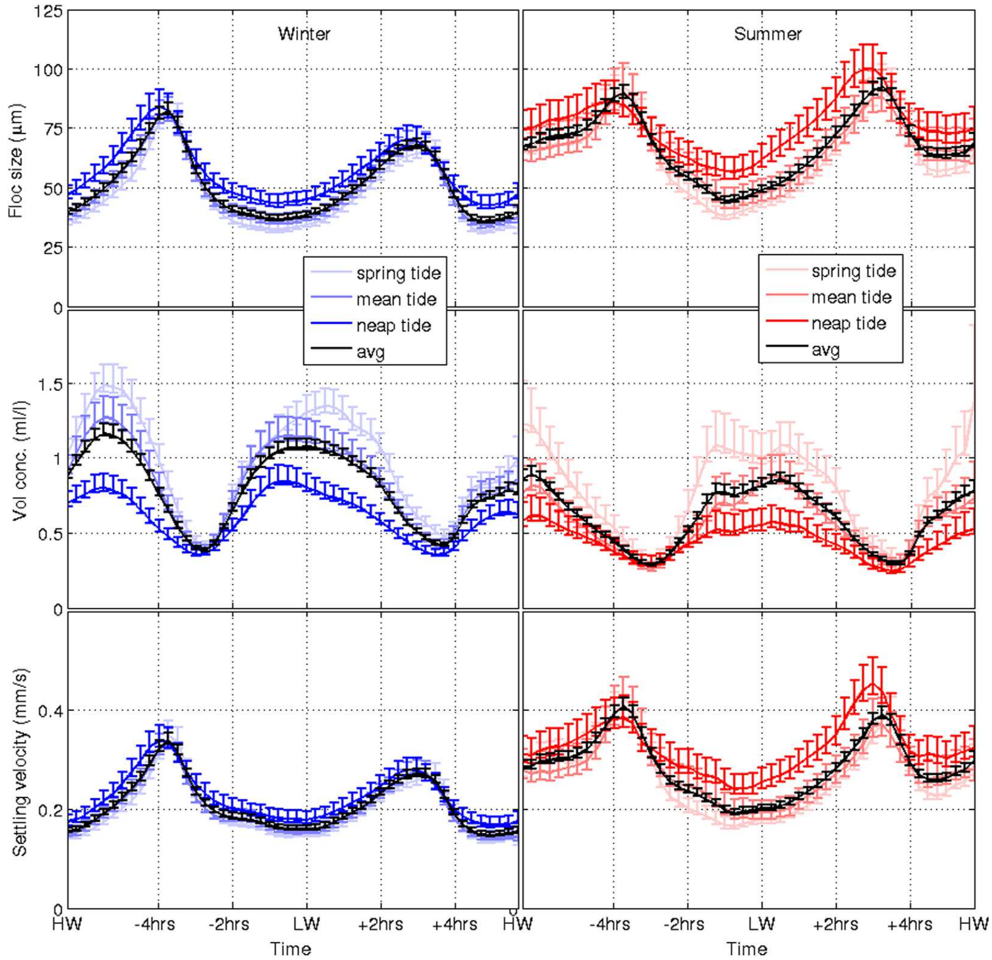

Figure 7. Ensemble averaged geometric mean floc size (µm), volume concentration (mL/L), and settling velocity (mm/s) at 2.0 mab during a tidal cycle in (left) winter and (right) summer (black line) and for different tidal ranges. The error bars are standard errors.

aggregation of flocculi and primary particles. When turbulent shear increases again then the microflocs disintegrate into their next smaller constituents.

The link with biological activity is shown in Figure 11, where the over 14 days averaged frequencies of the four aggregate groups of the flocs, floc sizes, SPM volume and mass concentration, and surface Chl concentrations are shown for the period 2005–2013. The Chl concentration increases during spring algae bloom in April and during a second bloom in July. Floc sizes increase from April onward and remain high until beginning of October. In winter, the mean floc sizes are between 45 and 60 µm and in summer between 50 and 100 µm. Highest mean floc sizes in summer have been measured end of June and August and lowest ones in July. The increase in floc size in April is mainly due to an increase in frequency of microflocs and a decrease in primary particles and flocculi frequency. The increase of macroflocs frequency starts in May and inversely follows the decrease of microflocs and primary particles frequency. Floc sizes are correlated with the algae blooms, although a time shift of about 1 month is observed. The increase in floc size in spring is correlated with a decrease of the SPM concentration at 2 mab and an increase in the near-bed ADP signal during whole the summer and in the OBS signal until beginning of July. The on average higher SPM concentrations during the months May and June correspond with the higher frequencies of macroflocs and the higher mean floc sizes, and thus higher settling fluxes during the same period. The OBS-derived SPM concentration at 0.2 mab has a less pronounced seasonal cycle than at 2 mab.

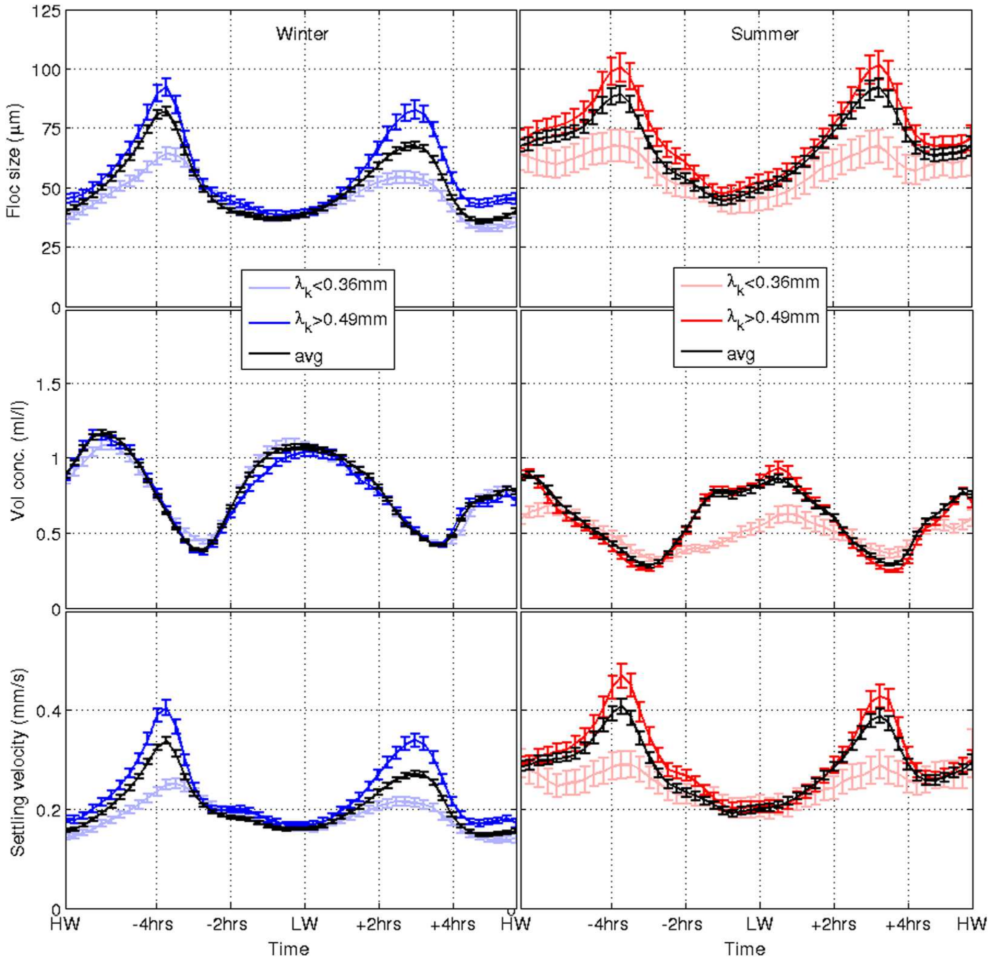

Figure 8. Ensemble averaged geometric mean floc size (μm), volume concentration (mL/L), and settling velocity (mm/s) at 2.0 mab during a tidal cycle in (left) winter and (right) summer (black line) and for high ($\lambda_k < 0.36$ mm, D33) and low ($\lambda_k > 0.49$ mm, D66) low-pass filtered Komogorov microscale conditions. These conditions correspond roughly with periods where the significant wave heights are lower than 0.4 m and greater than approximately 0.9 m. The error bars are standard errors.

5. Discussion

The seasonal differences in SPM concentration profile (Figure 4) and the different behavior of the SPM concentration at 0.2 and 2 mab during low and high turbulent conditions (Figure 6) indicate that the balance between turbulent mixing of the SPM (upward flux) and the settling velocity of each particle (downward flux) has changed. Variation in turbulent mixing is caused by tides, neap-spring cycles, wind forcing, and wave climate. Flocculation and thus settling velocity of flocs varies with the same physical forcings as well as with the presence of microbial products [*Maggi*, 2009]. Wind forcing, wave climate, and biological activity have a seasonal signal in the Belgian coastal area. The seasonality in wave height is, however, not sufficient to explain the observed seasonality [*Baeye et al*., 2011; *Fettweis et al*., 2014]. Similar the effect of wind forcing on the alongshore residual currents and thus on the advection of the SPM is similar in summer and winter. In other words, the frequency of storms with high wave heights or periods with wind direction that changes the alongshore residual flow are too low in the Belgian nearshore area to significantly alter the ensemble averaged values that have been presented above. The results suggest therefore that the seasonality is mainly caused by changes in floc size and settling velocity rather than turbulent mixing.

Table 2. Mean Frequency and Standard Deviation of Primary Particles, Flocculi, Micro and Macroflocs, and Geometric Mean and Multiplicative Standard Deviation of Settling Velocity (w_s) With a Yearly Constant Fractal Dimension of the Macroflocs[a]

	PP (%)	Flocculi (%)	Micro (μm)	Micro (%)	Macro (μm)	Macro (%)	w_s (mm/s)
Winter							
All data	6.1 ± 4.8	21.2 ± 12.4	66 ± 30	61.3 ± 15.0	277 ± 86	11.3 ± 10.6	0.20*/1.73
λ_k>0.49 mm	5.0 ± 4.4	19.8 ± 11.6	73 ± 34	63.6 ± 15.0	289 ± 92	11.6 ± 12.2	0.27*/1.79
λ_k<0.36 mm	7.0 ± 4.8	21.2 ± 12.4	58 ± 22	58.8 ± 14.4	257 ± 69	12.1 ± 9.3	0.19*/1.59
Summer							
All data	4.3 ± 4.4	15.1 ± 8.2	82 ± 34	65.9 ± 15.6	322 ± 96	14.7 ± 15.7	0.28*/1.63
λ_k>0.49 mm	3.6 ± 3.9	13.6 ± 7.2	86 ± 38	37.1 ± 16.7	332 ± 102	15.7 ± 18.4	0.29*/1.68
λ_k<0.36 mm	5.1 ± 4.6	17.7 ± 8.0	69 ± 23	62.5 ± 14.1	301 ± 83	14.7 ± 11.1	0.25*/1.53

[a]The data are further divided in two groups based on the low-pass filtered Kolmogorov microscale of turbulence (λ_k). These groups correspond roughly with periods where the significant wave heights are lower than 0.4 m and greater than approximately 0.9 m.

5.1. Seasonality in Flocculation

In shear-dependent flocculation, aggregation and breakage counteract each other in a flow and shear-varying tidal cycle [*Verney et al.*, 2009; *Lee et al.*, 2012; *Keyvani and Strom*, 2014]. In addition to shear-dependent flocculation, erosion could also increase the influx of large particles from the seabed into the

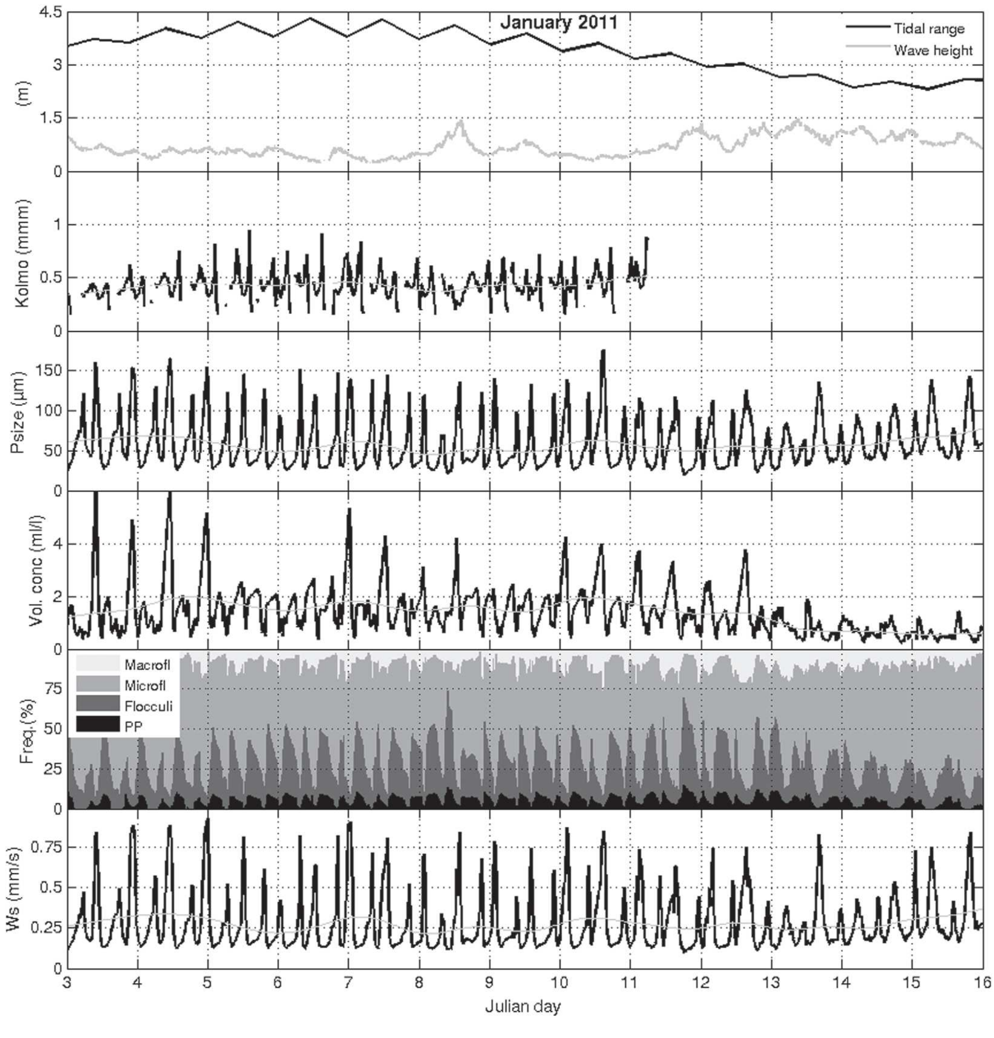

Figure 9. Time series of tidal range, significant wave height, Kolmogorov microscale, geometric mean floc size, the frequency of micro and macroflocs and flocculi, and primary particles and the settling velocity during about 10 days in January 2011.

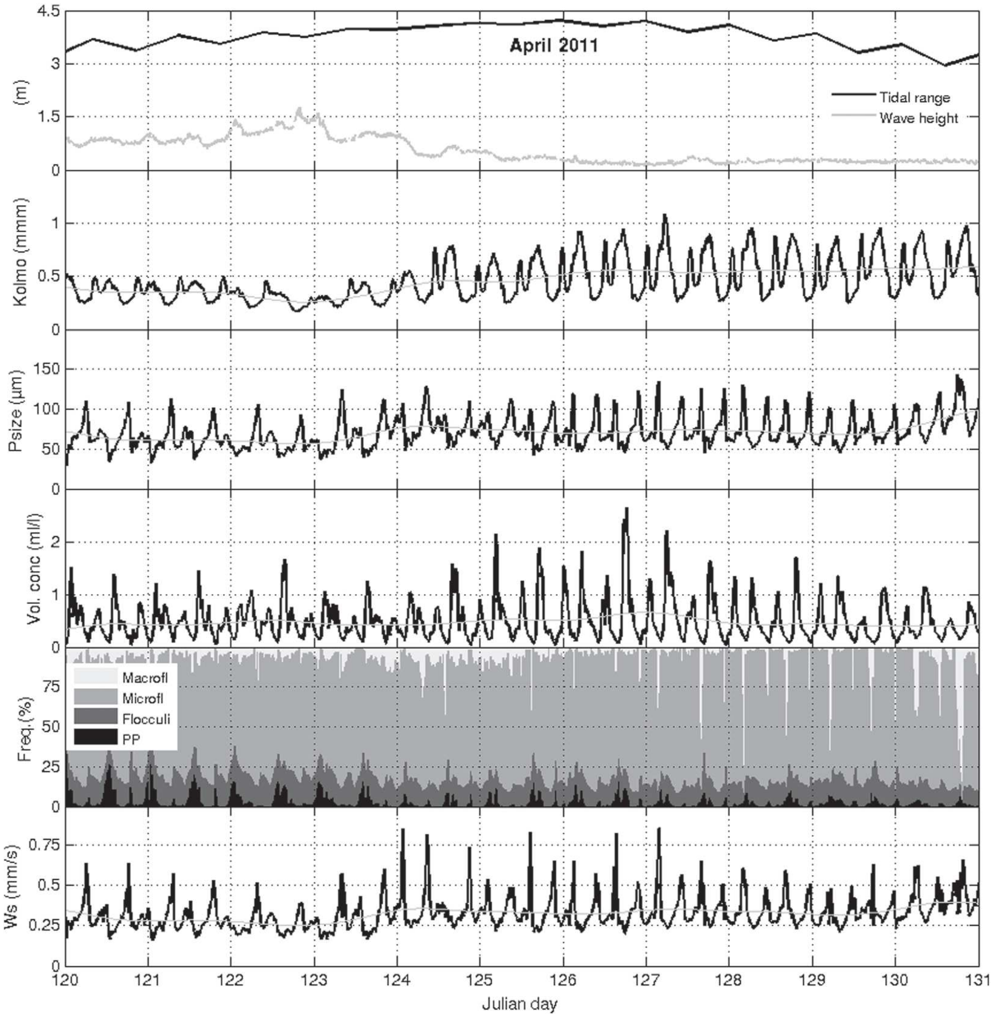

Figure 10. Time series of tidal range, significant wave height, Kolmogorov microscale, geometric mean floc size, the frequency of micro and macroflocs and flocculi, and primary particles and the settling velocity during about 10 days in April 2011.

water column [*Yuan et al.*, 2009], resulting thus in a mixture of cohesive and noncohesive sediment particles of various sizes in suspension. Previous research has shown that aggregates seem to be more armored against breakage in summer and the involvement of biologically mediated flocculation mechanisms besides the shear-dependent mechanism has been put forward to explain these observations [*Maggi*, 2009; *Lee et al.*, 2012; *Fettweis et al.*, 2014].

During maximum current velocities, which are the best condition for erosion of larger grains, most of the volume fraction of large particles generally decreases in our data (see Figures 9 and 10), pointing thus to mainly floc breakup and thus to cohesive sediments as the main constituents of the SPM. Floc size and settling velocities have been evaluated as a function of sea state characterized by the low-pass filtered Kolmogorov length scale. The results (Table 2 and Figure 9) show that the seasonality in floc size and settling velocity is only partially influenced by calm or stormy weather as the floc sizes remain higher in summer under various physical conditions. Erosion of larger particles from the seabed during storms, is therefore of minor importance to explain the seasonality at 2 m above the seabed. Biomediated flocculation is caused by the presence of microbial products, such as Transparent Extracellular Polymers (TEPs) that are released by algae and bacteria [*Logan et al.*, 1995; *Engel*, 2000; *Passow*, 2002]. The gluing capacity of these microbial exudates is known to enhance the building of organic-rich macroflocs [*Chen et al.*, 2005; *Droppo et al.*, 2005]. The phytoplankton bloom starts in early spring with a diatom bloom and shifts toward a phaeocystis bloom in April and May at the measuring

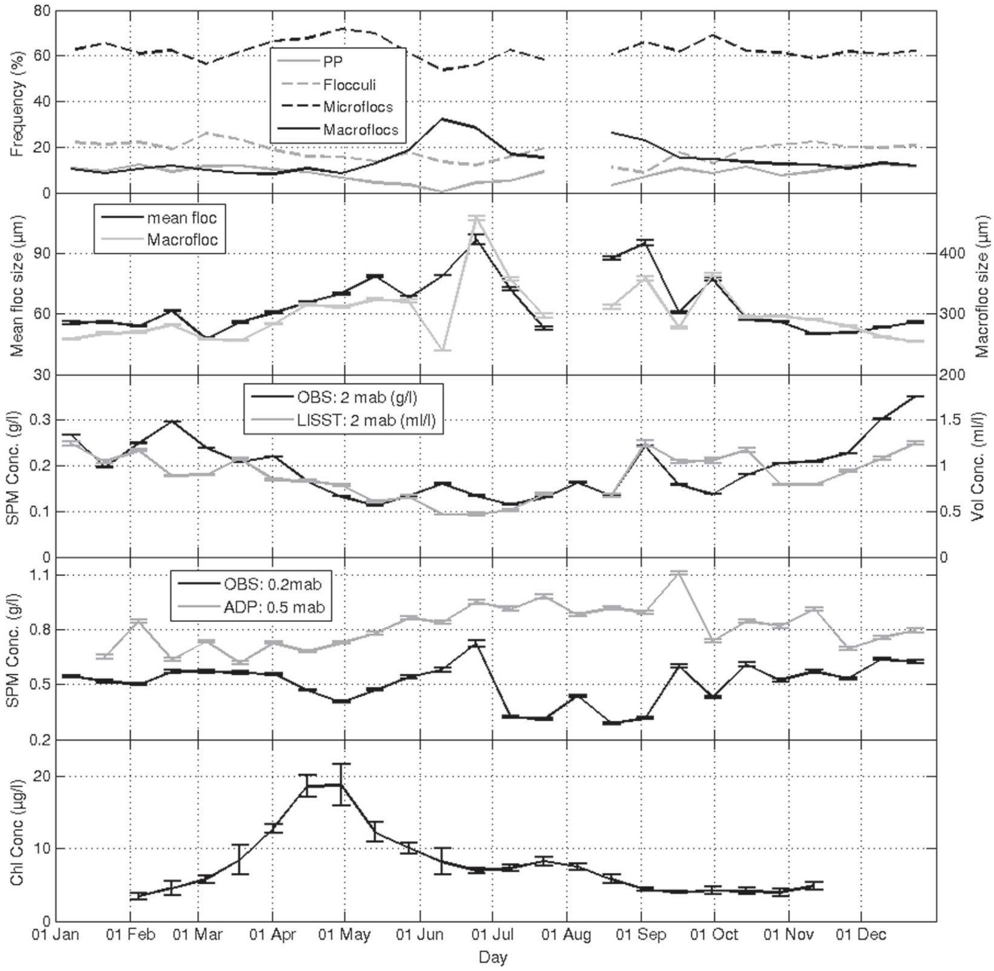

Figure 11. Two weekly averaged frequencies of primary particles, flocculi, microflocs, and macrolocs; mean and macrofloc size; SPM mass (OBS) and volume (LISST) concentration at 2 mab; SPM mass (OBS and ADP) concentration near the bed; and surface chlorophyll concentration. The Chl concentrations are from MERIS satellite and cover the period 2003–2011 [see *Fettweis et al.*, 2014], the other data are from the period 2005–2013. The error bars are standard errors.

location [*Lancelot et al.*, 1987]. Floc sizes show a significant increase in spring, followed by a decrease in July and again an increase in August and September (Figure 11). The decrease in July is possibly linked with the decrease of diatoms and phaeocystis concentrations, and hence TEP concentration, due to a shortage in nutrients and an increase in predation pressure by heterotrophic plankton species [*Rousseau et al.*, 2002]. Highest floc sizes are observed end of June and end of August, thus after the spring and summer blooms. Although the summer bloom is less pronounced, it results in Chl, heterotrophic bacteria and zooplankton concentration levels [*Lancelot et al.*, 2005] that are able to maintain high TEP concentration that generates these high floc sizes. These periods correspond with lower SPM concentrations in the water column, higher near-bed SPM concentrations, and higher frequencies of macroflocs.

5.2. Seasonality in SPM Concentration and the Occurrence of Lutoclines

Although the SPM concentration profiles do not prove the occurrence of lutoclines, they suggest, when extrapolated downward, higher SPM concentrations in the lowest 0.5 m above the seabed in summer and thus a higher probability of lutocline occurrence. The occurrence of fluffy layers of 0.05–0.10 m thickness has frequently been observed in bed samples from the measuring location. This is also confirmed by the ADV altimetry signal, which recorded variation in bed level occurring during a tidal cycle up to 20 cm. These variations are induced by sharp gradients in the SPM concentration that act as acoustic reflectors. The altimetry data show that the acoustic reflector is closer to the measuring volume of the ADV in winter than in summer. This may indicate a sharper gradient in the SPM concentration profile in summer than winter as is also suggested by the vertical profiles in Figure 4. The higher frequency of OBS saturation at 0.2 mab in summer than winter (section 3.2) supports this assumption, but the measuring techniques (acoustic and optic) are also blurring the results as OBS and ADP-derived SPM concentration are different in magnitude and as the mean OBS-derived SPM concentration at 0.2 mab is lower during summer in contrast with the ADP-derived SPM concentration (Table 1). The difference in mean SPM concentration between both data series is of the order of 50%. The underestimation of the ADP-derived SPM concentration at 1.8 mab with regard to the OBS-derived concentration reflects the uncertainty of the applied ADP calibration procedure and the correlation model. The ADP-derived SPM concentration at 0.5 mab is based on the calibration at 1.8 mab. The overestimation with respect to the 0.2 mab OBS-derived SPM concentration is possibly related to variations in SPM characteristics that have been observed at the measuring site during more extreme conditions (storm, maximum currents at spring tide), when sand is resuspended [*Fettweis et al*., 2012a]. Nevertheless, both data sets show a decreasing difference between winter and summer SPM concentration close to the bed, and suggest a higher SPM concentration in the very near-bed layer.

The higher summer SPM concentrations near the bed are supported by the data on floc size, settling velocity (Table 2 and Figure 11), and altimetry. The lower near-bed ADP-derived SPM concentration in winter during ebb and flood (Figure 3) and the larger difference in the altimetry signal in winter during a tide (8.5 cm in winter and 5.2 cm in summer) is probably a combination of the effects of lower settling velocities in winter, which enhances vertical mixing of the SPM, less stable near-bed SPM layers, and the fact that less SPM is present in the near-bed layer for resuspension. The higher near-bed SPM concentrations during slack water in winter are then caused by the lower settling velocities and the higher SPM concentrations in the water column. These result in a slower decrease of the SPM concentration at the near-bed measuring location.

The presence of TEPs has also an effect on the stability of mud layers and increases it erosion resistance [*Droppo et al*., 2001; *Black et al*., 2002; *Gerbersdorf et al*., 2008]. This would mean that in winter, the erosion resistance of the mud layer reduces as the stabilization effect of TEPs fades out. The possible effect of TEPs on the erosion resistance of the mud layers is visible in Figure 6, where the SPM concentration as a function of low-pass filtered Kolmogorov length scale is shown. During periods with higher wave-induced turbulence, the increase of SPM concentration near the bed is significantly larger in winter than in summer, which points to a better resistant of the mud layer against erosion in summer. The effects of seasonality in wave heights, although small (the mean significant wave height in winter is 0.75 m and in summer 0.63 m), are an additional, but not the main, explanation for the higher sensitivity of the SPM concentration in winter by wave-induced turbulence.

6. Conclusion

The long-term data series of SPM concentration, floc size, and settling velocity show a distinct seasonal signal. During summer, the SPM concentration is higher in the near bed, but lower higher up in the water column; during winter, the opposite is found. The floc size and settling velocity have an opposite seasonality: smaller flocs and thus settling velocities occur in winter and larger flocs and settling velocities in summer. Physical drivers such as wave heights and alongshore residual transports have a much weaker correlation with the observed seasonality. The seasonality in floc size and thus settling velocity is mainly the result of biological effects that enhances the size of the marine muddy flocs in summer. The results indicate that the SPM, or at least a significant part of it, stays in the area during summer and winter. In summer, the SPM is more concentrated in the near-bed layer, whereas in winter, the SPM is better mixed throughout the water column. The lower SPM concentrations in the water column during summer are thus compensated by higher near-bed SPM concentrations and possibly by a higher probability of occurrence of lutoclines.

The experimental approach was designed to measure the vertical SPM transport in the benthic boundary layer and cannot resolve accurately horizontal advection of SPM. The best way to resolve the horizontal dimension is using numerical sediment transport models as increasing the number of measuring locations is not an option due to the high costs and the still low horizontal resolution. Our results have shown that the near-bed processes do influence the SPM transport on different time scales and that significant part of the SPM fluxes occur in the benthic boundary layer. Simulations of the horizontal SPM advection should therefore incorporate the near-bed processes through, e.g., a physical-based bed shear stress model. Bed shear stress links the seafloor to the water column as it suspends sediments; influences and is influenced by the surface sediment texture and the microbathymetry; and contributes to turbulence generation, horizontal advection, and vertical mixing [*Dalyander et al*., 2013]. Models show promising results when the bed shear stress closure incorporates additional dissipation mechanisms (i.e., interparticle friction and collisions, and particle wake turbulence) that are important in the high SPM concentration layers occurring near the bed [*Bi and Toorman*, 2015].

Acknowledgment
The study was supported by the Maritime Access Division of the Ministry of the Flemish Community (MOMO project) and by the BRAIN-be program (BELSPO, INDI67 project). Ship Time RV Belgica was provided by BELSPO and RBINS–Operational Directorate Natural Environment. The wave data are from the Ministry of the Flemish Community (IVA MDK—afdeling Kust—Meetnet Vlaamse Banken). The mooring data can be obtained from the authors or from the Belgian Marine Data Centre (http://www.mumm.ac.be/datacentre). We thank L. Naudts, J. Backers, W. Vanhaverbeke, and K. Hindryckx for all technical aspects of instrumentation and moorings and F. Francken for data processing and archiving of the measurements. We would like to acknowledge the two reviewers for the pertinent comments that have significantly improved the manuscript.

References

Adriaens, R. (2015), Neogene and quarternary clay minerals in the southern North Sea, PhD thesis, 272 pp., KU Leuven, Leuven, Belgium.
Agrawal, Y., and H. Pottsmith (2000), Instruments for particle size and settling velocity observations in sediment transport, *Mar. Geol.*, *168*, 89–114.
Andrews, S., D. Nover, and S. Schladow (2010), Using laser diffraction data to obtain accurate particle size distributions: The role of particle composition, *Limnol. Oceanogr. Methods*, *8*, 507–526, doi:10.4319/lom.2010.8.507.
Arndt, S., G. Lacroix, N. Gypens, P. Regnier, and C. Lancelot (2011), Nutrient dynamics and phytoplankton development along an estuary–coastal zone continuum: A model study, *J. Mar. Syst.*, *84*, 49–66, doi:10.1016/j.jmarsys.2010.08.005.
Baeye, M., M. Fettweis, G. Voulgaris, and V. Van Lancker (2011), Sediment mobility in response to tidal and wind-driven flows along the Belgian inner shelf, southern North Sea, *Ocean Dyn.*, *61*, 611–622, doi:10.1007/s10236-010-0370-7.
Baeye, M., M. Fettweis, S. Legrand, Y. Dupont, and V. Van Lancker (2012), Mine burial in the seabed of high-turbidity area—Findings of a first experiment, *Cont. Shelf Res.*, *43*, 107–119, doi:10.1016/j.csr.2012.05.009.
Becker, M., K. Schrottke, A. Bartholomä, V. Ernstsen, C. Winter, and D. Hebbeln (2013), Formation and entrainment of fluid mud layers in troughs of subtidal dunes in an estuarine turbidity zone, *J. Geophys. Res.*, *118*, 2175–2187, doi:10.1002/jgrc.20153.
Berlamont, J., M. Ockenden, E. Toorman, and J. Winterwerp (1993), The characterisation of cohesive sediment properties, *Coastal Eng.*, *21*, 105–128.
Bi, Q., and E. A. Toorman (2015), Mixed-sediment transport modelling in Scheldt estuary with a physics-based bottom friction law, *Ocean Dyn.*, *65*, 555–587, doi:10.1007/s10236-015-0816-z.
Black, K. S., T. J. Tolhurst, D. M. Paterson, and S. E. Hagerthey (2002), Working with natural cohesive sediments, *J. Hydraul. Eng.*, *128*, 2–8, doi:10.1061/(ASCE)0733–9429(2002)128:1(2)).
Chen, M., S. Wartel, and S. Temmerman (2005), Seasonal variation of floc characteristics on tidal flats, the Scheldt estuary, *Hydrobiologia*, *540*, 181–195, doi:10.1007/s10750-004-7143-6.
Cross, J., W. A. M. Nimmo-Smith, R. Torres, and P. J. Hosegood (2013), Biological controls on resuspension and the relationship between particle size and the Kolmogorov length scale in a shallow coastal sea, *Mar. Geol.*, *343*, 29–38, doi:10.1016/j.margeo.2013.06.014.
Dalyander, P. S., B. Butman, C. R. Sherwood, R. P. Signell, and J. L. Wilkin (2013), Characterizing wave- and current- induced bottom shear stress: U.S. middle Atlantic continental shelf, *Cont. Shelf Res.*, *52*, 73–86, doi:10.1016/j.csr.2012.10.012.
Davies, E. J., W. A. M. Nimmo-Smith, Y. C. Agrawal, and A. J. Souza (2012), LISST-100 response to large particles, *Mar. Geol.*, *307-310*, 117–122, doi:10.1016/j.margeo.2012.03.006.
Downing, J. (2006), Twenty-five years with OBS sensors: The good, the bad, and the ugly, *Cont. Shelf Res.*, *26*, 2299–2318, doi:10.1016/j.csr.2006.07.018.
Droppo, I., G. Leppard, S. Liss, and T. Milligan (2005), *Flocculation in Natural and Engineered Environmental Systems*, CRC Press, Boca Raton, Fla.
Droppo, I. G., Y. L. Lau, and C. Mitchell (2001), The effect of depositional history on contaminated bed sediment stability, *Sci. Total Environ.*, *266*, 7–13.
Dyer, K. R. (1989), Sediment processes in estuaries: Future research requirements, *J. Geophys. Res.*, *94*(C10), 14,327–14,339.
Eisma, D. (1986), Flocculation and de-flocculation of suspended matter in estuaries, *Neth. J. Sea Res.*, *20*, 183–199.
Engel, A. (2000), The role of transparent exopolymer particles (TEP) in the increase in apparent particle stickiness during the decline of a diatom bloom, *J. Plankton Res.*, *22*, 485–497.
Fettweis, M. (2008), Uncertainty of excess density and settling velocity of mud flocs derived from in situ measurements, *Estuarine Coastal Shelf Sci.*, *78*, 428–436, doi:10.1016/j.ecss.2008.01.007.
Fettweis, M., J.-S. Houziaux, I. Du Four, V. Van Lancker, C. Baeteman, M. Mathys, D. Van den Eynde, F. Francken, and S. Wartel (2009), Long-term influence of maritime access works on the distribution of cohesive sediment: Analysis of historical and recent data from the Belgian nearshore area (southern North Sea), *Geo Mar. Lett.*, *29*, 321–330, doi:10.1007/s00367-009-0161-7.
Fettweis, M., M. Baeye, B. J. Lee, P. Chen, and J. C. R. Yu (2012a), Hydro-meteorological influences and multimodal suspended particle size distributions in the Belgian nearshore area (southern North Sea), *Geo Mar. Lett.*, *32*, 123–137, doi:10.1007/s00367-011-0266-7.
Fettweis, M., J. Monbaliu, B. Nechad, M. Baeye, and D. Van den Eynde (2012b), Weather and climate related spatial variability of high turbidity areas in the North Sea and the English Channel, *Methods Oceanogr.*, *3-4*, 25–29, doi:10.1016/j.mio.2012.11.001.
Fettweis, M., M. Baeye, D. Van der Zande, D. Van den Eynde, and B. J. Lee (2014), Seasonality of floc strength in the southern North Sea, *J. Geophys. Res. Oceans*, *119*, 1911–1926, doi:10.1002/2013JC009750.
Flagg, C. N., J. A. Vermersch, and R. C. Beardsley (1976), 1974 MIT New England shelf dynamic experiment (March 1974) data report, part II: The moored array, *Rep. 76-1*, Mass. Inst. of Technol., Cambridge, U. K.
Friedrichs, C. T., G. M. Cartwright, and P. J. Dickhudt (2008), Quantifying benthic exchange of fine sediment via continuous: Noninvasive measurements of settling velocity and bed erodibility, *Oceanogrphy*, *21*, 168–172.
Fugate, D. C., and C. T. Friedrichs (2002), Determining concentration and fall velocity of estuarine particle populations using ADV, OBS and LISST, *Cont. Shelf Res.*, *22*, 1867–1886.
Gerbersdorf, S. U., T. Jancke, P. Westrich, and D. M. Paterson (2008), Microbial stabilization of riverine sediments by extracellular polymeric substances, *Geobiology*, *6*, 57–69, doi:10.1111/j.1472–4669.2007.00120.x.
Gerritsen, H., J. G. Boon, T. van der Kaaij, and R. J. Vos (2001), Integrated modelling of suspended matter in the North Sea, *Estuarine Coastal Shelf Sci.*, *53*, 581–594.
Goossens, D. (2008), Techniques to measure grain size distributions of loamy sediments: A comparative study of ten instruments for wet analysis, *Sedimentology*, *55*, 65–96, doi:10.1111/j.365–3091.2007.00893.x.
Graham, G. W., E. J. Davies, W. A. M. Nimmo-Smith, D. G. Bowers, and K. M. Braithwaite (2012), Interpreting LISST-100X measurements of particles with complex shape using digital in-line holography, *J. Geophys. Res.*, *117*, C05034, doi:10.1029/2011JC007613.

Ha, H. K., J.-P. Y. Maa, K. Park, and Y. H. Kim (2011), Estimation of high-resolution sediment concentration profiles in bottom boundary layer using pulse-coherent acoustic doppler current profilers, *Mar. Geol.*, *279*, 199–209, doi:10.1016/j.margeo.2010.11.002.

Howarth, M. J., et al. (1993), Seasonal cycles and their spatial variability, *Philos. Trans. R. Soc. London A*, *343*, 383–403.

Jago, C. F., G. M. Kennaway, G. Novarino, and S. E. Jones (2007), Size and settling velocity of suspended flocs during a phaeocystis bloom in the tidally stirred Irish Sea, NW European Shelf, *Mar. Ecol. Prog. Ser.*, *345*, 51–62, doi:10.3354/meps07006.

Keyvani, A., and K. Strom (2014), Influence of cycles of high and low turbulent shear on the growth rate and equilibrium size of mud flocs, *Mar. Geol.*, *345*, 1–14, doi:10.1016/j.margeo.2014.04.010.

Kirby, R. (2011), Minimising harbour siltation—Findings of PIANC Working Group 43, *Ocean Dyn.*, *61*, 233–244, doi:10.1007/s10236-010-0336-9.

Kranenburg, C. (1994), On the fractal structure of cohesive sediment aggregates, *Estuarine Coastal Shelf Sci.*, *39*, 451–460.

Lacroix, G., K. Ruddick, J. Ozer, and C. Lancelot (2004), Modelling the impact of the Scheldt and Rhine/Meuse plumes on the salinity distribution in Belgian waters (southern North Sea), *J. Sea Res.*, *52*, 149–163, doi:10.1016/j.seares.2004.01.003.

Lancelot, C., G. Billen, A. Sournia, T. Weisse, F. Colijn, M. J. W. Veldhuis, A. Davies, and P. Wassman (1987), Phaeocystis blooms and nutrient enrichment in the continental coastal zones of the North Sea, *Ambio*, *16*, 38–46.

Lancelot, C., Y. Spitz, N. Gypens, K. Ruddick, S. Becquevort, V. Rousseau, G. Lacroix, and G. Billen (2005), Modelling diatom and *Phaeocystis* blooms and nutrient cycles in the Southern Bight of the North Sea: The MIRO model, *Mar. Ecol. Prog. Ser.*, *289*, 63–78.

Le Hir, P., P. Bassoullet, and H. Jestin (2000), Application of the continuous modeling concept to simulate high-concentration suspended sediment in a macrotidal estuary, *Proc. Mar. Sci.*, *3*, 229–247.

Lee, B. J., M. Fettweis, E. Toorman, and F. Molz (2012), Multimodality of a particle size distribution of cohesive suspended particulate matters in a coastal zone, *J. Geophys. Res.*, *117*, C03014, doi:10.1029/2011JC007552.

Lee, H. L., and P. L. Wiberg (2002), Character, fate, and biological effects of contaminated, effluent-affected sediment on the Palos Verdes margin, southern California: An overview, *Cont. Shelf Res.*, *22*, 835–840.

Logan, B. E., U. Passow, A. L. Alldredge, H.-P. Grossartt, and M. Simon (1995), Rapid formation and sedimentation of large aggregates is predictable from coagulation rates (half-lives) of Transparent Exopolymer Particles (TEP), *Deep Sea Res., Part II*, *42*, 203–214.

MacDonald, I. T., C. E. Vincent, P. D. Thorne, and B. D. Moate (2013), Acoustic scattering from a suspension of flocculated sediments, *J. Geophys. Res. Oceans*, *118*, 2581–2594, doi:10.1002/jgrc.20197.

Maggi, F. (2009), Biological flocculation of suspended particles in nutrient rich aqueous ecosystems, *J. Hydrol.*, *376*, 116–125, doi:10.1016/j.jhydrol.2009.07.040.

Markussen, T. N., and T. J. Andersen (2013), A simple method for calculating in situ floc settling velocities based on effective density functions, *Mar. Geol.*, *344*, 10–18, doi:10.1016/j.margeo.2013.07.002.

McAnally, W. H., C. Friedrichs, D. Hamilton, E. Hayter, P. Shrestha, H. Rodriguez, A. Sheremet, and A. Teeter (2007a), Management of fluid mud in estuaries, bays, and lakes. I: Present state of understanding on character and behavior, *J. Hydraul. Eng.*, *133*, 9–22, doi:10.1061/(ASCE)0733–9429(2007)133:1(9).

McAnally, W. H., A. Teeter, D. Schoellhamer, C. Friedrichs, E. Hayter, P. Shrestha, H. Rodriguez, A. Sheremet, and R. Kirby (2007b), Management of fluid mud in estuaries, bays, and lakes. II: Measurement, modeling and management, *J. Hydraul. Eng.*, *133*, 23–38, doi:10.1061/(ASCE)0733–9429(2007)133:1(23).

Mehta, A. J. (1986), Characterisation of cohesive sediment properties and transport processes in estuaries, in *Estuarine Cohesive Sediment Dynamics, Lecture Notes on Coastal and Estuarine Studies*, edited by A. J. Mehta, pp. 290–325, Springer-Verlag, Berlin Heidelberg.

Mehta, A. J. (1991), Understanding fluid mud in a dynamic environment, *Geo Mar. Lett.*, *11*, 113–118.

Mikkelsen, O., P. Hill, and T. Milligan (2006), Single-grain, microfloc and macrofloc volume variations observed with a LISST-100 and a digital floc camera, *J. Sea Res.*, *55*, 87–102, doi:10.1016/j.seares.2005.09.003.

Mikkelsen, O. A., and M. Pejrup (2001), The use of a LISST-100 laser particle sizer for in-situ estimates of floc size, density and settling velocity, *Geo Mar. Lett.*, *20*, 187–195.

Nauw, J. J., L. M. Merckelbach, H. Ridderinkhof, and H. M. van Aken (2014), Long-term ferry-based observations of the suspended sediment fluxes through the Marsdiep inlet using acoustic Doppler current profilers, *J. Sea Res.*, *87*, 17–29, doi:10.1016/j.seares.2013.11.013.

Passow, U. (2002), Transparent exopolymer particles (TEP) in aquatic environments, *Prog. Oceanogr.*, *55*, 287–333.

Rouhnia, M., A. Keyvani, and K. Strom (2014), Do changes in the size of mud flocs affect the acoustic backscatter values recorded by a Vector ADV?, *Cont. Shelf Res.*, *84*, 84–92, doi:10.1016/j.csr.2014.05.015.

Rousseau, V., A. Leynaert, N. Daoud, and C. Lancelot (2002), Diatom succession, silicification and silicic acid availability in Belgian coastal waters (southern North Sea), *Mar. Ecol. Prog. Ser.*, *236*, 61–73.

Sherwood, C., J. Lacy, and G. Voulgaris (2006), Shear velocity estimates on the inner shelf off Grays Harbor, Washington, USA, *Cont. Shelf Res.*, *26*, 1995–2018, doi:10.1016/j.csr.2006.07.025.

Stapleton, R. L., and D. A. Huntley (1995), Seabed stress determination using the inertia dissipation method and the turbulent kinetic energy method, *Earth Surf. Processes Landforms*, *20*, 807–815.

Thompson, C. E. L., C. L. Amos, T. E. R. Jones, and J. Chaplin (2003), The manifestation of fluid-transmitted bed shear stress in a smooth annular flume—A comparison of methods, *J. Coastal Res.*, *19*, 1094–1103.

Thorne, P. D., and D. M. Hanes (2002), A review of acoustic measurement of small-scale sediment processes, *Cont. Shelf Res.*, *22*, 603–632.

Thorne, P. D., C. E. Vincent, P. J. Hardcastle, S. Rehman, and N. D. Pearson (1991), Measuring suspended sediment concentrations using acoustic backscatter devices, *Mar. Geol.*, *98*, 7–16.

Toorman, E. A. (2002), Modelling of turbulent flow with cohesive sediment, *Proc. Mar. Sci.*, *5*, 155–169.

Trowbridge, J. H., and S. Elgar (2001), Turbulence measurements in the surf zone, *J. Phys. Oceanogr.*, *31*, 2403–2417.

van Ledden, M., Z.-B. Wang, H. Winterwerp, and H. de Vriend (2004), Sand–mud morphodynamics in a short tidal basin, *Ocean Dyn.*, *54*, 385–391, doi:10.1007/s10236-003-0050-y.

van Leussen, W. (1999), The variability of settling velocities of suspended fine-grained sediment in the Ems estuary, *J. Sea Res.*, *41*, 109–118, doi:10.1016/S1385-1101(98)00046-X.

Verney, R., R. Lafite, and J.-C. Brun-Cottan (2009), Flocculation potential of estuarine particles: The importance of environmental factors and of the spatial and seasonal variability of suspended particulate matter, *Estuaries Coasts*, *32*, 678–693, doi:10.1007/s12237-009-9160-1.

Voulgaris, G., and S. Meyers (2004), Temporal variability of hydrodynamics, sediment concentration and sediment settling velocity in a tidal creek, *Cont. Shelf Res.*, *24*, 1659–1683, doi:10.1016/j.csr.2004.05.006.

Wan, Y., D. Roelvink, W. Li, D. Qi, and F. Gu (2014), Observation and modeling of the storm-induced fluid mud dynamics in a muddy-estuarine navigational channel, *Geomorphology*, *217*, 23–36, doi:10.1016/j.geomorph.2014.03.050.

Whitby, K. (1978), The physical characteristics of sulfur aerosols, *Atmos. Environ.*, *41*, 25–49.

Winterwerp, J., A. Manning, C. Martens, T. de Mulder, and J. Vanlede (2006), A heuristic formula for turbulence-induced flocculation of cohesive sediment, *Estuarine Coastal Shelf Sci.*, *68*, 195–207, doi:10.1016/j.ecss.2006.02.003.
Winterwerp, J. C. (1998), A simple model for turbulence induced flocculation of cohesive sediment, *J. Hydraul. Eng.*, *36*, 309–326.
Winterwerp, J. C. (2002), On the flocculation and settling velocity of estuarine mud, *Cont. Shelf Res.*, *22*, 1339–1360.
Winterwerp, J. C. (2006), Stratification effects by fine suspended sediment at low, medium and very high concentrations, *J. Geophys. Res.*, *111*, C05012, doi:10.1029/2005JC003019.
Yuan, Y., H. Wei, L. Zhao, and Y. Cao (2009), Implications of intermittent turbulent bursts for sediment resuspension in a coastal bottom boundary layer: A field study in the western Yellow Sea, China, *Mar. Geol.*, *263*, 87–96, doi:10.1016/j.margeo.2009.03.023.

APPENDIX 2

Bijdragen

13th International Conference on Cohesive Sediment Transport Processes (INTERCOH), *7-11 September 2015, Leuven*

Dujardin A, Vanlede J, Van Hoestenberghe T, Van Poucke L, Fettweis M, Cardoso C, Velez C, Martens M. 2015. Factors influencing top sediment layer and SPM concentration in the Zeebrugge harbor.

Fettweis M, Baeye M, Verney R. 2015. Uncertainty of in situ SPM concentration measurements.

Fettweis M, Baeye M, Francken F, Van den Eynde D, Van Hoestenberghe T, Van Poucke L, Dujardin A, Martens C. 2015. In situ measurements of SPM concentration to evaluate the impact of the disposal of fine grained sediments from maintenance dredging.

Lee BJ, Bi Q, Toorman EA, Fettweis M, Weilbeer H. 2015. Two-Class Flocculation Kinetic Model: Development and Application to Large-scale, Multi-dimensional Cohesive Sediment Transport.

Thant S, Fettweis M, Baeye M, Monbaliu J. 2015. Wave systems and their impact on the seabed and water column turbidity in the Belgian coastal zone.

Van den Eynde D, Baeye M, Fettweis M, Francken F, Van Lancker V. 2015. Validation of modelled bottom shear stress under the influence of currents and waves using long-term measurements.

Factors influencing top sediment layer and SPM concentration in the Zeebrugge harbor

Dujardin Arvid[1], Joris Vanlede[2], Thomas Van Hoestenberghe[1], Luc Van Poucke[1], Michael Fettweis[3], Claudio Cardoso[1], Carlos Velez[1], Renaat De Sutter[1] and Chantal Martens[4]

[1] Antea Group, Buchtenstraat 9, B-9051 Gent, Belgium
E-mail: arvid.dujardin@anteagroup.com

[2] Flanders Hydraulics Research, Department of Mobility and Public Works, Flemish Government, Berchemlei 115, B-2140 Antwerp, Belgium

[3] Operational Directorate Natural Environment, Royal Belgian Institute of Natural Sciences, Gulledelle 100, B-1200 Brussels, Belgium

[4] Maritime Access Division, Department of Mobility and Public Works, Flemish Government, Tavernierkaai 3, B-2000 Antwerp, Belgium

The port of Zeebrugge (Belgium) suffers from significant siltation. To safeguard navigation, on average 5 million tons (dry matter) is yearly dredged inside the harbor (Dujardin *et al.*, in progress) and an additional 1.6 million tons (dry matter) in the access channel Pas van het Zand (Lauwaert *et al.*, 2006 & 2008), and disposed on authorized disposal sites in the Belgian part of the North Sea. Numerical model results indicate that a significant part of the disposed sediments recirculates back from the current disposal sites to the dredging areas (Van den Eynde and Fettweis, 2014). A field study, accompanied by an extensive monitoring campaign, was set up in 2013-2014 to verify whether using an alternative disposal site is influencing the SPM concentration and the top sediment layer in the harbor. In addition to the monitoring campaign and in order to better assess the results of the field study, the baseline system behavior was also characterized over a longer period (1999-2012).

The mechanisms causing the sediment from the North Sea to enter the harbor have been intensively studied the last decade (Dujardin *et al.*, 2009; Vanlede and Dujardin, 2014). The sediment dynamics inside of the harbor, however, are still largely unknown. The present study aims to quantify the influence of internal and external factors on the sediment dynamics within Zeebrugge harbor, based on both the 2013-2014 monitoring campaign and the longer period datasets. Possible factors external to the harbor are tide, wind, currents, wave climate, salinity and SPM concentration. The factors internal to the harbor are navigation, dredging operations and fresh water discharge.

For the 2013-2014 campaign, measurements inside and outside the port of Zeebrugge of various oceanographic and sediment parameters (SPM concentration, current velocity, waves, salinity, temperature, tides, wind, bathymetry, density of mud layers) were conducted during the whole duration of the experiment. The measurements outside the port are presented in Fettweis *et al.* (this volume). The monitoring inside the port was carried out at 4 locations. At each location, time series of currents, salinity, temperature, water elevation and SPM concentration were collected near the surface and near the bed. Measurements show for all locations that the maximum SPM concentration reaches more than 4g/l near the bed and up to 2g/l at the surface.

For the characterization of the baseline system behavior, a long-term dataset (1999-2012) is available of the height of the 210kHz and 33kHz reflector, fresh water inflow in the harbor, wind, wave, and tidal data, surface SPM data derived from satellite images (GRIMAS dataset) and dredging quantities. Within this dataset, bathymetric measurements were less frequent than during the 2013-2014 field study, except for the summer of 2012 (Dujardin *et al.*, 2014).

Correlations between different parameters are analyzed, both for the shorter (one year) and longer (13 year) period. Statistical relations were established based on the long-term dataset (Dujardin *et al.*, in progress) and the results from the 2013-2014 study were compared with the findings for the 1999-2012 period. In the harbor, local currents, tidal amplitude and SPM concentrations are significantly correlated. Daily variations in SPM concentrations and bathymetry (210kHz reflector level) are related to tides, storms, seasonal changes, ship movements and dredging operations.

References

Baeye M., M. Fettweis, G. Voulgaris and V. Van Lancker. 2011. Sediment mobility in response to tidal and wind-driven flows along the Belgian inner shelf, southern North Sea. Ocean Dynamics 61:611-622.

Dujardin A., S. Ides, G. Schramkowski, T. De Mulder and F. Mostaert. 2009. Haven van Zeebrugge – Optimalisatie maritieme toegankelijkheid: Onderzoek naar de water- en sedimentuitwisseling ter hoogte van de havenmond. Versie 3_0. WL Rapporten, 843_01. Waterbouwkundig Laboratorium, Antwerpen, Belgium. (in Dutch).

Dujardin A., J. Vanlede, S. Vos, T. Verwaest and F. Mostaert. 2014. Invloedsfactoren op de ligging van de top van de sliblaag in het CDNB: Deelrapport 1 – Casestudy “zomer 2012”. Versie 2.0. WL Rapporten, 00_078. Waterbouwkundig Laboratorium & Antea Group, Antwerpen, Belgium. (in Dutch).

Dujardin A., J. Vanlede, S. Vos, T. Verwaest and F. Mostaert. (in progress). Invloedsfactoren op de ligging van de top van de sliblaag in het CDNB: Deelrapport 2 – Analyse periode 1999 - 2011. Versie 1.0. WL Rapporten, 00_078. Waterbouwkundig Laboratorium & Antea Group, Antwerpen, Belgium. (in Dutch).

Fettweis M., M. Baeye, F. Francken, B. Lauwaert, D. Van den Eynde, V. Van Lancker, C. Martens and T. Michielsen. 2011. Monitoring the effects of disposal of fine sediments from maintenance dredging on suspended particulate matter concentration in the Belgian nearshore area (southern North Sea). Marine Pollution Bulletin 62:258–269.

Fettweis M., M. Baeye, T. Van Hoestenberghe, L. Van Poucke, A. Dujardin and V. Van Lancker. 2015. *In situ* measurements of SPM concentration to evaluate the impact of the disposal of fine grained sediments from maintenance dredging. Proc. Intercoh 2015 (this issue).

Lauwaert B., K. Bekaert, D. De Brauwer, M. Fettweis, H. Hillewaert, S. Hoffman, K. Hostens, K. Mergaert, I. Moulaert, K. Parmentier and J. Verstraeten. 2006. Synthesis report on the effects of dredged material disposal on the marine environment (licensing period 2004-'06). MUMM, ILVO Fisheries, Maritime Access Division, and Coast Division. Ostend, Belgium.

Lauwaert B., K. Bekaert, M. Berteloot, D. De Brauwer, M. Fettweis, H. Hillewaert, S. Hoffman, K. Hostens, K. Mergaert, I. Moulaert, K. Parmentier, G. Vanhoey and J. Verstraeten. 2008. Synthesis report on the effects of dredged material disposal on the marine environment (licensing period 2006-'08). MUMM, ILVO Fisheries, Maritime Access Division, and Coast Division. Ostend, Belgium. 109p.

Van den Eynde D. and M. Fettweis. 2014. Towards the application of an operational sediment transport model for the optimisation of dredging works in the Belgian coastal zone (southern North Sea). p.250-257. In: Dahlin H., N.C. Flemming, S.E. Petersson (Eds). Sustainable Operational Oceanography.

Vanlede J and A. Dujardin. 2014. A geometric method to study water and sediment exchange in tidal harbors. Ocean Dynamics, DOI 10.1007/s10236-014-0767-9.

Uncertainty of *in situ* SPM concentration measurements

Fettweis Michael[1], Matthias Baeye[1] and Romaric Verney[2]

[1] Operational Directorate Natural Environment, Royal Belgian Institute of Natural Sciences, Gulledelle 100, B-1200 Brussels, Belgium
E-mail: m.fettweis@mumm.ac.be

[2] Laboratoire Dyneco/Physed, IFREMER, BP 70, F-29280 Plouzané, France

The aim of the study is to assess the state of our understanding, to evaluate the confidence with which SPM concentration can be measured, and to identify human impact in the data series. Direct or indirect measurements of parameters are inherently associated with uncertainties (errors) due to a lack of accuracy of the measuring instruments, inadequate precision of the observations, and the statistical nature of the parameters. When using observations, understanding of the uncertainties is needed, in order to avoid speculative statements. Uncertainty will become an important issue for scientists and decision-makers in the future as they will be used to evaluate GES of the European marine areas and to predict the impact of human activities. Uncertainty in measured data can originate from different sources (Winter, 2007). Those that can be reduced by further study of the system and improving our state of knowledge, and those that are considered unknowable such as variability in the system beyond the existing time series, the chaotic nature of the system, and the indeterminacy of human systems (Dessai and Hulme, 2003).

SPM concentration can be measured using optical or acoustic sensors. The voltage output of Optical Backscatter Sensors (OBS) is converted to Formazine Technical Unit using solutions of formazine and SPM concentration by calibration against filtered water samples. After conversion to decibels, the backscattered acoustic signal strength (from an Acoustic Doppler Profiler) is corrected for geometric spreading, water attenuation, sediment attenuation (Kim *et al*., 2004) and is calibrated using the OBS-derived SPM concentration estimates (Fettweis, 2008). In general, acoustic backscattering is affected by sediment type, size and composition (Thorne *et al*., 1991; Hamilton *et al*., 1998; Bunt *et al*., 1999; Fugate and Friedrichs, 2002; Voulgaris and Meyers, 2004). OBS signals have primarily been designed to be most sensitive to SPM concentration; size effects are an order of magnitude lower than those of concentration, and flocculation effects are even smaller (Downing, 2006). Compared to optical devices, acoustic devices are more sensitive to coarser grain sizes and thus produce better estimates of the mass concentration of the coarser granular fraction. Changes in colour, size and density of the suspended sediments have been reported to influence the OBS results by a factor 10 to 20 (Sutherland *et al*., 2000). The latter is especially disturbing when using long-term time series of data of SPM concentration from OBS, as it is collected at a station near Zeebrugge and in the Seine Estuary, and where changes in sediment composition during e.g. a storm or fortnightly cycles have been reported (Baeye *et al*., 2011; Fettweis *et al*., 2012; Verney *et al*., 2013). Therefore a careful analysis of existing calibration data, of LISST data, and of acoustic and optical sensor data, has been carried out. Calibration of sensors (OBS and ADCP) is carried out during 6 tidal cycle measurements in the Belgian nearshore area and the Seine Estuary using *in situ* water samples. The analysis allows to evaluate calibration procedures of sensor output as a function of e.g. seasonal changes in composition and thus on the uncertainty of long-term time series of SPM concentration derived from acoustic and optical measurements of turbidity.

References

Baeye M., M. Fettweis, G. Voulgaris and V. Van Lancker 2011. Sediment mobility in response to tidal and wind-driven tidal flows along the Belgian ineer shelf, southern North Sea. Ocean Dynamics 61(5): 611-622.

Bunt J.A.C, P. Larcombe and C.F. Jago 1999. Quantifying the response of optical backscatter devices and transmissometers to variations in suspended particulate matter. Continental Shelf Research 19:1199–1220.

Dessai S. and M. Hulme 2003. Does climate policy need probabilities? Tyndall Centre for Climate Change Research, Working Paper 34, 42p.

Downing J. 2006. Twenty-five years with OBS sensors: the good, the bad, and the ugly. Continental Shelf Research 26:2299–2318.

Fettweis M. 2008. Uncertainty of excess density and settling velocity of mud flocs derived from in situ measurements. Estuarine Coastal and Shelf Science 78:428-436.

Fettweis M., M. Baeye, B.J. Lee, P. Chen and J.C.R. Yu 2012. Hydro-meteorological influences and multimodal suspended particle size distributions in the Belgian nearshore area (southern North Sea). Geo-Marine Letters 32:123-137.

Fugate D.C. and C.T. Friedrichs 2002. Determining concentration and fall velocity of estuarine particle populations using ADV, OBS and LISST. Continental Shelf Research 22:1867–1886.

Hamilton L.J., Z. Shi and S.Y. Zhang. 1998. Acoustic backscatter measurements of estuarine suspended cohesive sediment concentration profiles. Journal of Coastal Research 14:1213–1224.

Sutherland T.F., P.M. Lane, C.L. Amos and J. Downing 2000. The calibration of optical backscatter sensors for suspended sediment of varying darkness levels. Marine Geology 162:587-597.

Thorne P.D., C.E. Vincent, P.J. Hardcastle, S. Rehman and N.D. Pearson 1991. Measuring suspended sediment concentrations using acoustic backscatter devices. Marine Geology 98:7–16.

Verney R., G. Voulgaris, A. Manning, J. Deloffre and P. Bassoullet 2013. Quantifying suspended particulate matter (SPM) dynamics in estuaries: Combining acoustic and optical approaches. Proc. of the 12th Int. Conf. on Cohesive Sediment Transport Processes (INTERCOH), Gainesville, Florida.

Voulgaris G. and S. Meyers 2004. Temporal variability of hydrodynamics, sediment concentration and sediment settling velocity in a tidal creek. Continental Shelf Research 24:1659–1683.

Winter C. 2007. Evaluation of Sediment Transport Models. Sedimentary Geology 202:562-571.

In situ measurements of SPM concentration to evaluate the impact of the disposal of fine grained sediments from maintenance dredging

Fettweis Michael[1], Matthias Baeye[1], Thomas Van Hoesteberghe[2], Luc Van Poucke[2], Arvid Dujardin[2,3] and Chantal Martens[4]

[1] Operational Directorate Natural Environment, Royal Belgian Institute of Natural Sciences, Gulledelle 100, B-1200 Brussels, Belgium
E-mail: m.fettweis@mumm.ac.be

[2] Antea Group, Buchtenstraat 9, B-9051 Gent, Belgium

[3] Flanders Hydraulics Research, Department of Mobility and Public Works, Flemish Government, Berchemlei 115, B-2140 Antwerp, Belgium

[4] Maritime Access Division, Department of Mobility and Public Works, Flemish Government, Tavernierkaai 3, B-2000 Antwerp, Belgium

The aim of this study is to present and discuss the impact of disposal of fine-grained sediments on the SPM concentration and on the fluid mud dynamics in the turbid Belgian nearshore area (southern North Sea). Measurements show that the SPM concentration reaches more than 3g/l near the bed and up to 0.3g/l at the surface; lower values (<0.01g/l) occur more offshore (Fettweis *et al.*, 2010). The high SPM concentration results in high deposition of cohesive sediments that accumulate in man-made areas such as the ports and navigation channels. About 5 million tons (dry matter) per year of mainly fine-grained sediments is dredged in the port of Zeebrugge and is disposed on a nearby disposal site (Lauwaert *et al.*, 2008). The disposed sediments are quickly resuspended and transported away from the site. The results of a numerical study showed that a significant part recirculates back to the dredging places and that a relocation of the disposal site to another location at equal distance to the dredging area reduces this recirculation (Van den Eynde and Fettweis, 2014). In order to validate the model results a one year field study was set up in 2013-2014. During one month the dredged material was disposed at a new site and the efficiency of the new location was evaluated. Measurements inside and outside the port of Zeebrugge of various oceanographic and sediment parameters (SPM concentration, current velocity, waves, salinity, temperature, tides, wind, bathymetry, density of mud layers) were conducted during the experiment.

The measurements inside the port are presented in Dujardin *et al.* (this volume). The monitoring outside the port was carried out at two locations near the entrance of the port using instrumented tripods. Variations in SPM concentration were related to tides, storms, seasonal changes and human impacts. In order to evaluate the impact of the relocation of the disposal operations a statistical approach was used (Baeye *et al.*, 2011; Fettweis *et al.*, 2011). The measured SPM concentration time series during the relocation experiment were statistically compared against the population data. Both experiment samples and population are characterized by statistical properties, such as median, geometrical mean, standard deviation and probability density distribution. The analysis method is based on the concept of statistical populations and provides a tool to account for the complexities associated with natural dynamics and the need to evaluate quantitatively human impact. SPM concentration can be used as an indicator of environmental changes if sufficiently long time series are available that are representative of the natural variability.

References

Baeye M., M. Fettweis, G. Voulgaris and V. Van Lancker. 2011. Sediment mobility in response to tidal and wind-driven flows along the Belgian inner shelf, southern North Sea. Ocean Dynamics 61:611-622.

Dujardin A., J. Vanlede, T. Van Hoestenberghe, L. Van Poucke, M. Fettweis, C. Cardoso, C. Velez and C. Martens. 2015. Factors influencing top sediment layer and SPM concentration in the Zeebrugge harbor. Proc. Intercoh 2015. (this issue)

Fettweis M., F. Francken, D. Van den Eynde, T. Verwaest, J. Janssens and V. Van Lancker. 2010. Storm influence on SPM concentrations in a coastal turbidity maximum area (southern North Sea) with high anthropogenic impact. Continental Shelf Research 30:1417-1427.

Fettweis M., M. Baeye, F. Francken, B. Lauwaert, D. Van den Eynde, V. Van Lancker, C. Martens and T. Michielsen. 2011. Monitoring the effects of disposal of fine sediments from maintenance dredging on suspended particulate matter concentration in the Belgian nearshore area (southern North Sea). Marine Pollution Bulletin 62:258–269.

Lauwaert B., K. Bekaert, M. Berteloot, D. De Brauwer, M. Fettweis, H. Hillewaert, S. Hoffman, K. Hostens, K. Mergaert, I. Moulaert, K. Parmentier, G. Vanhoey and J. Verstraeten. 2008. Synthesis report on the effects of dredged material disposal on the marine environment (licensing period 2006-'08). MUMM, ILVO Fisheries, Maritime Access Division, and Coast Division. Ostend, Belgium. 128p.

Van den Eynde D. and M. Fettweis. 2014. Towards the application of an operational sediment transport model fort the optimisation of dredging works in the Belgian coastal zone (southern North Sea). p.250-257. In: Dahlin H., N.C. Flemming, S.E. Petersson (Eds). Sustainable Operational Oceanography.

In situ measurements of SPM concentration to evaluate the impact of the disposal of fine grained sediments from maintenance dredging

Michael Fettweis[1], Matthias Baeye[1], Frederic Francken[1], Dries Van den Eynde[1], Thomas Van Hoestenberghe[2], Luc Van Poucke[2], Arvid Dujardin[2,3], Chantal Martens[4]

[1] Royal Belgian Institute of Natural Sciences – Operational Directorate Natural Environment, Gulledelle 100, B-1200 Brussels, Belgium
[2] Antea Group, Buchtenstraat 9, B-9051 Gent, Belgium
[3] Flanders Hydraulics Research, Flemish Government, Department of Mobility and Public Works, Berchemlei 115, B-2140 Antwerp, Belgium
[4] Maritime Access Division, Flemish Government, Department of Mobility and Public Works, Tavernierkaai 3, B-2000 Antwerp, Belgium

Reducing maintenance dredging through relocation of disposal site

1. What is the recirculation of disposed fine grained sediments from the disposal site towards the dredging site?
2. Relocation of the disposal site (from ZBO to ZBW). Is the SPM concentration significantly decreasing near the dredging places?
3. What is the impact of disposal of fine-grained sediments on the SPM concentration in the turbid Belgian nearshore area (southern North Sea)?

The 19,100 TEU CSCL Globe enters the port of Zeebrugge on 17 January 2015. These type of ships have a large draft and increase maintenance dredging works.

Methods

In situ measurements and disposal sites

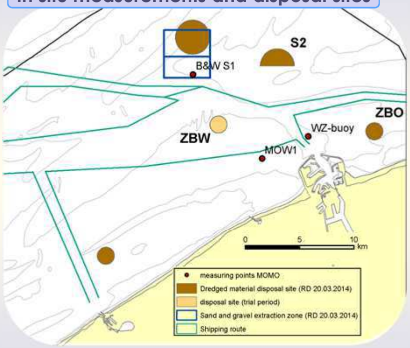

Belgian nearshore area near the port of Zeebrugge

Long time series of SPM concentration to resolve:

1) harmonic signals (tide, spring-neap cycle)
2) seasonal signal (+/- harmonic)
3) random signals (meteo, waves)

Design of the experiment

- 11 month with disposal site ZBO (as usual)
- 1 month with disposal site ZBW

Analysis of data

- as a function of residual alongshore flow, waves, tidal range, season: identify similar periods in time-series
- ensemble averaging
- statistical analysis

Tripod measurements at MOW1 & WZ buoy

SPM concentration (OBS ADP), Fluid mud layer (ADV altimetry), CTD, LISST, current velocity (ADV, ADP), turbulence (ADV)

Results

2013 SPM concentration time series at MOW1

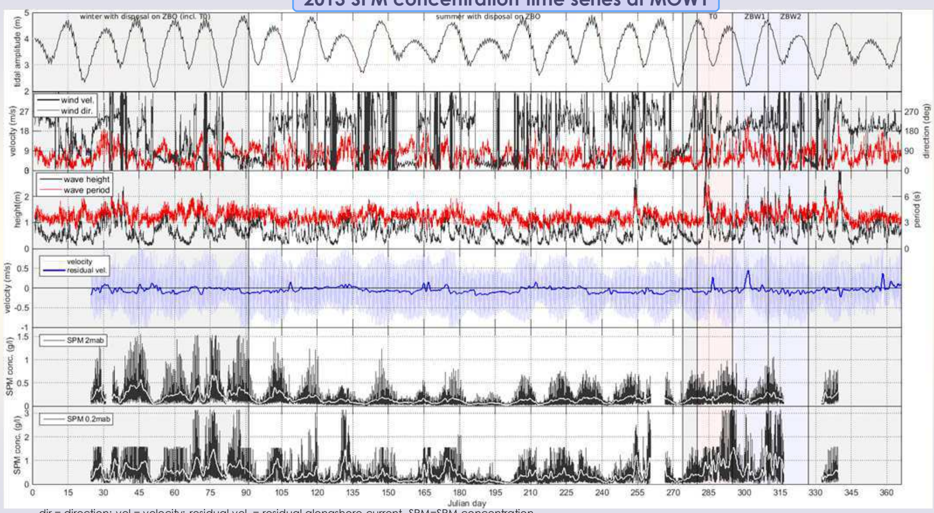

dir = direction; vel = velocity; residual vel. = residual alongshore current, SPM=SPM concentration

Ensemble averaged SPM conc. during a tide

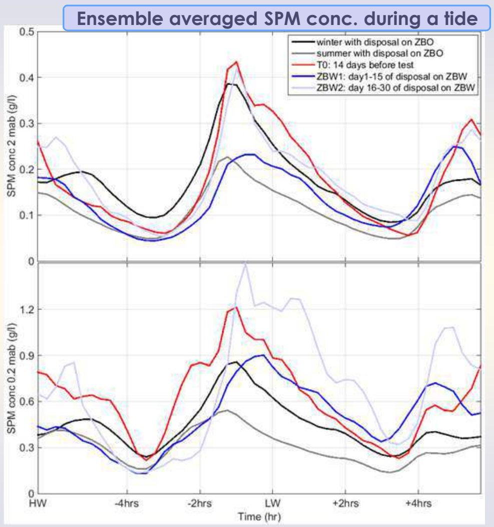

Conclusions

1. SPM dynamics, although dominated by tidal forcing, is significantly influenced by spring-neap cycles, seasons and meteo conditions.
2. This variability has been eliminated by using long time series and by choosing the same season (winter) and similar periods of meteo and residual currents (T0 & ZBW1).
3. The effect of disposal of fine grained matter on SPM concentration at MOW1 and WZ Buoy is about one order of magnitude lower than the natural SPM concentration.
4. During the ZBW-period the SPM concentration was lower than during T0 period. The decrease in SPM concentration is partially due to the fact another disposal site that is not influencing the SPM concentration at the measuring location (ZBW) was used.
5. The results indicate that sedimentation of mud in port and navigation channels situated in a high turbidity area can be reduced by a smart relocation of the disposal site.

Two-class flocculation kinetic model: development and application to large-scale, multi-dimensional cohesive sediment transport

Lee Byung Joon[1], Qilong Bi[2], Erik Toorman[2], Michael Fettweis[3] and Holger Weilbeer[4]

[1] School of Construction and Environmental Engineering, Kyungpook National University
2559 Gyeongsang-daero, Sangju, Gyeongbuk, 742-711, South Korea
E-mail: bjlee@knu.ac.kr

[2] Hydraulic Laboratory, Civil Engineering Department, KU Leuven
Kasteelpark Arenberg 40, Heverlee, 3001, Belgium

[3] OD Natural Environment, Royal Belgian Institute of Natural Sciences
Gulledelle 100, 1200 Brussels, Belgium

[4] Federal Waterways Engineering and Research Institute (BAW)
Wedeler Landstr. 157, 22559 Hamburg, Germany

Introduction

Fluid mud layer, composed of cohesive sediments, has been a serious problem in many waterways, docks and harbours. For example, Zeebrugge Harbour in Belgium has been reported to build up one- or two-meter thick fluid mud layer. Flocculation is known to be a key process for developing such fluid mud layers. Flocculation is a combined process of (1) aggregation of small mud particles to large flocs and (2) breakage of large flocs, depending on a turbulent shear condition. Cohesive sediments remain small in an open water (e.g. river or ocean), due to breakage under high turbulent shear. When entering/traveling into a closed water (e.g. harbour or dock), cohesive sediments aggregate to large, settleable flocs under low turbulent shear and finally settle/deposit on the bottom.

Most of flocculation models assume an equilibrium (or pseudo-equilibrium) condition and a single floc size, thus disregarding the two important aspects, (1) flocculation kinetics in a time and space and (2) bimodal (or multimodal) floc size distributions of cohesive sediments. Flocculation is a relatively slow process, taking several to ten hours to reach an equilibrium condition in a river, estuarine or coastal environment. Therefore, an empirical, equilibrium flocculation model may cause errors, when involving a time or spatial transition. For example, the Deurganckdok study (WL | Delft Hydraulics, 2006) reported that an equilibrium flocculation model resulted in under- (or over-) estimation of flocculation and sedimentation in a dock next to a turbulent river (i.e. at a transition). Also, flocculation often develops bimodal floc size distributions. This bimodal behaviour cannot be simulated with a conventional single-size flocculation model.

To minimize such errors, we developed a new flocculation kinetic model, based on Two-Class Population Balance Equation (TCPBE) (Eqn. (1)) (Lee *et al.*, 2011). The two discrete size groups of flocculi and flocs, as building blocks and aggregates, were found to approximate a bimodal floc size distribution of cohesive sediments (Lee *et al.*, 2012, 2014). This observation led us to develop a new two class population balance equation (TCPBE), which can track the concentration of size-fixed flocculi and the size and concentration of size-varying flocs as an approximation of a multimodal PSD.

$$[\frac{\partial N_i}{\partial t}]+[\frac{\partial u_x N_i}{\partial x}+\frac{\partial u_y N_i}{\partial y}+\frac{\partial u_z N_i}{\partial z}]-[\frac{\partial}{\partial x}\left(\frac{0.09\rho_w k_e^2}{S_c\varepsilon}\frac{\partial N_i}{\partial x}\right)+\frac{\partial}{\partial y}\left(\frac{0.09\rho_w k_e^2}{S_c\varepsilon}\frac{\partial N_i}{\partial y}\right)+\frac{\partial}{\partial z}\left(\frac{0.09\rho_w k_e^2}{S_c\varepsilon}\frac{\partial N_i}{\partial z}\right)]=\text{[redacted]}(agg/break)_i-\text{[redacted]}\frac{\partial N_i}{\partial z}$$

$$(agg/break)_{N_P}=\frac{\partial N_P}{\partial t}=-\frac{1}{2}\alpha_{PP}\beta_{PP}N_P N_P\left(\frac{N_C}{N_C-1}\right)-\alpha_{PF}\beta_{PF}N_P N_F+fN_C a_F N_F$$

$$(agg/break)_{N_F}=\frac{\partial N_F}{\partial t}=+\frac{1}{2}\alpha_{PP}\beta_{PP}N_P N_P\left(\frac{1}{N_C-1}\right)-\frac{1}{2}\alpha_{FF}\beta_{FF}N_F N_F+a_F N_F$$

$$(agg/break)_{M_F}=\frac{\partial M_F}{\partial t}=+\frac{1}{2}\alpha_{PP}\beta_{PP}N_P N_P\left(\frac{N_C}{N_C-1}\right)+\alpha_{PF}\beta_{PF}N_P N_F-fN_C a_F N_F$$

$$w_{s,i}=\Phi_{HS}\left(\frac{1}{18}\frac{(\rho_s-\rho_w)g}{\mu}D_P^{3-n_f}\frac{D_F^{n_f-1}}{1+0.15Re_i^{0.687}}\right)$$

$$\Phi_{HS}=(1-\phi)^a$$

(1)

(Nomenclature)

N_i = N_P, N_F, or M_F	$w_{s,i}$ = Floc Settling Velocity D_P, D_F = Diameter of Flocculi and Floc
N_C = Number of Flocculi in a Floc	n_f = Fractal Dimension
M_F = $N_F \times N_C$	Φ_{HS} = Factor for Hindered Settling
f = Flocculi Fraction Generated by Breakage	Φ = Factor for Hindered Settling

Model development and application: large-scale, multi-dimensional TCPBE-TELEMAC model.
For application to large-scale cohesive sediment transport, TCPBE is implemented to an open-source hydrodynamic and sediment transport model (TELEMAC in this study). We modify the original code of TELEMAC, adopting shear rate ($G = (\mathcal{E}/\nu)^{0.5}$) and settling velocity (w_s) as two key factors for controlling flocculation kinetics and sediment transport. At each time step in computation, TELEMAC calculates shear rates (G), which then control flocculation kinetics of TCPBE. On the other hand, TCPBE calculates floc settling velocities (w_s), which then determine floc sedimentation/deposition (i.e. sink) rates.
The combined TCPBE-TELEMAC model is applied to simulate cohesive sediment transport in Belgian near-shore area and Elbe Estuary in Germany. The results show that the TCPBE-TELEMAC model can more realistically simulate cohesive sediment processes (i.e. flocculation, advection, dispersion, sedimentation and deposition) than the equilibrium flocculation model. For example, the TCPBE-TELEMAC model can simulate a lag phase of flocculation at a time and spatial transition (e.g. from slack to peak flow; from an open ocean to a harbour), because it takes into account "kinetics". The conventional equilibrium flocculation model however does not consider kinetics nor the lag phase, so that it often develops steep gradient (or discontinuity) of flocculation at a time and spatial transition. In addition, because the TCPBE-TELEMAC model takes into account the bimodality with the two groups of flocculi and flocs, it can simulate background turbidity floating around in the water column. The single-class equilibrium flocculation model often develops zero turbidity, which is not real, because it does not differentiate turbidity-causing flocculi from flocs.

Further remarks: biologically-mediated TCPBE
The TCPBE model is theoretical but not empirical. This implies that the TCPBE model can easily add on other physical, chemical and biological processes without breaking the physics of flocculation. Thus, in future studies, the TCPBE model will be used as a generic model to adopt biologically-mediated flocculation. Especially, Extracellular Polymeric Substances (EPS) are known to scavenge and assemble biomass and sediment particles into large flocs (Engel *et al.*, 2004). Thus, the biologically-mediated TCPBE will include: (1) EPS formation kinetics controlled by microbial population dynamics and (2) particle aggregation and breakage kinetics between different particles species (i.e. EPS, biomass and minerals) (Fig. 1).

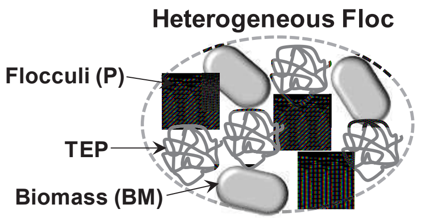

$$\rho_{Floc} = (1-e)(x_{TEP}\rho_{TEP} + x_{BM}\rho_{BM} + x_P\rho_P) + e\rho_{Water}$$

$$e = 1 - \left(\frac{D}{D_o}\right)^{n_f - 3}$$

Fig. 1. A schematic diagram of a biomass-sediment floc with heterogeneous composition and mathematical formula for calculating the density of a heterogeneous floc. x is the volume fraction of TEP, biomass or flocculi in a floc, e is the void fraction, D is the size of a floc and D_o is the size of a primary particle.

Acknowledgement
This research was supported by Basic Science Research Program through the National Research Foundation of Korea (NRF) funded by the Ministry of Education (No: 2014R1A1A2055622).

References
Engel A., S. Thoms, U. Riebesell, E. Rochelle-Newall and I. Zondervan. 2004. Polysaccharide aggregation as a potential sink of marine dissolved organic carbon. Nature 428:929-932.
Lee B.J., E. Toorman and M. Fettweis. 2014. Multimodal particle size distributions of fine-grained sediments: mathematical modeling and field investigation. Ocean Dynamics 64(3):429-441.
Lee B.J., M. Fettweis, E. Toorman and F. Molz. 2012. Multimodality of a particle size distribution of cohesive suspended particulate matters in a coastal zone. Journal of Geophysical Research 117. C03014.
Lee B.J., E. Toorman, F.J. Molz and J. Wang. 2011. A two-class population balance equation yielding bimodal flocculation of marine or estuarine sediments. Water Research 45(5):2131–2145.
WL | Delft Hydraulics. 2006. 3D slibtransport model Zeeschelde - Scenario 4: effect CDW op sedimentatie Deurganckdok, nieuw instrumentarium.

Two-Class Flocculation Kinetic Model: Development and Application to Large-scale, Multi-dimensional Cohesive Sediment Transport

Dept. of Construction and Environmental Engineering

B. Joon Lee[1], Qilong Bi[2], Erik A. Toorman[2], Michael Fettweis[3] and Holger Weilbeer[4]

1 School of Construction and Environmental Engineering, Kyungpook National University, South Korea (Info: bjlee@knu.ac.kr)
2 Hydraulics Laboratory, Department of Civil Engineering, Katholieke Universiteit Leuven, Belgium
3 OD Natural Environment, Royal Belgian Institute of Natural Sciences, Belgium
4 Federal Waterways Engineering and Research Institute (BAW), Hamburg, Germany

1 Flocculation is Dynamic!

Steady-state (Empirical) Flocculation Model

$W_s = f(Conc, Shear, Sal)$

Dynamic (Kinetic) Flocculation Model (Differential Equation)

$dNi/dt = f(Conc, Shear, Sal)$

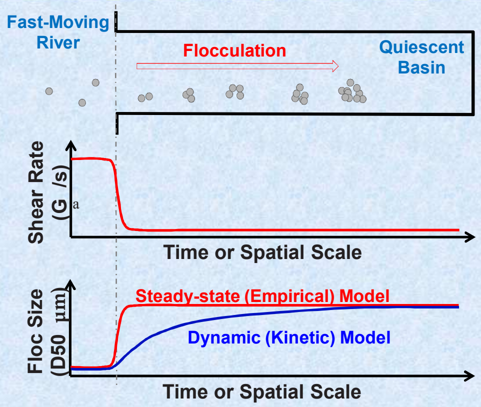

2 Flocculation causes Bimodality!

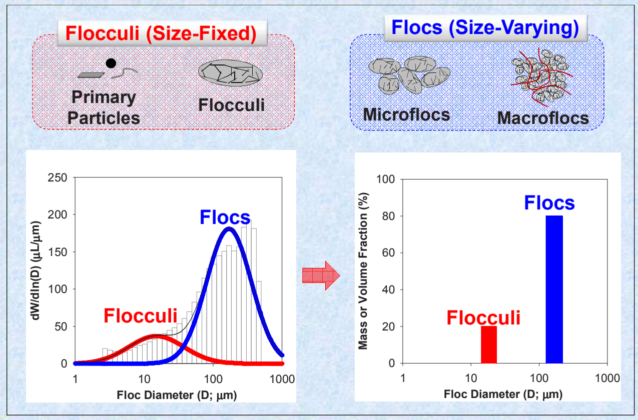

3 Implement TCPBE to TELEMAC to simulate Flocculation Dynamics and Bimodality

3.1 TCPBE-TELEMAC: Conceptual Model

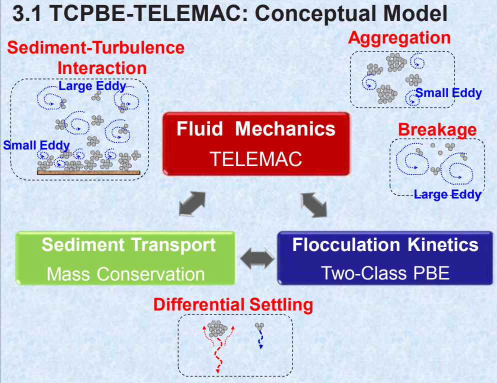

3.2 TCPBE-TELEMAC: Flocculation Kinetic Model (Two-Class PBE)

Three Dependent Variables (N_P, N_F, & M_F) and Partial Differential Equations

$$\left[\frac{\partial N_i}{\partial t}\right]+\left[\frac{\partial u_x N_i}{\partial x}+\frac{\partial u_y N_i}{\partial y}+\frac{\partial u_z N_i}{\partial z}\right]-\left[\frac{\partial}{\partial x}\left(\frac{0.09\rho_w k_e^2}{S_c\varepsilon}\frac{\partial N_i}{\partial x}\right)+\frac{\partial}{\partial y}\left(\frac{0.09\rho_w k_e^2}{S_c\varepsilon}\frac{\partial N_i}{\partial y}\right)+\frac{\partial}{\partial z}\left(\frac{0.09\rho_w k_e^2}{S_c\varepsilon}\frac{\partial N_i}{\partial z}\right)\right]=\pm(agg/break)_i-w_{s,i}\frac{\partial N_i}{\partial z}$$

$$(agg/break)_{N_P}=\frac{\partial N_P}{\partial t}=-\frac{1}{2}\alpha_{PP}\beta_{PP}N_PN_P\left(\frac{N_C}{N_C-1}\right)-\alpha_{PF}\beta_{PF}N_PN_F+fN_Ca_FN_F$$

$$(agg/break)_{N_F}=\frac{\partial N_F}{\partial t}=+\frac{1}{2}\alpha_{PP}\beta_{PP}N_PN_P\left(\frac{1}{N_C-1}\right)-\frac{1}{2}\alpha_{FF}\beta_{FF}N_FN_F+a_FN_F$$

$$(agg/break)_{M_F}=\frac{\partial M_F}{\partial t}=+\frac{1}{2}\alpha_{PP}\beta_{PP}N_PN_P\left(\frac{N_C}{N_C-1}\right)+\alpha_{PF}\beta_{PF}N_PN_F-fN_Ca_FN_F$$

$$w_{s,i}=\Phi_{HS}\left(\frac{1}{18}\frac{(\rho_s-\rho_w)g}{\mu}D_P^{3-n_f}\frac{D_F^{n_f-1}}{1+0.15Re_i^{0.687}}\right)$$

$$\Phi_{HS}=(1-\phi)^a$$

$N_i = N_P,\ N_F$, or M_F
N_C = No of Micro Flocs in a Macro Floc
$M_F = N_F \times N_C$
f = % Micro Flocs Generated by Breakage
$w_{s,i}$ = Settling Velocity
D_P, D_F = Diameter of Micro- and Macro-Floc
n_f = Fractal Dimension
Φ_{HS} = Factor for Hindered Settling
Φ = Factor for Hindered Settling

4 Biologically-mediated Flocculation: Conceptual Model

TEP (Transparent Extracellular Polymers) combine the Biological and Mineralogical Populations into a Floc.

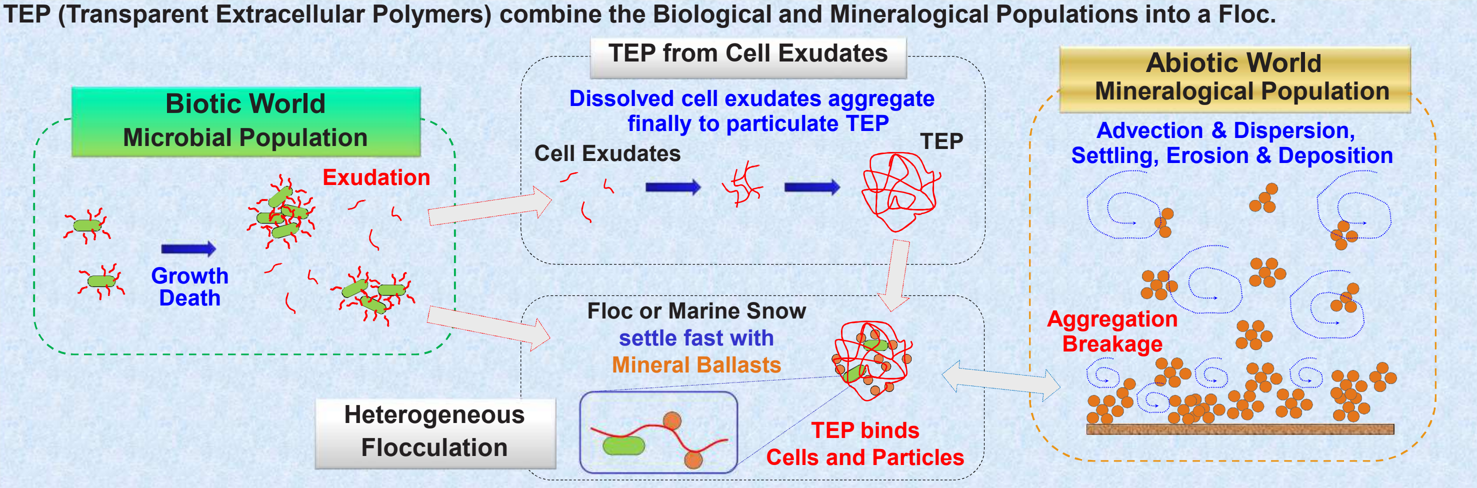

5 Biologically-mediated Flocculation: Mathematical Model

$$(A_i+B_i)-\frac{\partial(w_{s,i}N_i)}{\partial z}=\frac{dN_i}{dt}+\frac{\partial}{\partial x}(u_xN_i)+\frac{\partial}{\partial y}(u_yN_i)+\frac{\partial}{\partial z}(u_zN_i)+\frac{\partial}{\partial x}(u_xN_i)+\frac{\partial}{\partial y}(u_yN_i)+\frac{\partial}{\partial z}(u_zN_i)-\frac{\partial}{\partial x}\left(D_x\frac{\partial N_i}{\partial x}\right)-\frac{\partial}{\partial y}\left(D_y\frac{\partial N_i}{\partial y}\right)-\frac{\partial}{\partial z}\left(D_z\frac{\partial N_i}{\partial z}\right)$$

Flocculation Kinetics

Mineralogical Domain

$$\frac{dN_{Particle}}{dt}=\ldots$$

Biological Domain

$$\frac{dN_{Biomass}}{dt}=\ldots \qquad \frac{dN_{EPS}}{dt}=\ldots$$

Bio-Mineral Domain

$$\frac{dN_{Floc}}{dt}=\ldots$$

Acknowledgements: This research was supported by Basic Science Research Program through the National Research Foundation of Korea (NRF) funded by the Ministry of Education (No: 2014R1A1A2055622).

Extreme values of suspended particulate matter concentration and their relation to swell and wind sea in the Belgian coastal zone

Thant Silvy[1], Matthias Baeye[2], Michael Fettweis[2], Frederic Francken[2], Jaak Monbaliu[3] and David Van Rooij[4]

[1] MSc student Marine and Lacustrine Sciences and Management, Ghent University
E-mail: Silvy.Thant@gmail.com

[2] Operational Directorate Natural Environment (OD Nature), Royal Belgian Institute of Natural Sciences (RBINS), Gulledelle 100, B-1200 Brussels, Belgium

[3] Department of Civil Engineering, Katholieke Universiteit Leuven (KUL), Kasteelpark Arenberg 40, B-3001 Leuven

[4] Department of Geology and Soil Science, Renard Centre of Marine Geology (RCMG), Ghent University (UGENT), Krijgslaan 281 S8, B-9000 Gent

SPM concentration is one of the key parameters to describe the environmental status, and to evaluate and understand the impact of human activities in both nearshore and offshore areas (Fettweis and Van den Eynde, 2003; Dobrynin *et al.*, 2010). Long-term measurements are needed in order to resolve all variations in SPM concentration. Processes affecting SPM concentration are turbulence, tides, neap-spring cycles, meteorological events, season, and other long-term fluctuations. SPM concentration has been measured since 2005 at two coastal observatory sites in the high-turbidity zone off the Belgian coast. The measurements have been carried out using a benthic tripod that allowed measuring during all meteorological conditions, including storms.

The effects of storms on sediment re-suspension and SPM concentration have been investigated using meteorological and wave data from IVA MDK (afdeling Kust - Meetnet Vlaamse Banken). SPM concentration data from MOW1 (51.358°N, 3.098°E) and Blankenberge (51.329°N, 3.107°E) were estimated using the backscatterance data from a 3MHz acoustic Doppler profiling current meter. Because of the large amount (about 1500 days) of SPM concentration data, a detection algorithm for identifying extreme events was developed. This peak detection function allowed eventually cataloging the extreme SPM concentrations and relating them to storm events and wave system data.

Many events of extreme SPM concentration were detected and were related to one of the following specific extreme weather conditions: 1) NNW storms with high swell activity, 2) SW storms and 3) strong NE winds. The wave systems responsible all have a distinct effect on the degree of erosion of the seafloor bed sediments, the re-suspension of SPM concentration and the upward mixing of SPM through the water column. A NNW storm, characterized by swell waves, will cause a stronger erosion of bed sediments forming a high-concentrated suspension layer of SPM near the bottom in comparison to SW storms. The latter, characterized by wind sea, results in the absence of the benthic suspension layer. However, an enhanced upward mixing of SPM through the water column can be observed in contrast to the situation during NNW storms (Fig. 1). This is a consequence of the occurrence of a hindered re-suspension and settling of SPM due to the increased concentration (saturation concept), leading to a dense suspension and a reduced turbulence energy level. In this case, an upward mixing of SPM is attenuated since this is directly related to turbulent energy levels (Winterwerp, 2002; McAnally *et al.*, 2007; Winterwerp *et al.*, 2002, 2012). The SPM processes in the case of strong NE winds is different. Extreme SPM concentrations are mainly caused by advection of SPM from a more remote SPM source (e.g. Scheldt River).

Additionally, the interaction of different wave systems, together with water depth and sediment type will play an important role in understanding this variation in impact of different extreme weather conditions and the presence of extreme values of SPM concentration.

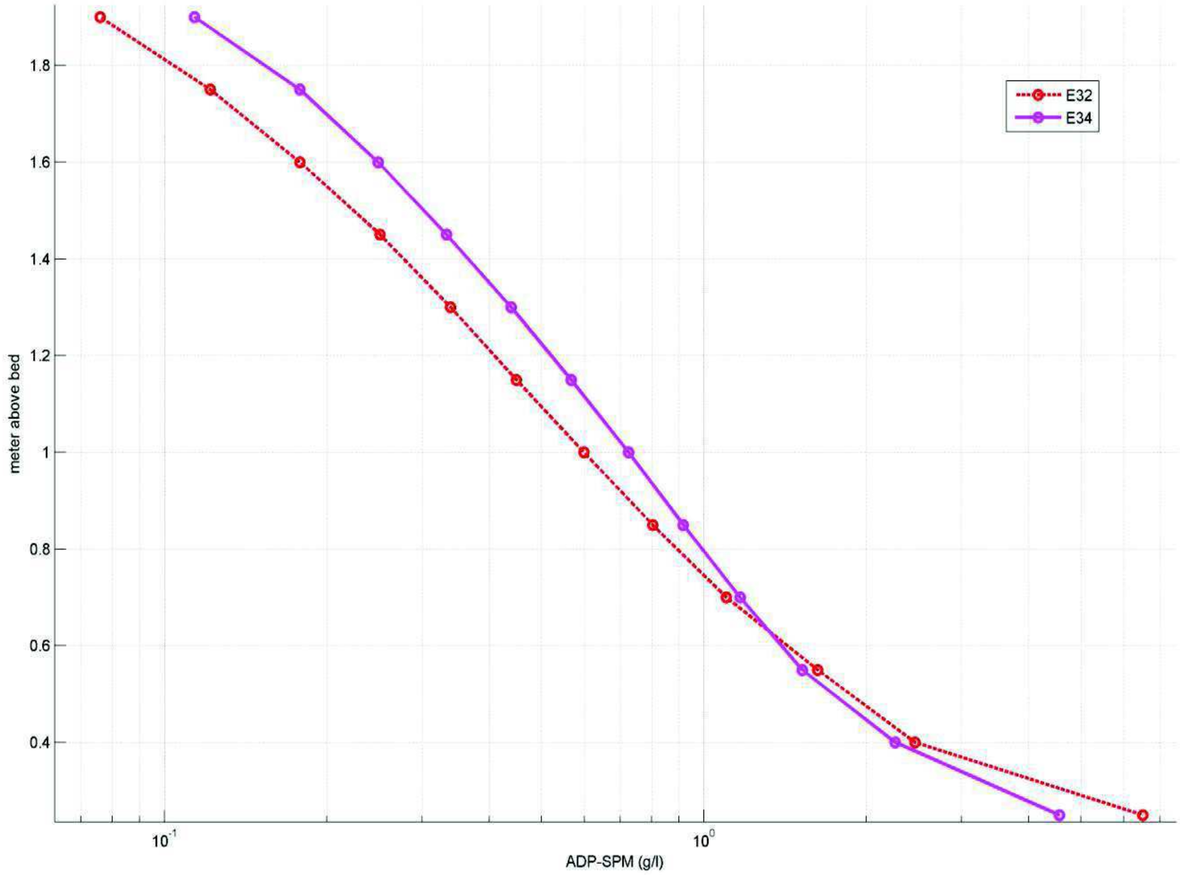

Fig. 4. Vertical profile of the averaged SPM concentration for a NNW storm event (E32, 10/10/2013) and a SW storm event (E34, 28/10/2013). SPM concentrations of E32 are higher at 0.3mab compared to E34, due to the higher erosion capacity of NNW storms. Concentrations at 1.8mab are higher for the SW event that is characterized by enhanced vertical mixing of SPM.

References

Dobrynin M., G. Gayer, A. Pleskachevsky and H. Günther. 2010. Effect of waves and currents on the dynamics and seasonal variations of suspended particulate matter in the North Sea. Journal of Marine Systems 82(1-2):1-20.

Fettweis M. and D. Van den Eynde. 2003. The mud deposits and the high turbidity in the Belgian–Dutch coastal zone, southern bight of the North Sea. Continental Shelf Research 23(7):669-691.

McAnally W.H., F. Asce, C. Friedrichs, D. Hamilton, E. Hayter, P. Shrestha, H. Rodriguez, A. Sheremet and A. Teeter. 2007. Management of fluid mud in estuaries, bays, and lakes. I: Present state of understanding on character and behavior. Journal of Hydraulic Engineering 133(1):9-22.

Winterwerp J.C. 2002. On the flocculation and settling velocity of estuarine mud. Continental Shelf Research 22(9):1339-1360.

Winterwerp J.C., A.W. Bruens, N. Gratiot, C. Kranenburg, M. Mory and E.A. Toorman. 2002. Dynamics of concentrated benthic suspension layers. Proc. 6th International Conference on Cohesive Sediment Transport, INTERCOH. Delft, the Netherlands.

Winterwerp J.C., G.J. de Boer, G. Greeuw and D.S. van Maren. 2012. Mud-induced wave damping and wave-induced liquefaction. Coastal Engineering 64:102–112.

Wave systems and their impact on the seabed and water column turbidity in the Belgian coastal zone

Silvy Thant[1], Matthias Baeye[2], Michael Fettweis[2], Frederic Francken[2], Jaak Monbaliu[3], David Van Rooij[4]

1 Antea Group, BU WATER, Buchtenstraat 9, B-9051 Gent
Email: silvy.thant@anteagroup.com; silvy.thant@gmail.com
2 Royal Belgian Institute of Natural Sciences (RBINS), Operational Directorate Natural Environment (OD Nature), Gulledelle 100, B-1200 Brussels
Email: Matthias.Baeye@mumm.ac.be
3 Katholieke Universiteit Leuven (KUL), Department of Civil Engineering, Kasteelpark Arenberg 40, B-3001 Leuven
4 Ghent University (UGENT), Department of Geology and Soil Science, Renard Centre of Marine Geology (RCMG), Krijgslaan 281 S8, B-9000 Gent

The impact of extreme weather conditions on SPM concentration

1. What is the impact of severe storms on sediment resuspension at the Belgian coastal zone? What is the SPM (suspended particulate matter) concentrations?
2. Are there different types of storms and do they have different impacts?
3. What are the wave and meteorological parameters associated with these storm events?

The "Sinterklaas"storm of December 5th 2013 struck the coast of Belgium and The Netherlands. At Ostend the highest waterlevel since 1953 was recorded.

Setting and Methods

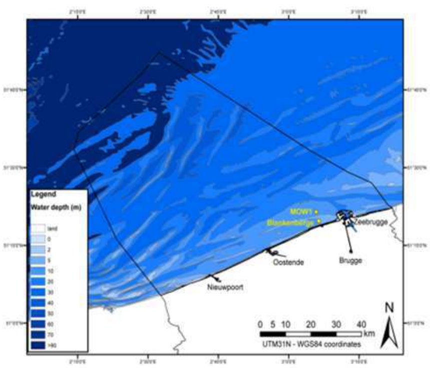

Timeseries of SPM concentration. Around day 330 an anomaly in SPM concentration occurs.

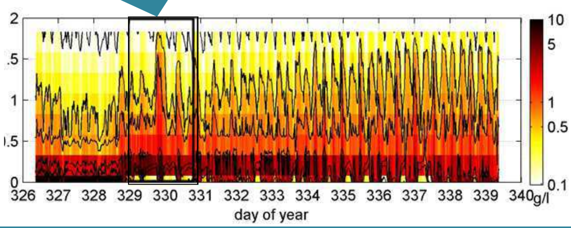

1. Long-term timeseries of SPM conc. at MOW1 and Blankenberge site
   - ADP data
   - 2008 – 2013 (1499 days)
   - filtering out harmonic signals (tide, spring-neap cycle)
   - extreme event detection
2. Wave and meteorological data of each extreme SPM concentration event

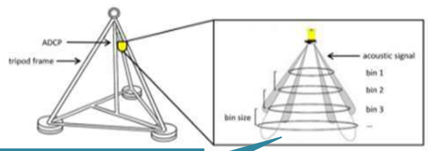

Backscatter data of an ADP used for SPM concentration

Results and discussion

NE winds

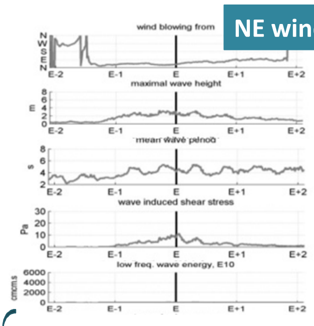

NE winds (no storm characteristics) combined with ebb tidal currents cause advection of sediment of the Westerscheld estuary

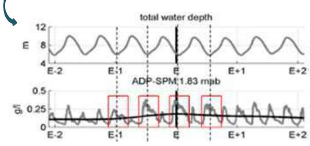

41 extreme events in SPM conc.

3 extreme weather types

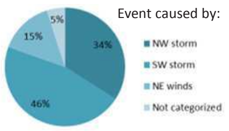

NW storm

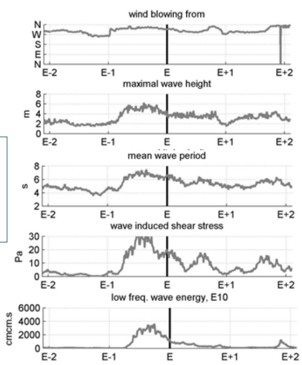

SW storm

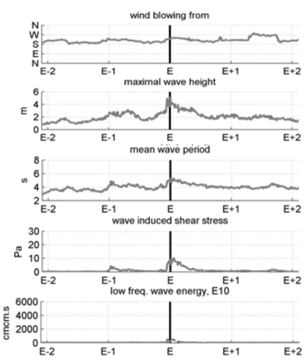

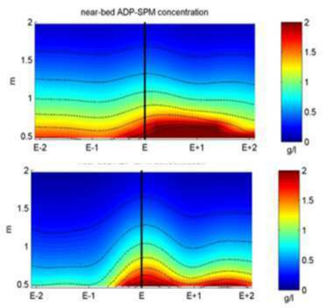

NW storms are characterised by low frequency waves (6s) causing serious erosion and very high SPM conc.

Erosion as well as SPM conc. caused by SW storms is lower compared to NW storms due to the lower shear stresses.

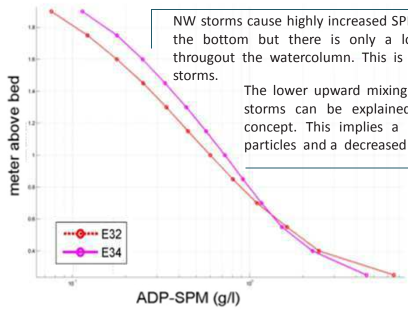

NW storms cause highly increased SPM concentrations at the bottom but there is only a low mixing of SPM througout the watercolumn. This is oppoite during SW storms.

The lower upward mixing capacity during NW storms can be explained by the saturation concept. This implies a hindered settling of particles and a decreased turbulent energy.

Conclusions

Extreme weather conditions (storms) are causing extreme values of SPM concentration at MOW1 and Blankenberge site **1**

3 weather conditions during extreme events:
- NE winds
- SW storms
- NW storms

Important: Hmax, P, E10, shear stress and wind direction **2**

Causing respectively:
1) advection of sediment from the mouth of the Westerschelde estuary in combination with ebb tidal currents,
2) resuspension of bed material with mixing of SPM higher up in the water column,
3) extreme resuspension and erosion of the bed but low upward mixing of the SPM in the water column. **3**

INTERCOH 2015
7 – 11 september, Leuven, Belgium

museum Operational Directorate Natural Environment OD Nature I OD Natuur I DO Nature

anteagroup

UNIVERSITEIT GENT

Validation of modelled bottom shear stress under the influence of currents and waves, using long-term measurements

Van den Eynde Dries, Matthias Baeye, Michael Fettweis, Frederic Francken and Vera Van Lancker

Suspended Matter and Seabed Monitoring and Modelling Group
Operational Directorate Natural Environment (OD Nature)
Royal Belgian Institute for Natural Sciences
Gulledelle 100, B-1200 Brussels, Belgium
E-mail: D.VandenEynde@mumm.ac.be

More than 2800 days of currents measurements with a benthic tripod and almost 400 days with a bottom mounted ADCP have been collected in the Belgian part of the North Sea during the period 2005-2013. These data have been used to derive the bottom shear stress from the current profile and the high frequency currents and have been used to validate the modelled bottom stresses. The validated model allows to get insight in the spatial and temporal variability of the bottom roughness.

Introduction
Bottom shear stress links the sea floor to the water column, and is a prime factor for the calculation of sediment transport, including erosion, resuspension and deposition, and bottom morphology. Bottom shear stress is influenced by a large number of factors, including the surface sediment texture, micro-bathymetry, benthic organisms, all influencing the bottom roughness.

In literature, many different methods are available for the calculation of the bottom shear stress, ranging from simple models, using a constant drag coefficient and depth-averaged currents, to complicated ones that take the different bottom boundary layers and the instantaneous bottom shear stresses in a wave cycle into account.

Comparison of the model results with measurements is not only important for validation of the model, but also to gain more insight in the variability of the bottom roughness, both in space and time. However, measuring bottom stresses is difficult and the (lack of) qualitative bottom stress measurements may hamper a sound validation of the model results.

Bottom shear stress measurements
Since 2005 more than 70 deployments have been carried out using benthic tripods. The frame was equipped with (1) a SonTek ADV Ocean point current sensor and a downward looking SonTek 3MHz ADP current profiler for currents; (2) a Sequoia LISST-100X Laser In-Situ Scattering & Transmissometer for particle size distribution and the volumetric concentration of the material in suspension; (3) a Sea-Bird SBE37 thermosalinograph for temperature and salinity; (4) optical backscatter sensors for turbidity in the water column. Furthermore RDI bottom mounted Acoustic Doppler Current Profilers, type Sentinel 1200 kHz Workhorse, were deployed to measure the complete current profile.

Over the period 2005-2013 more than 2100 days of current measurements are available from the tripods and about 400 days from the ADCPs. Most of the data (68%) were collected in the nearshore in the vicinity of the port of Zeebrugge (MOW1) (see Fig. 1.), but also at some more offshore stations current data were collected.

The bottom shear stress was derived from the current measurements using three methods. The first one calculates the bottom shear stress and bottom roughness, and their associated error ranges, from a least-square regression of the current profile for the lower part of the water column using the data from the ADP and ADCP (Wilkinson, 1983). In the second method, the bottom shear stress is calculated from the high frequency ADV current measurements using the second moment (turbulent) statistics (Andersen *et al.*, 2007). Since the bottom shear stress is assumed to be linearly related to the turbulent kinetic energy, it can be calculated from the variance of the current fluctuations (Stapleton and Huntley, 1995). Finally, the intertial dissipation method was applied, including a correction for the advection of waves (Trowbridge and Elgar, 2001; Sherwood *et al.*, 2006). In this method, the bottom shear stress is calculated as a function of the turbulent dissipation, derived from the energy spectrum of the currents.

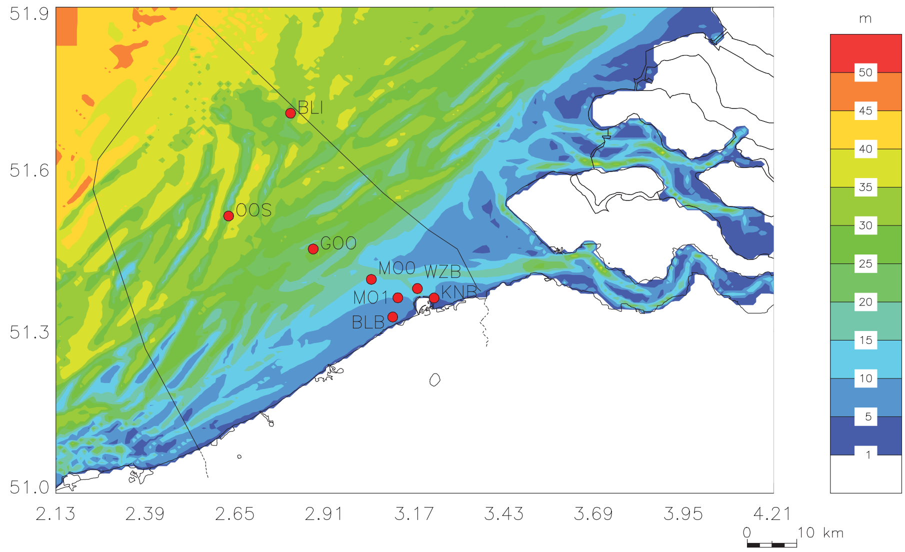

Fig. 1. Position of the measuring stations: OOS: Oosthinder, BLI: Bligh Bank, GOO: Gootebank, MO0: MOW0, BLB: Blankenberge, MO1: MOW1, WZB: WZ-Boei, KNB: Knokkebank.

Bottom shear stress calculations using a numerical model

The modules of Soulsby and Clarke (2005) and Malarkey and Davies (2012) have been used to calculate the bottom shear stress. Both modules parameterise the complex model results in an efficient way, so that they can be included in larger scale sediment transport models. Currents were calculated using a three-dimensional hydrodynamic model, based on the COHERENS software (Luyten, 2014), waves were calculated using an implementation of the WAM model (WAMDIG, 1988).

Acknowledgements

Data were acquired in several monitoring programmes [MOMO and MOZ4 (Flemish Government); ZAGRI and WinMON (private revenues)]. RV Belgica shiptime was provided by RBINS, OD Nature and Belgian Science Policy Office. The commander and crew of the RV Belgica, and the Measuring Service Ostend (RBINS, OD Nature) are acknowledged for logistical support.

References

Andersen T.J., J. Fredsoe and M. Pejrup. 2007. *In situ* estimation of erosion and deposition thresholds by Acoustic Doppler Velocimeter (ADV). Estuarine Coastal and Shelf Science 75:327–336.

Luyten P. (Ed.). 2014. COHERENS – A Coupled Hydrodynamical-Ecological Model for Regional and Shelf Seas: User Documentation. Version 2.6. RBINS Report, Operational Directorate Natural Environment, Royal Belgian Institute of Natural Sciences, Brussels, Belgium. 1554p.

Malarkey J. and A.G. Davies. 2012. A simple procedure for calculating the mean and maximum bed stress under wave and current conditions for rough turbulent flow based on Soulsby and Clarke's (2005) method. Computers & Geosciences 43:101-107.

Sherwood C.R., J.R. Lacy and G. Voulgaris. 2006. Shear velocity estimates on the inner shelf off Grays Harbor, Washington, USA. Continental Shelf Research 26:1995–2018.

Soulsby R.L. and S. Clarke. 2005. Bed shear-stresses under combined waves and currents on smooth and rough beds. Report TR 137. HR Wallingford, Wallingford, United Kingdom. 42p.

Stapleton K.R. and D.A. Huntley. 1995. Seabed stress determinations using the inertial dissipation method and the turbulent kinetic energy method. Earth Surface Processes and Landforms 20:807–815.

Trowbridge J. and S. Elgar. 2001. Turbulence measurements in the surf zone. Journal of Physical Oceanography 31:2403–2417.

WAMDIG: The WAM Development and Implementation Group. 1988. The WAM model: a third generation ocean wave prediction model. Journal of Physical Oceanography 18:1775-1810.

Wilkinson R.H. 1983. A method for evaluating statistical errors associated with logarithmic velocity profiles. Geo-Marine Letters 3:49–52.